**METEOR-BERICHTE**

**00-2**

# *DECOS / OMEX II*

**Cruise No. 43**
**25 November 1998 - 14 January 1999**

**Edited by:**

**Hans-Ulrich Schmincke, Gerhard Graf**

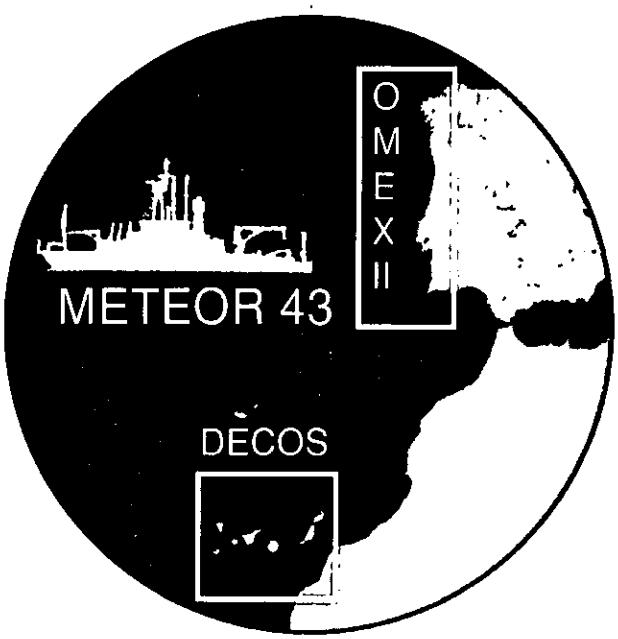


**Editorial Assistance:**

**Frank Schmieder**
**Fachbereich Geowissenschaften, Universität Bremen**

**Sebastian Krastel**
**GEOMAR, Kiel**

**Leitstelle METEOR**
**Institut für Meereskunde der Universität Hamburg**

**2000**

Table of Contents

**Abstract**

METEOR cruise M 43 consisted of two legs in the eastern Atlantic (25.11.1998 - 14.01.1999). The cruise started in Viana do Castelo (Portugal) and ended in Cadiz (Spain). The scientific crews changed in Las Palmas, Canary Islands (Spain), where the vessel had a stopover from 23.12.1998 - 28.12.1998.

The aim of METEOR cruise M 43/1 (Project DECOS, *Destruction and Construction of Seamounts*, 25.11.1998 - 23.12.1998) was to study the geodynamic evolution of intraplate volcanic edifices and their mantle sources along the boundary zone oceanic-continental lithosphere extending from the central to the western Canary Islands and as far south as the Saharan Seamount group focussing on the following questions: (1) Did the islands and seamounts sink into the lithosphere and, if so, what can be learned about the elastic thickness of the lithosphere? (2) At what depth below sea level do magmatic volatiles exsolve in significant amounts? (3) What is the regional distribution and volume of debris avalanche deposits? (4) How strongly did magmas evolve that erupted along the submarine ridges and seamounts? (5) Is there evidence for continental crust beneath the Canary Islands? (6) Does the character of the mantle sources change in time and regionally?

Submarine volcanoes on the flanks of the central and western Canary Islands and of six seamounts up to 500 km south of the Canary Islands (including Paps, Tropic, El Hierro and Endeavour Seamounts) were sampled by dredging at 180 stations and mapped by swath bathymetry. More than 60 % of the stations contained volcanic rocks varying widely in vesicularity, chemical and mineralogical composition, grain size, structures and therefore emplacement mechanisms and environment, and degree of alteration. The most common rock types are alkali basalt and basanite. Nephelinites dredged e.g. on the El Hierro submarine ridge suggest that highly undersaturated magmas may also erupt during the early stages of island growth possibly analogous to Loihi Seamount south of Kilauea Volcano. The large volumes of evolved rocks (trachytes, phonolites and rhyolites) on the submarine ridges of La Palma and El Hierro as well as on seamounts to the south have implications for the density substructure of the Canary Islands as well as plume flux and ascent rate of magmas and their residence time in shallow magma reservoirs. Fresh feldspars in many rocks will allow a detailed dating program, enabling a better understanding of the geodynamic evolution of the volcanic belt parallel to the continental-oceanic lithosphere boundary off NW Africa. The abundance of vesicles even in rocks dredged at more than 1000 m bsl, commonly scoriaceous lapillistones, is thought to be due to high volatile contents of the alkalic magmas, necessitating recalibration of vesicle geobarometers to determine initial water depth of eruption. It also means that the density structure in the interior of large seamounts needs to be re-evaluated and the likelihood for flank failures maybe larger in large seamounts whose upper 1000-2000 m bsl is dominantly composed of highly unstable lapilli deposits. The submarine ridges south of La Palma and El Hierro, discrete rift zones, about 3-5 km wide and up to 40 km long with steep lateral and terminal slopes, are capped by abundant seamounts suggesting locally developed conduit systems. The dominantly linear volcanic structures (NNE-SSW and NW-SE) mirror those of the islands, possibly reflecting the stress field of the lithosphere. Seamounts south of the Canary Islands are more common than previously known, evidence that the boundary zone between continental and oceanic lithosphere acts as a preferred zone for magma ascent (leaky lithosphere boundary). Volcanic activity along the submarine ridges of La Palma and El Hierro appear to be very young and the prominent volcano Hijo de Tenerife between Gran Canaria and Tenerife that erupted spectacular bombs of intermediate rocks containing both peridotite nodules and possibly Mesozoic sandstone xenoliths may still be active. All lavas emplaced at more than ca. 600 m depth on the flanks of the Canary Islands - our minimum water depth for dredging - show evidence for subaqueous emplacement. The boundary between submarine and subaerial volcano growth is thus shallow, implying that the

islands have been relatively stable with respect to sea level and that the recently proposed sinking of Tenerife by some 2500 m is untenable. South of El Hierro, a 30 km² debris avalanche area was mapped in detail and debris avalanche material – probably of Pliocene age (Roque Nublo Group) - was sampled in the channel between Gran Canaria and Fuerteventura. This helps to clarify the run-out distance and possibly timing of these flank collapses based on the change in composition of lavas with age. Bathymetric data combined with other recent data sets will provide a rather complete bathymetric map of the seafloor around the Canary Islands, greatly facilitating future marine geological and geophysical work in the area.

Leg 43/2 was carried out to investigate particle transport from the narrow shelf of the Iberian Peninsula to the continental slope in the frame of the EU-Project OMEX II (Ocean Margin Exchange programme). The special issue of this cruise was to quantify sedimentation, bottom near particle transport, the hydrographical regime, and the exchange of biogases during winter, in order to compare these results with those of other seasons and other settings of shelf-continentals slope systems. In spite of the poor weather conditions most data have been successfully taken. A prominent result is given by the findings that the Nazaré Canyon turned out to provide a focussing of sediment and a rapid transport from the shelf to the deep-sea.

## Zusammenfassung

Die 43. Reise des deutschen Forschungsschiff METEOR fand in zwei Abschnitten vom 25.11.1998 bis 14.1.1999 im Ostatlantik statt. Die Expedition begann in Viana do Castelo (Portugal) und endete in Cadiz (Spanien). Zwischen den beiden Fahrtabschnitten wurde der Hafen von Las Palmas, Kanarische Inseln (Spanien) angelaufen (23.12. – 28.12.1998), wo die wissenschaftliche Besatzung wechselte.

Hauptziel der METEOR-Fahrt M 43/1 (Project DECOS, *Destruction and Construction of Seamounts,* 25.11.1998 - 23.12.1998) war es, die geodynamische Evolution ozeanischer Intraplattenvulkane und ihrer Mantelquellen in der Grenzzone ozeanische - kontinentale Lithosphäre im Gebiet der zentralen und westlichen Kanarischen Inseln und der Saharan Seamountgruppe im Süden genauer zu untersuchen, und zwar mit folgenden Schwerpunkten: (1) Sind die Inseln und Seamounts in die Lithosphäre eingesunken, und welche Schlüsse können über die elastische Mächtigkeit der Lithosphäre daraus gezogen werden? (2) In welcher Wassertiefe beginnt eine signifikante Blasenbildung? (3) Wie verbreitet sind Schuttlawinen? (4) Wie stark differenziert sind die submarin eruptierten Magmen? (5) Gibt es Anzeichen für Kontinentale Kruste? (6) Ändert sich die Zusammensetzung der Mantelquellen mit dem Grad der Entwicklung einer Insel und regional?

Die submarinen Flanken der Inseln Tenerife und Gran Canaria, Vulkanbauten entlang der submarinen Rücken südlich von La Palma und El Hierro, sowie die Flanken von sechs Seamounts (Tropic Seamount, Endeavour Seamount, El Hierro Seamount, Paps Seamount und zwei kleinere Seamounts) bis zu 500 km südlich der Kanaren wurden auf insgesamt 180 Stationen beprobt und bathymetrisch kartiert. Vulkanische Gesteine, auf gut der Hälfte der Stationen gewonnen, umfassen ein großes kompositionelles Spektrum (Nephelinite bis zu plagioklasreichen Alkalibasalten, seltene intermediäre Gesteine sowie Trachyte, Phonolithe und Rhyolithe) sowie unterschiedliche Blasigkeit und Frische (Grad der Alteration). Nephelinite vom vermuteten submarinen Frühstadium bei Hierro ähneln wegen des Auftretens von hoch $SiO_2$-untersättigten Laven dem Loihi-Stadium vom Kilauea Vulkan (Hawaii). Die unerwartete Häufigkeit hochdifferenzierter Gesteine entlang der submarinen Rücken von La Palma und El Hierro sowie in den

südlichen Seamounts lassen auf niedrige Plumeflux Raten und lange Aufenthaltszeiten in Magmareservoiren schließen. Genaue Altersbestimmungen werden sich aufgrund der frischen Feldspateinsprenglinge in Trachyten und Phonolithen durchführen lassen. Die Häufigkeit von hochblasigen Gesteinen - überwiegend basaltischen Lapillisteinen - bis in Wassertiefen größer 1000 m läßt auf einen hohen Volatilengehalt der Magmen schließen. Dies bedingt eine niedrige Dichte und große Instabilität der Vulkangebäude und erfordert eine Neukalibrierung des Blasengeobarometers für submarine vulkanische Gesteine zur Bestimmung der Eruptionstiefe. Die detailliert untersuchten submarinen Rücken südlich von La Palma und El Hierro, ungefähr 3-5 km breit und bis zu 40 km lang, sind von zahlreichen Seamounts bedeckt und stellen vulkanische Riftzonen dar. Ihre überwiegend NNE-SSW und NW-SE orientierten vulkanischen Lineamente ähneln denen auf den Inseln und spiegeln möglicherweise das lithosphärische Spannungsfeld wider. Die vulkanischen Gesteine auf den submarinen Rücken sind ausweislich ihrer Frische sehr jung. Die spektakulären Bomben aus intermediären Vulkaniten des prominenten Vulkans Hijo de Tenerife zwischen Tenerife und Gran Canaria deuten andauernde vulkanische Tätigkeit an. Die bis in Flachwasserbereiche von < 600 m gedredgten Gesteine sind ausnahmslos submarin eruptiert, so daß eine Absenkung der Inseln maximal wenige 100 m betragen haben kann und nicht 2500 m, wie für Tenerife postuliert. Durch die bathymetrische Kartierung mittels HYDROSWEEP wurden zahlreiche Seamounts entdeckt, Hinweis auf intensive magmatische Aktivität im Grenzbereich kontinentale-ozeanische Lithosphäre (leaky lithosphere boundary). Im Süden von El Hierro wurde eine Schuttlawinenablagerung von 30 km$^2$ Ausdehnung bathymetrisch kartiert, und vermutlich pliozäne (Roque Nublo) Schuttlawinenablagerungen wurden zwischen Gran Canaria und Fuerteventura gedredgt. Die bathymetrische Detailkartierung kombiniert mit vorhandenen Daten wird die Grundlage für eine bathymetrische Karte des gesamten Kanarenarchipels darstellen, wichtige Planungsgrundlage für weitere geologische und geophysikalische Arbeiten in diesen Gebiet.

Abschnitt 43/2 untersuchte im Rahmen des EU-Projektes OMEX II (Ocean Margin Exchange programme) den Partikeltransport vom schmalen Schelf vor der iberischen Halbinsel auf den Kontinentalhang. Der spezielle Anlass dieser Fahrt war, die Prozesse des bodennahen Partikeltransportes, der Sedimentation, die hydrographischen Randbedingungen und den Austausch von Biogasen speziell in der Wintersituation zu quantifizieren, um sie mit entsprechenden anderen Jahreszeiten und mit anderen Schelf-Kontinentalhang-Situationen vergleichen zu können. Trotz schlechter Wetterbedingungen konnten die meisten Daten erfolgreich gewonnen werden. Herausragende Ergebnisse sind die Befunde im südlich gelegenen Nazaré Canyon, die belegen, dass Canyons den Schelfexport fokussieren und für einen schnellen Transport vom Schelf bis in die Tiefsee sorgen.

## 1 Research Objectives

During Leg M43/1 (Project DECOS, Destruction and Construction of Seamounts) submarine volcanoes on the flanks of the Canary Islands, especially their submarine rift systems and isolated cones and seamounts within and south of the Canary Island Archipelago, were sampled by dredging and mapped by swath bathymetry and a subbottom profiling system (Fig. 1). The goal of the cruise was to develop criteria to distinguish different types of seamounts and submarine flank volcanoes by their structure, general lithology, composition, age and therefore their origin. We wanted to reconstruct the development of submarine volcanoes depending on the composition of the magma, eruption rate and water depth. Active magmatic degassing was studied by taking reconnaissance water samples. A second aim of the cruise was to document major debris avalanche and debris flow deposits in more detail that resulted from the failure of subaerial and submarine flanks of some island volcanoes. With these data we hope to contribute to a better understanding of the evolution of the magma sources and volcanism in the boundary area between the oceanic and continental lithosphere off Northwest Africa.

Leg M 43/2 served the multidisciplinary joint project of the European Union OMEX II (Ocean Margin Exchange; period: 1997-2000), in which 40 institutes participate. During the first application phase, research was focused on the region between Meriadzek Terrace and Porcupine Sea-Bight, whereby benthic work concentrated on a transect over Goban Spur (Celtic Sea), an example for a broad shelf. During phase II the five sub-projects focused their research on the continental slope between northern Spain to Lisbon as an example for a very narrow shelf, which is affected by upwelling processes. The major aims were:

(1) Assessment of the physically controlled advective and diffusive transport processes at different shelf edges to elaborate a numerical 3-D model.

(2) Quantification of biologically influenced vertical transport processes in along -and cross-slope direction, which result in the material exchange at continental slopes. Also in this context, a numerical model to describe processes at continental slopes has to be elaborated.

(3) Characterisation and balancing of bio-geochemical processes, which are relevant for material fluxes of carbon, nutrients and bio-reactive elements.

(4) Analysis of transport, sedimentation, accumulation as well as deposition of particles under different oceanographic conditions. Characterisation of the bottom nepheloid layer at the European continental slope. Studies of the importance of benthos communities for the carbon flux into the sediment.

5) Quantification and modelling of the exchange of carbon and biogas through the water-air-boundary layer at the continental slope.

The specific aim of this leg was to determine physical conditions and biogeochemical fluxes during the winter season.

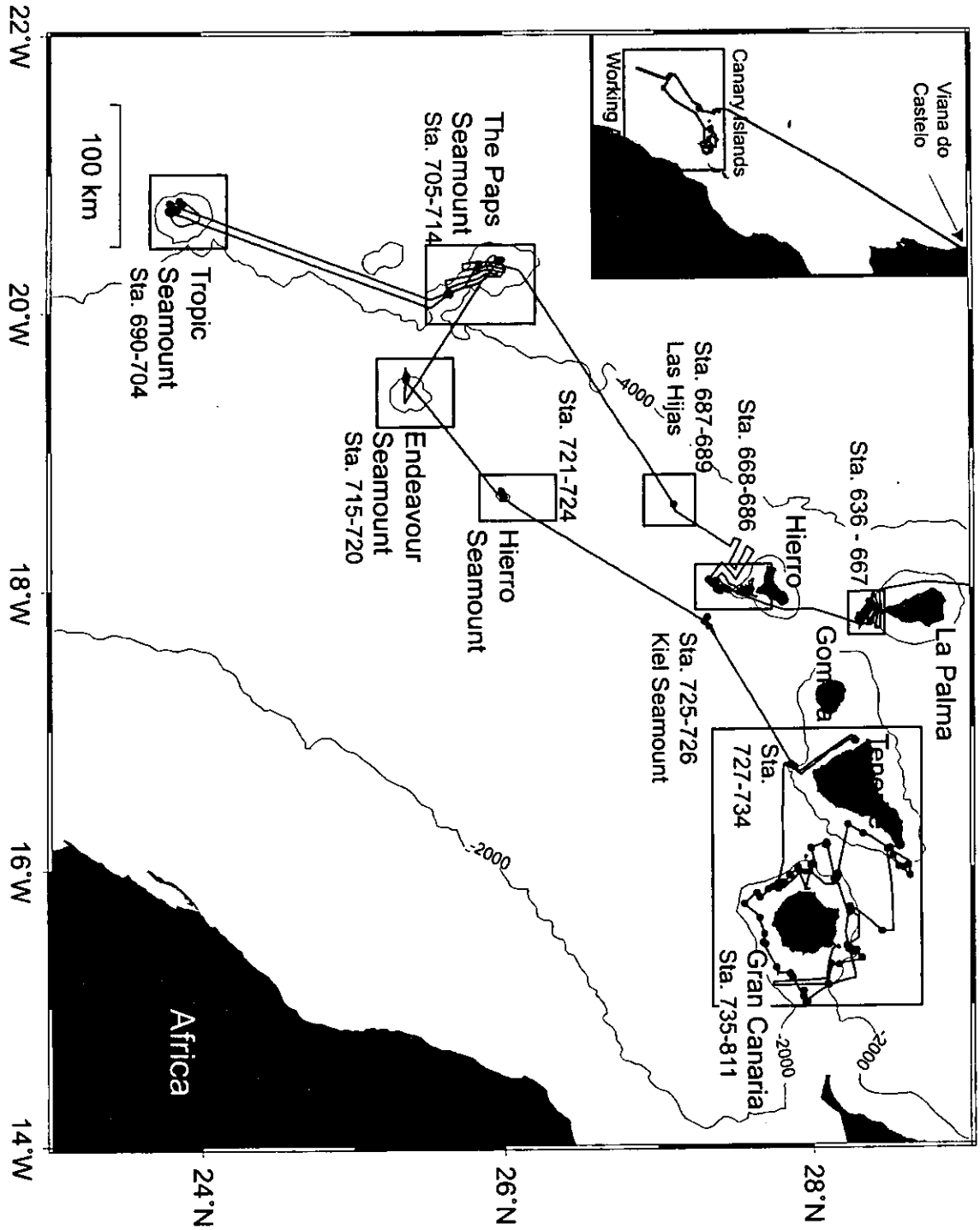


**Figure 1:** Overview map showing the ship tracks of METEOR cruise M43/1 and the main study areas within and south of the Canary Island Archipelago. Also marked by squares are the more detailed maps of individual target areas.

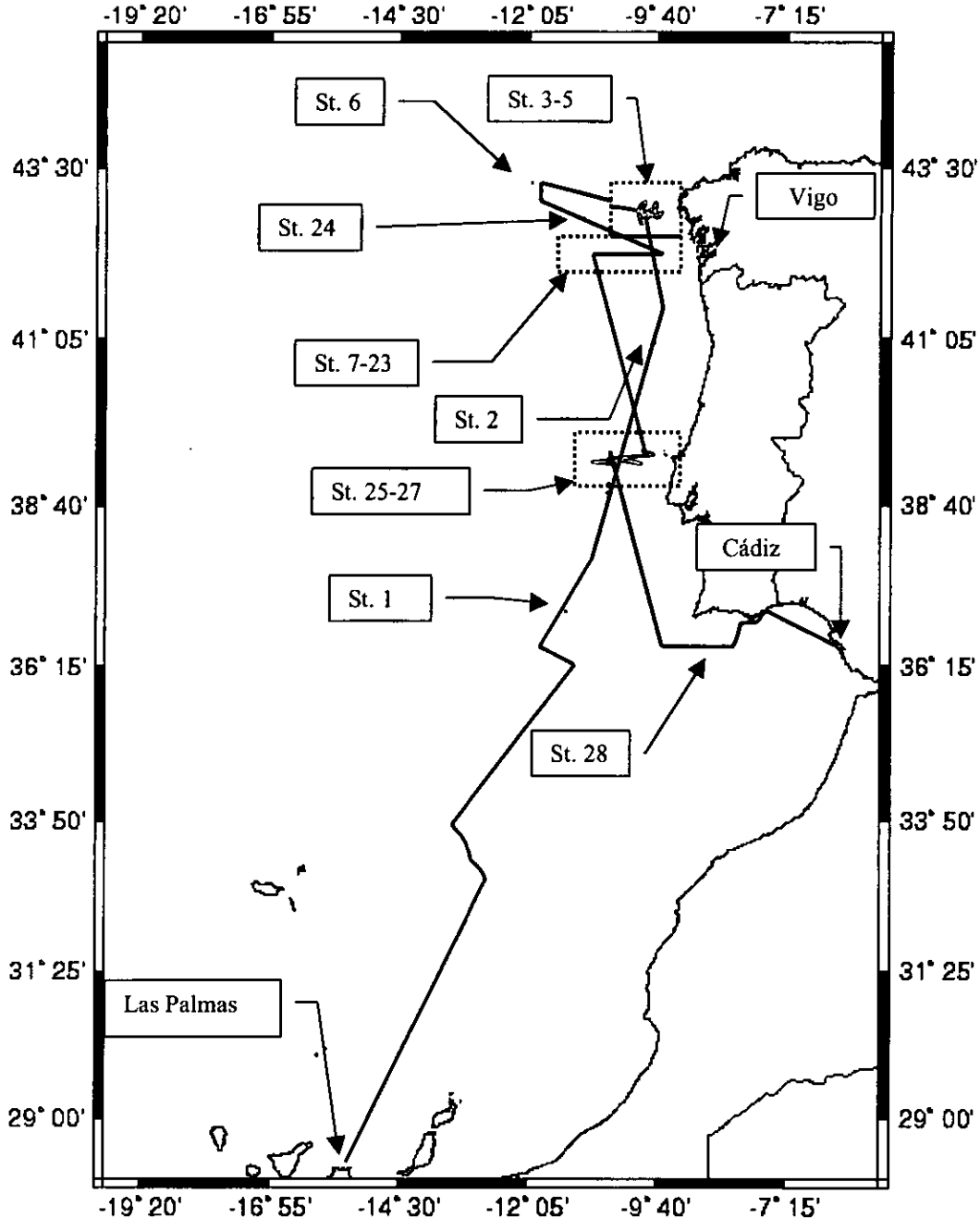


**Figure 2:** Cruise track M43/2.

**Table 1:** Legs and chief scientists of METEOR cruise no. 43

| **Leg M43/1** | **Leg M43/2** |
|---|---|
| 25. November 1999 - 23. December 1999 | 28. December - 14. January 1999 |
| Viana do Castello - Las Palmas | Las Palmas - Malaga Cadiz |
| Chief Scientist: Prof. Dr. H.-U. Schmincke | Chief Scientist: Prof. Dr. G. Graf |
| **Coordination**: Prof. Dr. Hans-Ulrich Schmincke | |
| **Master (RV METEOR)**: Captain M. Kull | |

## 2 Participants

**Table 2:** Participants of METEOR cruise no. 43

Leg M43/1

| Name | Specialty | Institute |
|---|---|---|
| Schmincke, Hans-Ulrich (Chief Scientist) | Volcanology | GEOMAR |
| Abratis, Michael, Dr. | Geochemistry | GEOMAR |
| Bassek, Dieter, Technician | Meteorology | DWD |
| Bayon, Germain, M. Sc. Geology | Geochemistry | SOC |
| Burri, Thomas, Student | Geology | UBE |
| Gurenko, Andrey, Dr. | Petrology | GEOMAR |
| Halmer, Martina, Dipl. Geol. | Volcanology | GEOMAR |
| Hansteen, Thor, Dr. | Petrology | GEOMAR |
| Hendry, Morag, B.Sc.(Hons.) | Geology | UCD |
| Hippler, Dorothee, Student | Geology | UF |
| Jacobs, Birgit, Dipl. Geophys. | Geophysics | IfG |
| Krastel, Sebastian, Dr. | Geophysics | GEOMAR |
| Leverty, Karl, B.Sc. | Geology | TCD |
| Lipka, Ulrike, Student | Geology | UF |
| Mata, Joao, Ph.D | Geochemistry | ULI |
| Meisel, Sören, Student | Geology | UJ |
| Öhmke, Holger, Technician | Technician | RASL |
| Pautlitz, Dirk, Student | Geophysics | IfG |
| Sachs, Peter, Dr. | Mineralogy | GEOMAR |
| Schimanski, Alex, Dipl. Geol. | Geology | IfG |
| Schmidt, Ralf, Dipl. Geol. | Volcanology | GEOMAR |
| Stroncik-Treue, Nicole, Dipl. Geol. | Geochemistry | GEOMAR |
| Strüfing, Reinhard, Dipl. Met. | Meteorology | DWD |
| Sumita, Mari, Dr. | Volcanology | GEOMAR |
| Troll, Valentin, Dipl. Geol. | Volcanology | GEOMAR |
| Urbanski, Nico, Dipl. Geol. | Volcanology | GEOMAR |
| Vespermann, Dirk, Dipl. Geol. | Volcanology | GEOMAR |
| Wienecke, Martin, Dr. | Geochemistry | IfG |

**Table 2:** continued

Leg M43/2

| Name | Speciality | Institute |
|---|---|---|
| Graf, Gerhard | Chief scientist | UR |
| Behr, Hein Dieter | Meteorology | DWD |
| Blohm-Sievers, Elke | Microbiology | MPI |
| Borges, Alberto | Geochemistry | UL |
| Bouma, Hilda | Benthosbiology | NIOO |
| Clement, Sian | Oceanograghy | UNWB |
| Franke, Uli | Benthosbiology | UR |
| Friis, Karsten | Geochemistry | IfM - Kiel |
| Garcia, Carla | Geology | UCTRA |
| Heeschen, Katja | Geochemistry | GEOMAR |
| Joao Luis da Silva Curdia | Benthosbiology | UCTRA |
| Kähler, Anja | Benthosbiology | GEOMAR |
| Karpen, Volker | Benthosbiology | GEOMAR |
| Keir, Robin | Geochemistry | GEOMAR |
| Lavaleye, Marc | Benthosbiology | NIOZ |
| Lowry, Roy | Data mangment | BODC |
| Moodley, Leon | Benthosbiology | NIOO |
| Nachtigall, Kerstin | Planktology | IfM - Kiel |
| Ochsenhirt, Wolf-Dieter | Meteorology | DWD |
| Peine, Florian | Benthosbiology | UR |
| Peinert, Rolf | Planktology | IfM - Kiel |
| Philip, Eva | Benthosbiology | GEOMAR |
| Pielenz, Holger | Benthosbiology | UR |
| Rehder, Gregor | Geochemistry | GEOMAR |
| Schmidt, Sabine | Geochemistry | UCTRA |
| Spyres, Georgina | Geochemistry | PML |
| Thomsen, Laurenz | Benthosbiology | GEOMAR |
| Torres, Ricardo | Oceanograghy | UNWB |
| Witzel, Karl-Paul | Microbiology | MPI |

**Table 3:** Participating Institutions

| | |
|---|---|
| BODC | Bidston Observatory, POL-CCMS<br>Birkenhead, Merseyside L43 7RA, UK |
| DWD | Deutscher Wetterdienst, Geschäftsfeld Seeschiffahrt<br>Bernhard-Nocht-Str. 76, D-20359 Hamburg, Germany |
| GEOMAR | GEOMAR Forschungszentrum für marine Geowissenschaften<br>Wischhofstr. 1-3, D-24148 Kiel, Germany |
| IfG | Institut für Geowissenschaften der Universität Kiel<br>Olshausenstraße 40, D-24118 Kiel, Germany |
| IfM | Institut für Meereskunde an der Universität Kiel<br>Düsternbrooker Weg 20, D-24105 Kiel, Germany |
| MPI | Max-Plank-Institut für Limnologie<br>August-Thienemann-Str. 2, D-24306 Plön, Germany |
| NIOO | Netherlands Institute of Ecology<br>Center for Estuarine and Coastal Ecology (CEMO)<br>Korringaweg 7, 4401 NT Yerseke, The Netherlands |
| NIOZ | Netherlands Institute of Sea Resaerch<br>Postbox 59, Den Burg (Texel) 1790 AB, The Netherlands |
| PML | Plymouth Marine Laboratory, PML-CCMS<br>West Hoe, Plymouth PL1 3DH, UK |
| RASL | Röntgen Analytik Service Dr. Frank Lechtenberg,<br>Katenkoppel 12, D-25524 Itzehoe, Germany |
| SOC | Southampton Oceanography Centre<br>European Way, Empress Dock, Southampton SO 14 3ZH, UK |
| TCD | Trinity College, Dep. of Geology<br>Dublin 2, Ireland |
| UBE | Mineralogisch-Petrologisches Institut der Universität Bern<br>Baltzerstraße 1, CH-3012 Bern, Switzerland |
| UCD | Cardiff University, Department of Earth Science<br>PO Box 914, Main Building, Park Place, Cardiff CF1 3YE, UK |
| UCTRA | Universidade do Algarve<br>P- 8000 Faro, Portugal |
| UF | Geologisches Institut der Albert-Ludwigs Universität Freiburg<br>Albertstraße 23b, D-79104 Freiburg, Germany |
| UJ | Friedrich-Schiller Universität Jena, Institut für Geowissenschaften<br>Burgweg 11, D-07743 Jena, Germany |

**Table 3:** continued

| | |
|---|---|
| UL | Univ. Liege<br>B-4000 Sart Tilman, Belgium |
| ULI | Universidade de Lisboa, Departamento de Geologia<br>Faculdade de Ciencias, Campo Grande C2-5° Piso, 1600 Lisboa, Portugal |
| UNWB | School of Ocean Sciences, Univ. Bangor<br>Menai Bridge, Gwynedd LL 59 5EY, UK |
| UR | Universität Rostock, Meeresbiologie<br>Freiligrathstrasse 7/8, D-18055 Rostock, Germany |

# 3 Research Program

## 3.1 Leg M43/1

The goal of METEOR Cruise M43/1 was a detailed survey by bathymetric mapping and dredging of the submarine ridges south of La Palma and El Hierro, the Saharan Seamounts and the submarine flanks around Gran Canaria and Tenerife to obtain a better understanding of the destructive and constructive processes during the evolution of large intraplate volcanic edifices in the sea (Fig. 1).

*Constructive processes*
Volcanic activity on oceanic islands occurs synchronously on land and on the submarine flanks. The subaerial part of oceanic islands generally makes up less than 5% of the total volume. Our understanding of the growth processes and growth rates of volcanic islands therefore depends critically on the interpretation of bathymetric data, sidescan studies, submersible studies and sampling by dredging.

Several questions are relevant in the framework of the M43/1 project. Seamounts to be studied could represent:

- very young intraplate volcanoes in the submarine eruptive stage, perhaps precursors to an island;
- older submarine volcanoes which never reached the island stage;
- subsided and eroded former volcanic islands.

Eruptions in the recent past probably occurred both along the submarine southern extension of the rift zones of La Palma and El Hierro but possibly also at the submarine slopes of Tenerife and Gran Canaria. The most useful geobarometers to determine the initial water depth of eruption are the vesicularity of hyaloclastite particles and the sulfur content of fresh glasses. Types and mechanisms of the submarine eruptions, the composition and age of the lavas and hyaloclastites and therefore their petrologic significance are unknown and one of the aims of this research project.

*Destructive processes*
Oceanic islands become reduced in height and subaerial volume by slow erosive and alteration processes, by catastrophic failure and by sinking into the lithosphere. Large volcanoes are known to commonly experience flank failure, a process also characteristic for volcanic islands. Based on morphology and degree of dislocation, submarine landslides can be grouped into two major types: 1) slumps and 2) debris avalanches. Slumps are slow rotary movements of largely undeformed masses along discrete shear planes. In contrast, debris avalanches are fast long-runout mass movements in which fragmentation has reduced the landslide mass to individual blocks during sudden, catastrophic failures (MOORE ET AL., 1989; 1994). Submarine slumps and debris avalanches appear to be more common in the Canaries than in the Hawaiian Islands and also occur during late stages in the volcanic evolution of an island.

*Evolution of magmas, magma sources and the lithosphere-volcano system*
The spectrum of chemical and mineralogical compositions of volcanic rocks from oceanic islands raises several questions:
How many different mantle sources with contrasting geodynamic significance (plume, asthenosphere, oceanic and continental lithosphere) can be distinguished from each other? How strongly are magmas differentiated and by what processes?

The 3000 km long belt of islands and seamounts along the north-western African continental margin between 20°N and 35°N, here referred to as the East Atlantic Intraplate Volcanic Prov-

ince, extends from the Madeira Island Group through the Canary Islands to the Cape Verde Islands, and therefore does not fit easily with the model of relatively small ocean island hot spots. The large number of islands and seamounts, their irregular distribution and the long evolution of volcanism on some of the islands (more than 15 million years for islands such as Porto Santo, Fuerteventura, Lanzarote, Gran Canaria and possibly La Gomera), as well as their close proximity to the coast of Africa are reasons to believe that their origin is due to rising mantle diapirs as well as the boundary between continental and oceanic lithosphere (SCHMINCKE, 1982).

This East Atlantic intraplate volcanic province represents an end-member of hot spot provinces in several aspects: the large number of islands and seamounts and their long evolution of volcanism would require a large number of long-lived mantle plumes of different sizes. The relationship between large fracture zones and the position and dynamic evolution of the Canaries advocated by some authors is controversial. Fracture zones on the African mainland such as the South Atlas Fault extension to the Canary Islands as well as the influence of fracture zones formed at the Mid-Atlantic Ridge were called on to explain the position and evolution of the Canary Islands.

The regional geodynamic relationships between the Canary Islands and the group of seamounts in the south as well as the Las Hijas Seamounts south-west of El Hierro found by us in 1997 is unknown. Apart from the general decrease in age of the shield phases of the Canary Islands from east to west, there seems to be no systematic age distribution of the volcanism in the East Atlantic. Volcanoes and seamounts running NNE-SSW, however, seem to be aligned sub-parallel to the African coast and therefore to the transitional area between continental and oceanic lithosphere. One aim of the present research project is to help clarify this large-scale geodynamic problem using the composition and age of the rocks.

The regional magma development shall be mapped by analyzing rocks from a large area to understand the composition and lateral extent of melting domains in the mantle. Central is the question if the development of the Canary Islands can be best understood in terms of hot spots or if other mechanisms, configurations of melting anomalies or old fracture systems are more important for the development of volcanism and magmatism in the entire volcanic belt off northwest Africa.

By analyzing the lithology and composition of dredged volcanic rocks we also hope to better understand the volcanic and magmatic evolution of seamounts which may or may not have experienced long-term systematic changes in magma production rates and magma composition, the latter of which is observed in the subaerial part of many volcanic islands.

The dredged lavas and hyaloclastites of submarine volcanoes at depths between 500 m and 2500 m bsl on the flanks of Tenerife, Gran Canaria, La Palma and El Hierro shall help (1) to determine the boundary between submarine and subaerial development, which should help clarifying the rate by which islands and seamounts subside due to the load on the lithosphere; (2) to determine the main eruptive centers, magma composition and therefore magma sources below the islands; (3) to calibrate geobarometers of alkalic volatile-rich magma depending on the depth of eruption.

## 3.2 Leg M43/2

*Carbon remineralisation by the benthic community*

Remineralisation of organic matter takes place already during carbon transport processes occurring in the water column. Parameterisation of the subsequent processes acting in the benthal will be required to estimate the fraction of carbon that is recycled back into the ocean versus that which is permanently buried. A better understanding of the biological, chemical and physical processes and the measurement of the corresponding rates are required for a balance of carbon flux through the sediment.

Measurements of benthic respiration rates, biomass production and activity are necessary to estimate the role of benthic organisms for the carbon flux through the sediment. Recent results from the temperate north-east Atlantic demonstrated a strong seasonality in benthic biomass production, respiration and activity rates which were coupled with sedimentation events. The major part of benthic carbon consumption goes into respiration, in the range of 80-95% of total benthic carbon consumption.

The main objective of the benthic program is the quantification of the biologically mediated carbon flux through the sediment by following the benthic reaction (remineralisation, burial rates) toward sedimentation pulses. The canyon areas will be studied in detail.
Additionally, a comparative study on the coral *Lophelia* living on the Iberian slope and on the Galicia Bank will be carried out. While the first population is potentially under the influence of the production in the upwelling zone, the one on Galicia Bank lives under more oceanic, on presumably nutrient poor, conditions. Comparisons of growth rates and elemental tracers in the calcium matrix, for instance, may shed light if there is an effect of the nearby continent.

*Processes within the bottom boundary layer*
At continental margins bottom nepheloid layers are commonly found. Lateral particle fluxes in the benthic boundary layer [BBL] far exceed the vertical fluxes from the euphotic zone. The fluxes are dominated by fast sinking particles whereas the mass of particles consists of fine slow sinking particles.

Aim of the project is the investigation of the following processes: particle transport within internal boundary layers, especially in canyons and gullies along the shelf edge, sedimentation, accumulation and mass fluxes of particulate matter. With the help of CTD-water samplers and a transmissiometer, samples shall be taken in the deep sea and in the canyon area at the continental margin. With the help of the BIOPROBE bottom water sampler, flow velocity and light transmission will be determined and water samples at 5,10, 20 and 40 cm height above the sea floor will be taken. A particle camera will take video pictures of aggregates. Gravity cores will be used to determine sediment accumulation rates. Benthic flow simulation chambers will give information on sediment stability and particle behaviour. Thorium analyses will be done and sediment transport studies will be carried out along the shelf edge.

*Microbial studies of aggregate dynamics in the benthic boundary layer*
The focus of this group will be to study microbial activities and the genetic structure of the microbial communities in the water column, in the benthic boundary layer and the surface sediments on a transect across the continental margin of the OMEX area. These results will give information on the origin of particles in the BBL. Measurements of the microbial activities will address the role of bacteria in the dynamics of organic carbon across the continental margin.

To elucidate the genetic composition of the microbial communities PCR will be used with DNA-extracts from water and sediment samples to retrieve sequences of the genes coding for either 16S rRNA or the functional enzyme ammonia-monooxygenase of ammonia-oxidising bacteria. Sequence-specific electrophoresis of the PCR-products will give an overview of the species-composition within this group of bacteria. Cloning and sequencing of the PCR-products is used for identification and phylogenetic classification by DGGE. Samples will be retrieved from Niskin bottles, the bottom water sampler and the multiple corer.

*Processes in the water column*
The goal of the OMEX project is to determine spatial and temporal variability in the exchange of particulate and dissolved organic matter at the continental margin and thereby the role of the margins in regional elemental cycling and carbon sequestration. In this second phase, emphasis has shifted from the Goban Spur, with a gradual, wide slope and weak upwelling, to the Iberian

Margin with its steep slope and strong periodic up- and downwelling cycles. As part of a multidisciplinary joint approach the Institut für Meereskunde has deployed two moorings equipped with sediment traps, in situ pumps and current meters at the mid- and outer slope along a transect at 42°38'N, in water depths of 1500 m and 2230 m. During the current period of deployment (March 1998 - Jan 1999), a number of interesting features occurred at the Iberian Margin, the imprint of which we will record in the traps by use of bulk and marker variables and radionuclide analyses of samples. We thus hope to link processes occurring at the sea surface, as seen by remote sensing and recorded on OMEX cruises, to temporal and spatial patterns of vertical and lateral particle flux. Using samples of suspended particulate matter over this 9- month deployment period collected by the newly developed in situ pumps, we will gain insights in the qualitative and quantitative patterns of SPM flux and the role of scavenging that leads to settling. Moorings IM2 and IM3 at positions 42°38.5'N, 9°42.3'W and 42°37.5'N, 10°01.5'W respectively will be recovered yielding 100 sediment trap samples, 60 in situ pump samples and 9 months of current meter data from 5 RCMs. The moorings will not be redeployed. Gradients in suspended particulate matter along- and across the slope will be determined by water column sampling and in situ pump deployments. Special emphasis will be given to sampling of the surface, intermediate and benthic nepheloid layers that will be determined using a transmissiometer and nephelometer attached to the CTD. Bulk and marker variables will be determined in these samples and used to determine gradients in these properties around the mooring positions. Additionally ADCP measurements will give information on the surface current regime.

*Distribution of Surface $pCO_2$, $\delta^{13}C$, $\Sigma CO_2$, $CH_4$, and Radiocarbon*

Workpackage II of the OMEX Project is concerned with mesoscale variability of carbon and related fluxes in the shelf and slope waters of the Iberian Margin. Two of the objectives within this part of OMEX are (a) to trace principal water masses and their sources and (b) to assess the net air-sea exchange flux of $CO_2$ as well as the penetration of anthropogenic $CO_2$ in the region. In connection with the latter objective, the partial pressure of $CO_2$ in surface water as well as in the air will be surveyed continuously underway using two different equilibrator systems (intercalibration). The vertical distribution of the $^{13}C/^{12}C$ ratio in dissolved inorganic carbon will be determined on samples collected from the CTD casts in the shorebased Leibniz Laboratory at the University of Kiel. Since anthropogenic $CO_2$ produced by burning of fuel fuels carries a low $^{13}C/^{12}C$ ratio, these measurements provide an indication of the penetration of this $CO_2$ into the water column. The measurements also give an indication of the nature of the seasonal cycle of the biological pump of carbon in the area, which is dependent on upwelling and the net production of carbon.

The vertical and horizontal distribution of methane provides a contribution to the first objective above, the tracing of water masses. In relatively young deep waters, it appears that methane is oxidised on about a 50-year time scale. The proximity of possible sediment sources on the continental slope as well as the presence of water masses with ages less than 100 years in the upper 2000 meters in this region indicates that methane may provide a useful supplement to the information that one obtains from salinity, temperature and dissolved oxygen.

The vertical distribution of radiocarbon will be determined on samples collected from one or more deep CTD stations. This will also be valuable in connection with the tracing of water masses. By comparison to previous determinations 17 years ago, it should be possible to observe the temporal change in the radiocarbon distribution due to uptake of bomb-produced $^{14}C$.

*Determination of the net total radiation at sea*

The knowledge of the spatial and temporal distribution of the net total radiation and its components at the sea-surface is important for numerous meteorological and oceanographic investigations. On the cruise of the vessel the following radiation components will be recorded: global

solar radiation and atmospheric radiation. The other components closing the radiation balance equation - reflected solar radiation and terrestrial surface radiation - will be computed with the aid of numerical models tested in former cruises in the Atlantic Ocean. Further, direct solar radiation, sunshine duration, and UV-B global radiation will be measured

## 4 Narrative of the Cruise

### 4.1 Leg M43/1

The scientific crew boarded FS METEOR in Viana do Castelo on November 23rd and 24th, 1998. The scientific party included one scientist each from Berne University, Dublin University, Lisbon University, Southampton Oceanography Centre, Cardiff University, and Jena University, 2 scientists from Freiburg University, 2 meteorologists from the German Sea Weather Office, 4 scientists from Kiel University and 14 colleagues from GEOMAR Research Center. The ship departed from Viana do Castelo on November 25th 1998, 10:00 o'clock. After three days of transit, which were used for scientific meetings and set-up of the equipment, work began on November 28th at 14:42 by employing the systems PARASOUND and HYDROSWEEP north of La Palma.

Beginning on the morning of November 29th and ending December 2nd, 35 stations were dredged along the South La Palma Ridge, interrupted by some additional HYDROSWEEP mapping, to delineate the morphology of the ridge in detail for better placing dredge stations. A rich suite of rocks was dredged on the northern part of the ridge which extends to about 1000 m below sea level. Dredging on the apparently older seamounts on the southern half of the ridge, which are generally more strongly manganese-encrusted and covered by calcareous crusts, was less successful.

The 40 km long South El Hierro Ridge southeast of the island was mapped BY HYDROSWEEP and dredged successfully in 19 stations between December 2nd and 5th, with dredging starting on December 3rd at 08:00. Very fresh, glassy basalts were recovered along the proximal ridge section. Pumiceous alkali feldspar-rich trachytic rocks were dredged in the central part of the ridge. The seafloor south of El Hierro was mapped on our way to Las Hijas Seamounts by HYDROSWEEP and PARASOUND on December 5th in order to delineate a large debris avalanche fan in more detail.

Las Hijas Seamount group was reached on December 5th, dredged successfully at 3 stations, recovering large amounts of trachytic rocks. Paps Seamount was mapped in detail by HYDROSWEEP on December 6th. Tropic Seamount, the southernmost point of the cruise, was reached December 7th, dredged successfully at 15 stations (conglomerates, basalts, trachytes and volcaniclastic rocks) and left December 8th at 21:00. Paps Seamount was reached December 9th in the morning and was sampled at 10 stations with moderate results until December 10th 17:00. Endeavour Seamount was reached December 11th, dredged successfully at 6 stations and left December 11th at 19:00. El Hierro Seamount was reached December 11th at 21:00 and dredged at 4 stations until December 12th 6:00. An unnamed seamount - here called Kiel Seamount - 45 km southeast of the island of El Hierro was reached December 12th at 15:00 and was dredged at two stations.

Work in the third major region began when the southeastern point of Tenerife was reached December 13th. Dredging at the southwest flank northwest of Los Gigantes produced some basalt. Definite submarine lava was dredged following HYDROSWEEP mapping along the coast of Tenerife near Punta de la Rasca during the night December 13th to 14th. Following another stretch of HYDROSWEEP profiling between Tenerife and Gran Canaria, dredging along the southwestern flank of Gran Canaria began December 14th at 11:30. Most remarkably, this and the following dredges produced submarine rhyolitic and basaltic lavas corresponding exactly to the Güigüi, Horgazales and Lower Mogán formations on land, except that the flows dredged had been emplaced under water. Thus important evidence that the island has remained relatively stable with respect to sea level since the initial shield phase some 15 million years ago was gathered at the beginning of dredging the flanks of Gran Canaria. Dredging continued along several profiles along the southwest slope until December 15th. Following HYDROSWEEP profiling and a brief stop near Barranco de Güigüi, the wild part of Gran Canaria where all the Miocene formations are exposed, dredging some 12 km west of Güigüi in the evening of December

15th recovered remarkable glassy lava or welded ignimbrite. The flows appear to have entered the ocean possibly a few km offshore the present coastline because they occur at some 100 m asl along the coast and became quenched and contorted under water.

El Hijo de Tenerife Seamount, a conical volcano some 600 m high, discovered during METEOR Cruise M24 in April 1993 (SCHMINCKE AND RIHM, 1994) was dredged on December 16th in the hope to sample a young volcano on the lower eastern submarine slopes of Tenerife, an area of frequent albeit small earthquakes. The catch was spectacular with large amounts of bomb-like poorly vesicular but extremely fresh mafic phonolite with phenocrysts of amphibole and mica and many angular rock fragment inclusions. Evidence is strong that many fragments were produced by explosive activity remarkably similar to phreatomagmatic eruptions on land. Basically a small Pico de Teide is here growing under the sea. Water samples were taken just above the top of the volcano at different water depths. Dredging along the steep northwest flank of Gran Canaria off Agaete produced ol-, cpx-phyric basalts similar to those dredged off the southern flanks, again compositionally resembling picritic lavas near Agaete.

On the afternoon of the 17th until the late afternoon of the 18th, cone-shaped morphological features and ridges on the eastern submarine flank of Tenerife were dredged as far north as the tip of Anaga Peninsula. Basaltic lapillistones, in some places containing abundant fresh sideromelane, are most common. Dense basalts were recovered in some dredges. Water samples were taken at ODP drill Site 954, 40 km N of Gran Canaria where pore solutions and effervescent $CO_2$ in the drill cores had indicated young volcanism (SCHMINCKE AND SUMITA, 1998). Dredging on the northern flank of Gran Canaria commenced early December 19th with fresh Miocene (?) shield basalts being recovered in several dredges. Dredging of a broad submarine ridge extending north of the coast near Arucas proved technically impossible because of abundant undersea cables crossing the area. Dredging of the prominent and wide submarine ridge off La Isleta, the northeastern peninsula of Gran Canaria, began before noon on December 19th, following a stretch of HYDROSWEEP mapping not covered in detail previously. Ol-, cpx-phyric basalts were recovered. Dredging continued until early afternoon of December 22 off the east and south coasts of Gran Canaria with variable success in water depths between 600 and 1500 m bsl. Highlights were the recovery of complex breccias most likely from the flanks of debris avalanche blocks of Pliocene age (Roque Nublo debris avalanche) due east of Gran Canaria, fresh glassy phonolite lava off the southeast coast, probably Miocene Fataga Formation lavas that entered the sea about 11 million years ago, and additional samples of Miocene glassy rhyolite lava off Barranco de Veneguera due south of the island. HYDROSWEEP mapping of previously uncovered areas west and north of Gran Canaria was carried out until the morning of December 23rd. The vessel entered the port of Las Palmas at 8:00 on 23.12.1998.

## 4.2 Leg M43/2

The cruise started on 28th December, 1998, at 10:45 am, in Las Palmas under perfect weather conditions and with all scientific equipment delivered in time. 29 scientists from 6 different nations (Germany, Belgium, France, The Netherlands, United Kingdom, Portugal) were on board, representing the OMEX II programme of the European Union. This programme of the EU aims to study fluxes across the ocean margin and processes along European shelf breaks facing the North Atlantic Ocean. The expected transit time to the northern Portuguese upwelling area was 3.5 days.

Due to deteriorating weather conditions, cruise speed had to be reduced already during the second day and finally we had to stop in order to wait for a heavy storm to pass the scheduled study site. On January 1st the first samples were taken with a CTD in the outflow of the Mediterranean water, where high methane concentrations were detected (Station 1). To follow the sur-

face currents to the North, 4 drifter buoys from the University of Bangor were deployed on 41° N, which were from there on continuously tracked by satellites. On January 3rd the main working transect off Vigo was reached but due to heavy seas, CTD casts were cancelled. Surface water was then sampled and current measurements were performed. The next day a long term sediment trap deployment was released and successfully recovered and thus one major aim of the cruise was achieved. Another mooring, which had been damaged by fishermen, could not be recovered. On January 6th METEOR reached the Galicia Bank and due again to increasingly bad weather conditions, it was not risked to release a Dutch mooring from the NIOZ institute, Texel. This deployment of artificial hard substrate for the study of deep-sea corals was still working as was indicated by a successful hydrophone contact and it was decided to recover this experiment in spring.

Within the next 5 days weather conditions improved and a full transect at 42° N including all water and sediment samplers could be covered (Stations 7 to 23). A total of 30 CTD casts and many sediment cores were carried out from the shelf down to a water depth of 2500 m. This transect was a success and provided the first winter data for this key area of the OMEX programme. During the following days another transect in the Nazaré Canyon was also sampled, in order to study both the distribution of particles in the lower water column and the benthic biomass and activity (Stations 25-27). With a detailed bathymetric map provided by the British colleagues it was possible to sample directly in the central conduit of the Canyon. This Canyon serves as modern conduit of organic matter and pollutants to the deep sea and will be of great interest for future work.

Although the cruise was relatively short and the weather often being bad, the scientific programme carried out was very successful and the whole OMEX community was very happy with the results. On our way back to Cadiz an additional CTD was taken for the study of the Mediterranean outflow and in support of another European project a PARASOUND and HYDROSWEEP profile was run off the city of Faro. On January 13, METEOR reached the port of Cadiz in the early evening and immediately entered a dry dock .

# 5 Preliminary Results

## 5.1 Leg M43/1 (Marine Geosciences)

(H.-U. Schmincke, S. Krastel, T. Hansteen, M. Sumita)

### 5.1.1 Hydroacoustic Systems

During cruise M43/1, the shipboard acoustical systems HYDROSWEEP and PARASOUND were used on a 24 hour schedule to record continuous high resolution bathymetric and sediment echosounding profiles. Data were collected in the areas dredged and also in many previously unmapped intervening areas.

#### 5.1.1.1 PARASOUND

*Method*

The sedimentechographic system PARASOUND of Krupp Atlas Elektronik can be used for penetrating the uppermost sediments to a maximum depth of 50 m below the seafloor. The system submits a primary frequency of 18.0 kHz which is superimposed by a second primary frequency between 21.5 kHz and 23.5 kHz resulting in a differential frequency between 3.5 kHz and 5.5 kHz. Due to the parametric pulse, the horizontal resolution is better than for classical 3.5 kHz echosounders. The opening angle of the transmitted beam is only 4°. The source signal is a sinusoidal wavelet with a duration of two periods. Digitizing and recording of the echosounding seismograms was done with the software package ParaDigMa (SPIESS, 1992). The system converts the analogue data to digital data and stores them on an external hard disk. The storage of the data to a hard disk and not to 9-track tapes was done on FS METEOR during this cruise for the first time. The seismograms were sampled at 40 kHz with a typical registration length of 266 ms for a depth window of 200 m. The pre-processed data were plotted online with a vertical depth scale of several hundred meters to eliminate frequent changes in window depth. The seismograms were filtered with a wide bandpass of 2.5-5.5 kHz. These plots provided a first impression of variation in sea floor morphology, sediment coverage and sediment patterns along the ship's track.

Occasionally the storage of the data was interrupted and it was not possible to start recording without a shutdown of the system and change of hard disk. Some data were lost during these periods. This problem could not be solved during the cruise.

*Preliminary Results*

Several different facies are visible on the PARASOUND records. First analysis of the PARASOUND data shows three main facies:

1. Very steep slopes of the islands and seamounts: These areas are characterized by a very rough relief with numerous canyons and gullies. Usually the slope is so steep that the signal is scattered away from the vessel and therefore no signals were recorded. In other cases the bottom echo is discontinuous due to the rough relief. No subbottom echoes can be identified indicating a hard and compact seafloor.
2. More gently dipping slopes of the islands and seamounts: At a greater distance off the coast and off the top of the seamounts, the bottom echo is becoming more continuous and some subbottom echoes are visible (Fig. 3a). The sediments are not well-stratified. Hyperbolas and overlapping echoes are still common in these areas. The input of material transported downslope is very high. Numerous canyons are cut into the seafloor. They were probably carved into the submarine flanks of the islands/seamounts by sedimentary mass flows which originated on land or further upslope. Some areas are affected by giant landslides (slumps and debris avalanches) such as the area south of El Hierro,

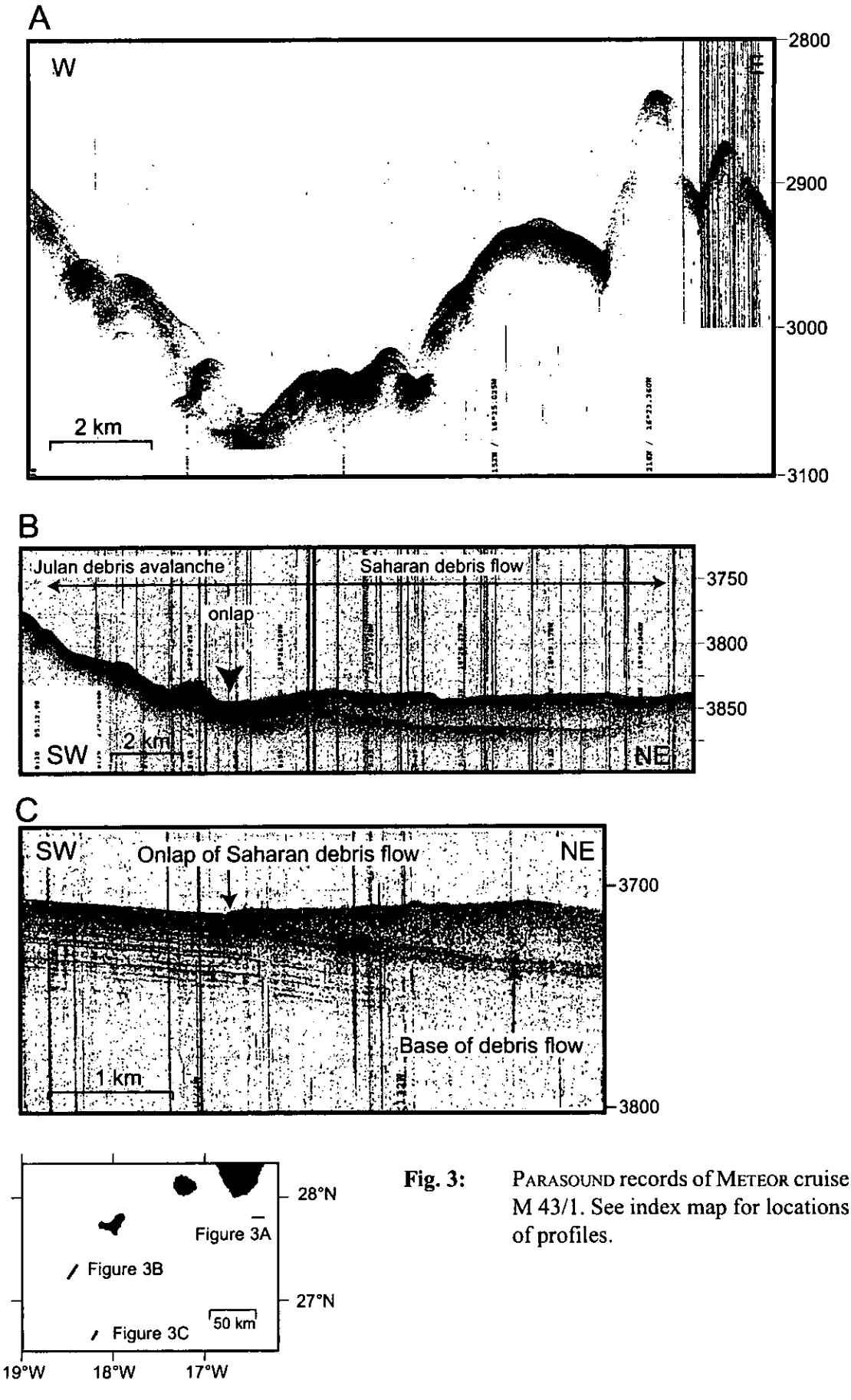


**Fig. 3:** PARASOUND records of METEOR cruise M 43/1. See index map for locations of profiles.

which is characterized by large debris-slide deposits. At a distance of 45 km off the coast of El Hierro, these deposits are overlain by the Saharan debris flow, which was generated on the west African continental margin (MASSON ET AL., 1992). The debris flow is clearly visible on the Parasound records (Figs. 3b, 3c).

3. Flat sedimentary basins: The sedimentary basins are characterized by a strong and continuous bottom echo. Several subbottom echoes run parallel to the seafloor (Fig. 3c). Some of the strong subbottom echoes may indicate volcaniclastic material with a high impedance contrast to the pelagic sediments. These reflectors probably correlate with high input of volcanic material due to redeposition or increased volcanic activity.

#### 5.1.1.2 HYDROSWEEP

The swath bathymetric system HYDROSWEEP of Krupp Atlas Elektronik is used for mapping the water depth. The seafloor is sampled by 59 beams of well known pre-defined angles. The total swath width is 90°, giving a coverage of 2 times the ocean depth. Data are stored on magnetic tapes.

Data processing on board was done with the HYDROMAP system. Contour-plots with a scale of 1:50,000 and 50 m contour-intervals were used for selecting suitable sites for dredging. Since bad weather conditions (especially wind and waves from the port side) causes problems with the system, the data processing of the multibeam echosounder often resulted in gaps. Results of the bathymetric mapping are discussed in Chapter 5.1.4.

### 5.1.2 Rock Sampling and Descriptions

#### 5.1.2.1 Methods

*Dredging*

Purpose: Sampling of rocks (parts of lava flows or loose blocks) occurring in either smooth-surfaced or topographically rough areas such as seamounts and volcanic ridges.

Principle: Steel teeth mounted on a metal frame tear off pieces of lava flows or incrustations or help collecting loose blocks as the dredge is towed along the sea floor. Samples are collected in a chain bag in the larger dredges, and at metal rails inside the smaller drum dredges. The main tools for the recovery of lavas, blocks and consolidated volcaniclastic and carbonate rocks were three types of dredges, including drum dredges and two types of chainbag-dredges with rectangular and oval iron frames (Fig. 4). The rectangular chainbag-dredge has sawteeth cut into the iron frame, whereas the tube- and oval chainbag dredges have welded or bolted teeth.

Wire length, water depth and wire tension measured by a calibrated tensiometer were displayed online via the ship's computer network. A separate analogue system was used to produce tensiometer-records on paper. Wire tension during operation varied between 0 and about 6 tons, with maximum values of about 8 tons. Dredging was carried out by first putting out the required cable length from the moving ship followed by dredge hauling with the ship held at a fixed position relative to the seafloor.

The chainbag dredges proved to be the better suited for dredging seamounts and island flanks because of the high abundance of smooth-surfaced carbonate and manganese crusts. Dredging was performed at a total of 177 stations (Table 4, also see chapter 7.1.1):

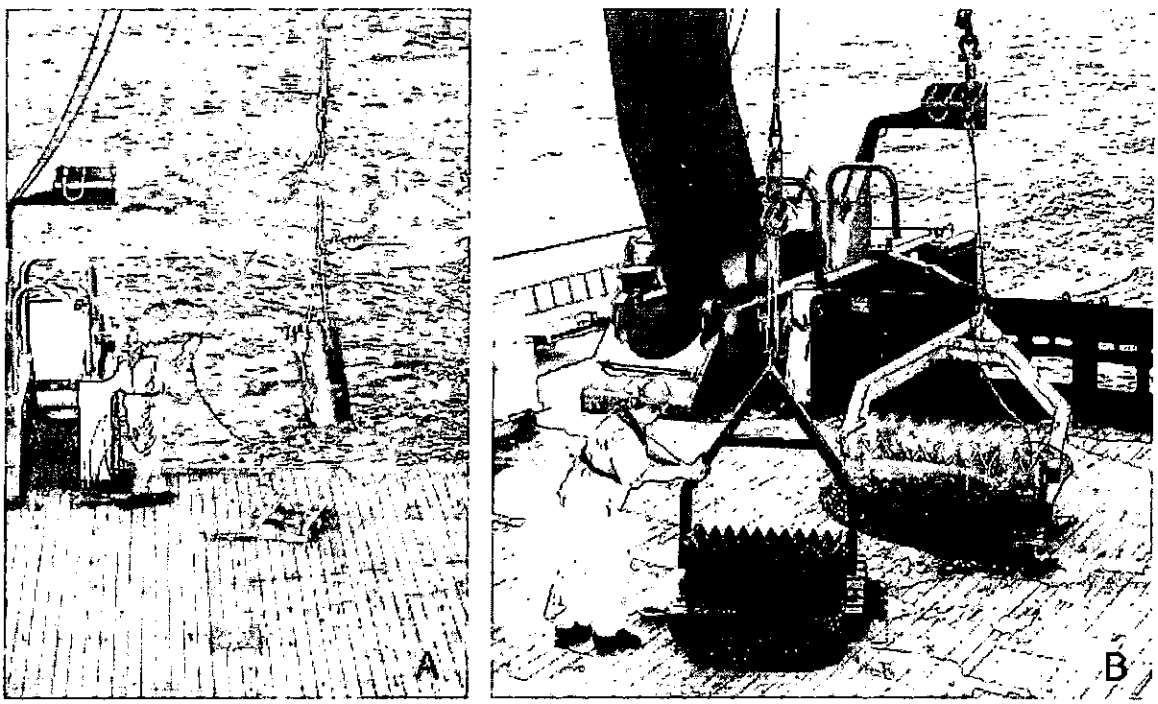


**Figure 4:** Photograph of the three main dredge types used on board: Drum dredge and 2 chain dredges of different design (see text for discussion).

*Thin section preparation*

Thin sections were produced on the vessel in a specially equipped laboratory. Rock slabs considered suitable for thin sections were cut, cleaned and dried followed by impregnation. Another period of drying was required after the impregnation prior to grinding and polishing one side of the rock slip until a smooth, even and flat surface was created. This flat side of the slip was then glued on to a standard microscope slide using an epoxy resin. The glue takes about 24 hours to harden properly before the rock slip can be cut a second time to a thickness of approximately 1 mm. Then the slip was ground on a rotating plate with grinding powder of various grain size. When the rock slip is about 0.05 mm it is becoming transparent and the finest grain size of grinding powder is applied in order to work the slip down to a thickness of 0.035 mm. At this stage, the grinding had to be done manually to guarantee constant thickness throughout the rock slip. Having reached the required thickness of 0.03-0.025 mm, a cover slip was fixed with Canada-balsam in order to protect the upper side of the rock slide. After a short period in open air to allow the Canada-balsam to solidify sufficiently, the thin section was ready for petrographic analysis.

*Preparation for geochemical analysis*

Solid rocks including good-quality glassy crusts and in some cases picked grains cleaned ultrasonically were cut into convenient pieces for crushing on-board, as a preparation for geochemical analyses. The cut samples were cleaned, dried, crushed, sieved, desalinated and powdered. Preparation procedures included:

1. Crushing using a jaw-crusher followed by removal of the smallest grain sizes by sieving.
2. Desalination of the crushed rocks through several passes of water washing, the last step of the procedure being filtering with ultrapure water.
3. Ball-milling the crushed and washed samples into fine powders suited for diverse geochemical analysis.

**Table 4:** List of dredged stations

| M43-1 | Date | Type of dredge | Time seafloor (UTC) | Latitude | Longitude | Water depth (m) | Number of samples | Rock type (NR*: No recovery) |
|---|---|---|---|---|---|---|---|---|
| ***1. South La Palma Ridge*** | | | | | | | | |
| 636 | 29.11.1998 | TD | 9:07 | 28° 26,1 N | 17° 51,3 W | 630 | | NR* |
| 637 | | TD | 11:47 | 28° 26,4 N | 17° 51,0 W | 498 | | NR* |
| 637b | | TD | 13:07 | 28° 26,5 N | 17° 51,1 W | 510 | | NR* |
| 637c | | TD | 13:59 | 28° 26,5 N | 17° 51,1 W | 472 | | NR* |
| 637d | | KD | 15:03 | 28° 26,5 N | 17° 51,1 W | 513 | | NR* |
| 638 | | TD | 16:36 | 28° 25,5 N | 17° 51,7 W | 924 | 18 | Basalt fragments and basaltic lapillistones |
| 639 | | TD | 18:21 | 28° 23,9 N | 17° 51,9 W | 1091 | 5 | Fresh basalt lava and lapillistones |
| 640 | | TD | 20:15 | 28° 23,0 N | 17° 52,6 W | 1681 | | NR* |
| 641 | | TD | 22:54 | 28° 21,7 N | 17° 54,3 W | 2735 | 1 | Hemipelagic sediment |
| 642 | 30.11.1998 | TD | 7:35 | 28° 21,8 N | 17° 52,1 W | 1572 | | NR* |
| 643 | | TD | 9:46 | 28° 18,2 N | 17° 48,2 W | 1628 | | NR* |
| 644 | | TD | 12:06 | 28° 18,3 N | 17° 45,8 W | 1505 | | NR* |
| 645 | | TD | 13:43 | 28° 18,3 N | 17° 45,8 W | 1398 | 1 | Carbonates |
| 646 | | KD | 15:45 | 28° 18,2 N | 17° 45,8 W | 1550 | 5 | Carbonates and basalts |
| 647 | | KD | 18:37 | 28° 18,4 N | 17° 45,8 W | 1340 | | Coral debris |
| 648 | | KD | 20:30 | 28° 18,7 N | 17° 46,7 W | 1443 | 3 | Basaltic rocks |
| 649 | | KD | 22:30 | 28° 18,8 N | 17° 46,5 W | 1361 | 3 | Coral debris |
| 650 | 01.12.1998 | KD | 1:19 | 28° 19,7 N | 17° 47,8 W | 1142 | 1 | Coral debris |
| 651 | | KD | 3:39 | 28° 19,2 N | 17° 48,2 W | 1334 | 1 | Carbonate, partly volcaniclastic |
| 652 | | RD | 6:49 | 28° 19,2 N | 17° 48,2 W | 1054 | | NR* |
| 653 | | TD | 8:13 | 28° 19,3 N | 17° 48,3 W | 1002 | 1 | Basaltic lapillistone |
| 654 | | RD | 9:41 | 28° 19,4 N | 17° 48,1 W | 910 | 1 | Carbonate, partly volcaniclastic |
| 655 | | RD | 12:00 | 28° 20,4 N | 17° 49,2 W | 1132 | | Coral debris |
| 656 | | RD | 14:11 | 28° 20,6 N | 17° 49,7 W | 1236 | 4 | Coral debris |
| 657 | | RD | 16:24 | 28° 21,9 N | 17° 51,1 W | 1247 | 12 | Basalt lava and scoria |
| 658 | | RD | 18:56 | 28° 23,0 N | 17° 51,8 W | 1251 | 16 | Basalt pillow lava |
| 659 | | RD | 21:04 | 28° 23,6 N | 17° 51,9 W | 1325 | | NR* |
| 660 | | RD | 23:53 | 28° 24,0 N | 17° 51,7 W | 924 | 3 | Basalt lava |
| 661 | 02.12.1998 | RD | 1:03 | 28° 23,9 N | 17° 50,6 W | 1052 | 1 | Coral debris |
| 662 | | RD | 3:03 | 28° 23,5 N | 17° 50,0 W | 1202 | 2 | Trachyte |
| 663 | | RD | 7:07 | 28° 22,1 N | 17° 45,6 W | 2072 | 5 | Volcaniclastic sediment |
| 664 | | RD | 9:58 | 28° 25,7 N | 17° 49,7 W | 719 | 13 | Basaltic lapillistone |
| 665 | | RD | 11:27 | 28° 26,3 N | 17° 50,6 W | 372 | 4 | Basalt |
| 666 | | RD | 13:24 | 28° 23,6 N | 17° 50,0 W | 1233 | 3 | Trachyphonolite and basalt |
| 667 | | RD | 16:30 | 28° 18,9 N | 17° 44,5 W | 1996 | 3 | Basaltic lava and lapillistone |
| ***2. South Hierro Ridge*** | | | | | | | | |
| 668 | 03.12.1998 | RD | 8:29 | 27° 36,5 N | 18° 0,2 W | 757 | 9 | Basalt and lapillistones |
| 669 | | RD | 9:41 | 27° 35,9 N | 18° 0,1 W | 595 | 4 | Basalt lava and lapillistones |
| 670 | | RD | 10:58 | 27° 35,9 N | 17° 59,1 W | 346 | 1 | Basaltic lapillistones |
| 671 | | RD | 12:10 | 27° 34,3 N | 17° 58,6 W | 832 | 3 | Basalt and volcaniclastics |
| 672 | | RD | 13:29 | 27° 35,1 N | 17° 58,9 W | 554 | 3 | Carbonate, partly volcaniclastic |
| 673 | | RD | 15:00 | 27° 33,6 N | 17° 58,3 W | 898 | 3 | Basalt and volcaniclastics |
| 674 | | RD | 16:40 | 27° 33,4 N | 17° 58,9 W | 964 | 3 | Basaltic lapillistones |
| 675 | | RD | 18:33 | 27° 32,0 N | 17° 48,9 W | 975 | 5 | Basalt and coral debris |
| 676 | | RD | 21:08 | 27° 27,7 N | 18° 0,0 W | 1689 | 4 | Basalt and coral debris |
| 677 | 04.12.1998 | RD | 23:17 | 27° 26,8 N | 18° 0,4 W | 1539 | 3 | Limestone and manganese crust |
| 678 | | RD | 1:29 | 27° 25,7 N | 18° 1,1 W | 1694 | 3 | Felsic lapillistone |
| 679 | | RD | 4:01 | 27° 23,0 N | 18° 2,0 W | 2173 | 3 | Felsic lapillistone |
| 680 | | RD | 6:24 | 27° 22,1 N | 18° 2,4 W | 2403 | 1 | Hemipelagic sediments |
| 681 | | RD | 9:03 | 27° 21,3 N | 18° 3,0 W | 2677 | 2 | Hemipelagic sediments |
| 682 | | RD | 11:55 | 27° 22,6 N | 18° 3,8 W | 3117 | 1 | Volcaniclastic sediments |
| 683 | | RD | 15:12 | 27° 23,2 N | 18° 0,3 W | 2871 | 1 | Hemipelagic sediments |
| 684 | | RD | 17:31 | 27° 23,9 N | 18° 0,6 W | 2319 | 4 | Hemipelagic sediments, basalt |
| 685 | | RD | | 27° 24,4 N | 17° 59,4 W | 2520 | | - No contact to sea floor - |
| 686 | | RD | 21:54 | 27° 20,0 N | 18° 4,3 W | 2654 | 1 | Manganese crust |
| ***3. Las Hijas Seamount*** | | | | | | | | |
| 687 | 05.12.1998 | RD | 11:30 | 27° 6,6 N | 18° 36,7 W | 2550 | 10 | Felsic lava |
| 688 | | RD | 14:15 | 27° 7,2 N | 18° 36,2 W | 2434 | 3 | Limestone, managanese crust |
| 689 | | RD | 17:09 | 27° 6,1 N | 18° 36,6 W | 2862 | 8 | Felsic lava |
| ***4. Tropic Seamount*** | | | | | | | | |
| 690 | 07.12.1998 | RD | 6:18 | 23° 47,7 N | 20° 47,5 W | 3603 | | NR* |
| 691 | | RD | 9:28 | 23° 48,1 N | 20° 45,9 W | 3077 | 2 | Hemipelagic sediments, manganese crust |
| 692 | | RD | 13:13 | 23° 50,0 N | 20° 45,1 W | 1875 | 5 | Limestone, basalt, felsite |
| 693 | | RD | 15:17 | 23° 50,5 N | 20° 44,7 W | 1142 | 4 | Limestone, basalt, felsite |
| 694 | | KD | 17:51 | 23° 51,5 N | 20° 48,8 W | 2770 | 4 | Basalt |
| 695 | | KD | 20:10 | 23° 51,9 N | 20° 48,1 W | 2000 | 2 | Coral debris, managnese crust |
| 696 | | KD | 22:35 | 23° 52,0 N | 20° 47,9 W | 1872 | 2 | NR* |

**Table 4:** continued

| M43-1 | Date | Type of dredge | Time seafloor (UTC) | Latitude | Longitude | Water depth (m) | Number of samples | Rock type ( NR*: No recovery) |
|---|---|---|---|---|---|---|---|---|
| 697 | 08.12.1998 | RD | 1:22 | 23° 52,8 N | 20° 47,4 W | 1477 | 2 | Felsite breccia, limestone |
| 698 | | RD | 4:42 | 23° 47,0 N | 20° 44,4 W | 2447 | | NR* |
| 699 | | RD | 6:53 | 23° 47,3 N | 20° 44,2 W | 2023 | 5 | Limestone, basalt, felsite |
| 700 | | RD | 9:07 | 23° 48,1 N | 20° 43,7 W | 1454 | | Coral debris, limestone |
| 701 | | RD | 11:18 | 23° 47,3 N | 20° 44,3 W | 2010 | | NR* |
| 702 | | RD | 13:52 | 23° 47,4 N | 20° 44,1 W | 2054 | 5 | Limestone, felsite |
| 703 | | RD | 16:33 | 23° 47,3 N | 20° 44,3 W | 2052 | 6 | Limestone, basaltic lapillistone, felsite |
| 704 | | RD | 19:35 | 23° 47,6 N | 20° 44,3 W | 2077 | 2 | Manganese crust |
| ***5. Paps Seamount*** | | | | | | | | |
| 705 | 09.12.1998 | RD | 10:07 | 25° 38,3 N | 20° 8,8 W | 2297 | 1 | Hyaloclastite, manganese crust, coral debris |
| 706 | | RD | 12:29 | 25° 38,9 N | 20° 8,0 W | 2105 | ? | Felsic pumiceous lapillistone |
| 707 | | KD-WS | 15:17 | 25° 37,8 N | 20° 7,9 W | 2312 | 8 | Pillow lava, lapillistone, Fe-rich manganese crust |
| 708 | 09.12.1998 | KD-WS | 20:06 | 25° 50,4 N | 20° 21,1 W | 2579 | | NR* |
| 709 | | KD-WS | 23:04 | 25° 50,4 N | 20° 20,1 W | 2582 | 1 | Manganese crust, Claystone |
| 710 | 10.12.1998 | KD-WS | 2:09 | 25° 49,9 N | 20° 19,5 W | 2991 | 1 | Volcaniclastic sediment |
| 711 | | KD-WS | 7:14 | 25° 58,0 N | 20° 22,1 W | 2038 | 2 | Vesicular basalt and fresh partially melted glass (slag) |
| 712 | | KD-WS | 9:46 | 25° 59,5 N | 20° 22,9 W | 2118 | | NR* |
| 713 | | RD | 12:44 | 25° 58,0 N | 20° 22,2 W | 2048 | 1 | Manganese crust and carbonate |
| 714 | | RD | 15:43 | 25° 57,9 N | 20° 23,0 W | 2076 | 7 | Basaltic lapillistone, manganese crust, carbonate |
| ***6. Endeavour Seamount*** | | | | | | | | |
| 715 | 11.12.1998 | RD | 4:00 | 25° 21,6 N | 19° 32,8 W | 2077 | 4 | Basaltic lapillistones |
| 716 | | RD | 6:16 | 25° 21,6 N | 19° 32,5 W | 1817 | 3 | Basaltic lapillistones |
| 717 | | RD | 8:25 | 25° 21,5 N | 19° 31,4 W | 1429 | 1 | Intermediate volcanic rock |
| 718 | | RD | 10:10 | 25° 21,5 N | 19° 30,9 W | 1000 | 1 | Vesicular basalt, manganese crust, limestone, coral debris |
| 719 | | RD | 11:37 | 25° 21,5 N | 19° 30,5 W | 698 | 1 | Coral debris, limestone |
| 720 | | RD | 12:45 | 25° 21,4 N | 19° 30,2 W | 447 | | Carbonate with manganese crust |
| ***7. Hierro Seamount*** | | | | | | | | |
| 721 | 11.12.1998 | RD | 22:04 | 25° 59,1 N | 18° 42,9 W | 2440 | 7 | Medium grained basalt |
| 722 | 12.12.1998 | RD | 0:32 | 25° 59,7 N | 18° 41,9 W | 1953 | 2 | Carbonate rocks and manganese crusts |
| 723 | | RD | 2:47 | 25° 59,9 N | 18° 41,2 W | 1574 | 1 | Manganese crust |
| 724 | | RD | 4:40 | 26° 0,3 N | 18° 40,2 W | 1138 | 1 | Carbonate rocks, manganese crust, coral debris |
| ***8. Kiel Seamount*** | | | | | | | | |
| 725 | 12.12.1998 | RD | 17:14 | 27° 19,4 N | 17° 48,1 W | 3525 | | NR* |
| 726 | | RD | 21:41 | 27° 18,4 N | 17° 46,4 W | 3385 | 2 | aphyritic vesicular basalt |
| ***9. Los Gigantes*** | | | | | | | | |
| 727 | 13.12.1998 | RD | 11:29 | 28° 15,9 N | 16° 55,2 W | 818 | 4 | Felsite and basalt |
| 728 | | RD | 12:53 | 28° 16,2 N | 16° 54,6 W | 700 | 2 | Coral debris, pumiceous rock |
| 729 | | RD | 14:38 | 28° 16,1 N | 16° 54,6 W | 617 | | Coral debris, sponges |
| 730 | | RD | 15:48 | 28° 16,2 N | 16° 54,5 W | 520 | 1 | Bioclastic limestone, sponges |
| 731 | | RD | 16:47 | 28° 16,3 N | 16° 54,5 W | 367 | 1 | Cpx-, ol-phyric basalt |
| ***10. Punta de la Rasca*** | | | | | | | | |
| 732 | 13.12.1998 | RD | 22:43 | 27° 51,7 N | 16° 44,6 W | 2503 | 1 | Hemipelagic sediment |
| 733 | 14.12.1998 | RD | 1:22 | 27° 52,1 N | 16° 44,0 W | 2099 | 4 | Fine-grained basalt and volcaniclastics |
| 734 | | RD | 4:00 | 27° 53,1 N | 16° 43,3 W | 1942 | 1 | Vesicular basalt |
| ***11. Off Barranco de Veneguera and Barranco de Tasartico*** | | | | | | | | |
| 735 | 14.12.1998 | RD | 11:57 | 27° 47,0 N | 15° 53,7 W | 1596 | 1 | Hemipelagic sediment |
| 736 | | RD | 13:44 | 27° 46,8 N | 15° 52,9 W | 954 | 5 | Fresh dense quenched rhyolite lava VL |
| 737 | | RD | 15:14 | 27° 46,7 N | 15° 51,5 W | 593 | 4 | Diverse volcanic rocks, carbonate crust |
| 738 | | RD | 16:36 | 27° 46,7 N | 15° 51,0 W | 450 | | NR* |
| 739 | | RD | 18:39 | 27° 48,9 N | 15° 53,7 W | 1173 | 2 | Pl-phyric basalt (Horgazales formation) |
| 740 | | RD | 20:20 | 27° 49,0 N | 15° 53,5 W | 929 | | Hemipelagic sediment |
| 741 | | RD | 22:08 | 27° 48,8 N | 15° 53,5 W | 1000 | 1 | Hemipelagic sediment |
| 742 | 15.12.1998 | RD | 0:00 | 27° 48,5 N | 15° 52,7 W | 973 | | NR* |
| 743 | | RD | 1:48 | 27° 48,5 N | 15° 52,7 W | 854 | 3 | ol-, cpx-phyric basalt |
| 744 | | RD | 4:00 | 27° 51,1 N | 15° 56,8 W | 1286 | 3 | ol-, cpx-phyric basalt |
| 745 | | RD | 5:36 | 27° 51,2 N | 15° 56,7 W | 1056 | | NR* |
| 746 | | RD | 7:02 | 27° 51,2 N | 15° 56,5 W | 881 | | NR* |
| 747 | | RD | 8:59 | 27° 51,2 N | 15° 56,6 W | 1008 | | Coral debris |
| 748 | | RD | 11:51 | 27° 54,2 N | 16° 0,1 W | 1247 | 2 | Cpx-phyric basalt |
| 749 | | RD | 13:26 | 27° 54,5 N | 15° 58,7 W | 974 | 5 | Aphyric and ol-, px-, pl-phyric basalt |
| ***12. Off Barranco de Güigüi Grande and Güigüi Chico*** | | | | | | | | |
| 750 | 15.12.1998 | RD | 20:33 | 27° 59,4 N | 16° 1,5 W | 1685 | 6 | Quenched glassy fsp phyric lava |
| 751 | | RD | 22:39 | 27° 59,2 N | 16° 1,0 W | 1405 | 2 | Ditto |

**Table 4:** continued

| M43-1 | Date | Type of dredge | Time seafloor (UTC) | Latitude | Longitude | Water depth (m) | Number of samples | Rock type ( NR*: No recovery) |
|---|---|---|---|---|---|---|---|---|
| 752 | 16.12.1998 | RD | 1:41 | 28° 0,0 N | 16° 1,5 W | 1706 | | NR* |
| 753 | | RD | 4:42 | 27° 59,2 N | 16° 8,5 W | 2171 | | NR* |
| 754 | | RD | 6:30 | 27° 59,3 N | 16° 8,3 W | 1901 | | Coral debris |
| ***13. Hijo de Tenerife*** | | | | | | | | |
| 755 | 16.12.1998 | RD | 9:17 | 28° 5,0 N | 16° 10,7 W | 2100 | 13 | Slightly vesicular "bombs" of intermediate composition |
| 756 | | RD | 11:19 | 28° 5,2 N | 16° 10,6 W | 1966 | 6 | Ditto |
| 757 | | TD | 13:24 | 28° 5,2 N | 16° 10,4 W | 1893 | 6 | Ditto |
| 758 | | RO | 16:02 | 28° 5,4 N | 16° 10,1 W | 1667 | | Water sapmle |
| 759 | | RD | 17:34 | 28° 5,2 N | 16° 10,4 W | 1884 | 5 | "Bombs" and volcaniclastics of intermediate comp. |
| ***14. Submarine flank Gran Canaria, off Agaete*** | | | | | | | | |
| 760 | 16.12.1998 | RD | 21:09 | 28° 8,1 N | 15° 55,2 W | 1576 | | Hemipelagic sediment |
| 761 | | RD | 23:18 | 28° 8,2 N | 15° 54,8 W | 1368 | 2 | Ditto |
| 762 | 17.12.1998 | RD | 0:54 | 28° 8,2 N | 15° 54,5 W | 1093 | | Basalt |
| 763 | | RD | 2:57 | 28° 9,0 N | 15° 55,9 W | 1768 | 1 | Basalt, coral debris |
| 764 | | RD | 4:42 | 28° 9,1 N | 15° 55,6 W | 1378 | | NR* |
| 765 | | RD | 5:59 | 28° 9,2 N | 15° 55,4 W | 1073 | 4 | Basalt |
| 766 | | RD | 8:14 | 28° 9,4 N | 15° 57,5 W | 2548 | | Coral debris |
| 767 | | RD | 10:40 | 28° 9,7 N | 15° 56,6 W | 1796 | 2 | Basalt |
| ***15. Submarine flank Tenerife, off Güimar and Anaga*** | | | | | | | | |
| 768 | 17.12.1998 | RD | 15:01 | 28° 13,4 N | 15° 18,4 W | 988 | 3 | Basalt |
| 769 | | RD | 16:00 | 28° 19,2 N | 16° 14,4 W | 653 | | Ooze and coral debris |
| 770 | | RD | 23:01 | 28° 36,3 N | 16° 0,6 W | 2305 | 2 | Basaltic scoria |
| 771 | 18.12.1998 | RD | 1:56 | 28° 37,0 N | 15° 56,4 W | 2970 | 1 | Basalt |
| 772 | | RD | 5:24 | 28° 34,4 N | 15° 59,9 W | 2386 | 1 | Hemipelagic sediment |
| 773 | | RD | 9:14 | 28° 32,9 N | 16° 0,2 W | 2061 | 8 | Lapillistone |
| 774 | | RD | 11:56 | 28° 30,6 N | 16° 5,0 W | 1273 | 4 | Basalt and lapillistone |
| 775 | | RD | 14:35 | 28° 29,3 N | 16° 8,3 W | 541 | 2 | Basalt |
| 776 | | RD | 16:03 | 28° 29,4 N | 16° 8,3 W | 436 | 2 | Basalt |
| 777 | | RD | 18:55 | 28° 28,35 N | 16° 7,84 W | 1055 | | Hemipelagic sediment |
| ***16. ODP Site 954 and . Submarine flank Gran Canaria, off Galdar*** | | | | | | | | |
| 778 | 19.12.1998 | RO | 1:50 | 28° 26,3 N | 15° 32,0 W | 3480 | | Water sample |
| 779 | 19.12.1998 | RD | 5:31 | 28° 14,0 N | 15° 43,0 W | 1268 | 2 | Basalt |
| 780 | | RD | 7:28 | 28° 13,8 N | 15° 42,9 W | 965 | 2 | Basalt |
| 781 | | RD | 9:30 | 28° 14,5 N | 15° 40,8 W | 1617 | 1 | Hemipelagic sediment |
| ***17. Gran Canaria, off La Isleta*** | | | | | | | | |
| 782 | 19.12.1998 | RD | 11:20 | 28° 14,1 N | 15° 40,7 W | 1446 | | NR* |
| 783 | | RD | 15:15 | 28° 12,9 N | 15° 25,8 W | 772 | 2 | Basaltic lapillistone, basalt |
| 784 | | RD | 17:24 | 28° 13,6 N | 15° 24,1 W | 1293 | 1 | Hemipelagic sediment, coal |
| 785 | | RD | 19:56 | 28° 15,3 N | 15° 23,9 W | 1932 | | Hemipelagic sediment |
| 786 | | RD | 22:25 | 28° 16,5 N | 15° 23,9 W | 2801 | | Ditto |
| 787 | 20.12.1998 | RD | 1:49 | 28° 15,7 N | 15° 23,0 W | 2162 | | Ditto |
| 788 | | RD | 5:03 | 28° 18,7 N | 15° 20,4 W | 3078 | | Hemipelagic sediment |
| 789 | | RD | 8:31 | 28° 9,8 N | 15° 17,7 W | 1882 | 1 | Basaltic lapillistone |
| 790 | | RD | 10:59 | 28° 6,9 N | 15° 18,0 W | 1228 | 4 | Picrite, beach rock |
| 791 | | RD | 14:22 | 28° 5,6 N | 15° 9,3 W | 1467 | 3 | Limestone coral debris |
| 792 | | RD | 16:06 | 28° 6,0 N | 15° 9,0 W | 1305 | 1 | Coral debris |
| 793 | | RD | 19;27 | 27° 56,4 N | 15° 6,5 W | 1603 | 4 | Basalt, breccia |
| 794 | | RD | 22:00 | 27° 57,7 N | 15° 1,4 W | 1637 | 10 | Phonolite breccia, basalt |
| 795 | 21.12.1998 | RD | 0:30 | 27° 56,1 N | 15° 3,9 W | 1606 | 1 | Manganese crusts |
| 796 | | RD | 3:10 | 27° 52,0 N | 15° 12,3 W | 1413 | 1 | Calcarenite |
| 797 | | RD | 5:23 | 27° 51,2 N | 15° 13,8 W | 1214 | | Hemipelagic sediment |
| 798 | | RD | 8:14 | 27° 45,8 N | 15° 16,5 W | 1258 | 1 | Manganese crusts, carbonaze |
| 799 | | RD | 11:37 | 27° 40,7 N | 15° 27,2 W | 1515 | | Hemipelagic sediment |
| ***18. Gran Canaria, off SE coast*** | | | | | | | | |
| 800 | | RD | 13:36 | 27° 41,5 N | 15° 26,6 W | 1146 | 4 | Rhyolite breccia with fresh glass |
| 801 | | RD | 15:50 | 27° 41,2 N | 15° 31,1 W | 1340 | 1 | Hemipelagic sediment |
| 802 | | RD | 18:09 | 27° 39,4 N | 15° 38,3 W | 1130 | | NR* |
| 803 | | RD | 21:21 | 27° 33,6 N | 15° 44,6 W | 1475 | 7 | Corals |
| 804 | | RD | 23:52 | 27° 38,3 N | 15° 49,2 W | 1332 | | NR* |
| 805 | 22.12.1998 | RD | 1:51 | 27° 39,7 N | 15° 47,1 W | 882 | | NR* |
| 806 | | RD | 3:48 | 27° 42,8 N | 15° 50,9 W | 1227 | | NR* |
| 807 | | RD | 5:48 | 27° 44,6 N | 15° 51,9 W | 1332 | | NR* |
| 808 | | RD | 7:45 | 27° 46,4 N | 15° 53,0 W | 1261 | 3 | Glassy felsic lava |
| 809 | | RD | 9:52 | 27° 46,8 N | 15° 53,0 W | 1052 | 3 | Obsidian |
| 810 | | RD | 11:49 | 27° 48,9 N | 15° 53,6 W | 1052 | | NR* |
| 811 | | RD | 13:09 | 27° 48,6 N | 15° 53,9 W | 1290 | 1 | Hemipelagic sediment |

### 5.1.2.2 Rock Types Dredged and Their Interpretation

Rocks dredged were described in three different stages using successively smaller sub-sets of samples. An initial description was carried out when the dredge came on board. The samples were first washed by freshwater on deck and were then examined in the dredge laboratory where typical specimens were sawed. The profiling time between sampling sites was used for initial rock descriptions (macroscopic description, photography). The dredged rocks were grouped into sample types. One or more reference samples were selected from each group. The thin-sections slabs and, where appropriate, small samples for crushing were then transferred to the onboard laboratories for crushing and thin section preparation.

Small pieces of typical reference samples were kept in the microscopy lab for detailed description and for comparison with new, incoming samples. This second stage of visual examination was carried out under a stereomicroscope aided by handlens examination of the cut and dried surface. This information was transferred to specially prepared forms. The hand specimen description and estimation of e.g. vesicle sizes, volume % of vesicles, volume % of phenocrysts etc. was optimized based on a reconnaissance thin section examination under the petrographic microscope. Altogether 150 thin sections were prepared from the rocks recovered. This information was then transferred into a table (see chapter 7.1.2).

*Classification of Rock Types*

In the absence of chemical data, we classified the rocks based on hand specimen and thin section description into the following simple categories: Basalts (aphyric, ol-phyric, cpx-, pl- phyric etc.), intermediate rocks, lighter colored when fresh, no phenocrysts or only minor pyroxene, and evolved rocks, phonolitic where feldspathoids were found (such as in some tuffs on the South La Palma Ridge) or trachytes where no silica-undersaturated mineral phases were found in thin section. Large clear phenocrysts in the evolved rocks were called alkali feldspar or anorthoclase which is the most common large alkali feldspar phenocryst phase in the trachytes, phonolites and rhyolites of the Canary Islands. Dark mica in these rocks was called phlogopite based on the composition of dark mica on both Gran Canaria and Tenerife.

*Basaltic Rocks*

The range in volcanic rock types dredged is large. Alkali basalts dominate. Most are phyric with olivine and clinopyroxene phenocrysts in varying relative proportions and volumes. Clinopyroxene- and olivine-rich basaltic rocks (picrites) were dredged on both the South El Hierro Ridge and the SW and NW coast of Gran Canaria. Plagioclase phenocrysts occur in some rocks. Three-phase or even 4 phase (ol, cpx, pl, amph) basalts are rare. Nephelinites characterized by practically exclusively clinopyroxene in the groundmass - the criterion for their classification - were recovered in a few dredges. On the older Canary Islands and in Hawaii, such lavas normally occur during the post-erosional stage. The basaltic rocks dredged were generally quickly cooled (tachylitic) and practically invariably vesicular along the El Hierro and La Palma Ridges, commonly around 50 vol.%. Those dredged along the flanks of Tenerife and Gran Canaria, in contrast, are generally nonvesicular to sparsely vesicular. Glassy, quenched basalt is common either as a rim of larger basalt fragments, pillows, thin sheet flows etc. Vesicles in many basalts are partially filled with glassy or tachylitic, commonly vesicular matrix melt that has been sucked in between spherulites when the gas contracted in the quickly cooled lava. Incompletely palagonitized fresh sideromelane is not uncommon in some vesicular lapilli. More fully crystallized basalts are rare.

*Intermediate Rocks*
Two main types of intermediate rocks were recovered. In two dredges on the South La Palma Ridge, intermediate rocks are characterized by amphibole and minor feldspar phenocrysts with traces of apatite microphenocrysts and/or abundant groundmass clinopyroxene. At Tropic Seamount, intermediate rocks show a complex mineralogy including both plagioclase - commonly corroded - amphibole, pyroxene and altered olivine. Mafic clats are also common in the more evolved rocks from this seamount.

*Felsic Rocks*
Solid felsic lava, mostly non-vesicular, some in the form of felsite breccias, as well as microvesicular to pumiceous felsite were dredged on the submarine ridges of La Palma and El Hierro, on Las Hijas, Tropic and Hijo de Tenerife Seamounts and along the submarine flanks of Gran Canaria. These evolved rocks occur as dense blocks, part of larger rock masses, but also commonly as both pyroclastic and hydroclastic particles which are distinguished by their vesicularity. Dredging was repeated successfully on some of these localities suggesting that these rock bodies are large, several tens of meters if not hundreds of meters in dimension and most likely represent extrusive domes. Several compositional types of evolved rocks were dredged. Most common are fine-grained, highly evolved felsic lavas that are either practically aphyric or contain 1-15 vol.% of alkali feldspar and also some plagioclase phenocrysts. Magnetite/ilmenite, amphibole, phlogopite and titanite are common minor components with titanite being common at Tropic Seamount and phlogopite in the evolved rocks from South La Palma Ridge and off Tenerife. All three compositional groups of felsic rocks known from the Canary Islands were dredged: excellent, fresh, glassy rhyolite on Gran Canaria, mafic phonolite on Hijo de Tenerife, some phonolite tuffs on La Palma and in some areas, such as the submarine flank of El Hierro and the seamounts Las Hijas and Tropic, very abundant trachyte. The corollary of the unexpected abundance of highly evolved rocks and volcanic structures both within the archipelago as well as on the southern seamounts, implies that a large number of seamounts and other structures along this passive margin are probably of evolved composition.

The Hijo de Tenerife mafic phonolite is a fine-grained to glassy, slightly vesicular rock with 3 vol.% phenocrysts, almost exclusively aegirine-augite and dark mica with very rare feldspars and some xenocrystic olivine up to several cm in size. The striking aspect of this fresh and very young rock is the abundance of angular, generally only partially heated rock fragments including ultramafic xenoliths, basalts, olivine xenocrysts, basement sediments etc. as well as basaltic schlieren (magma mixing).

*Volcaniclastic Rocks*
The term lapillistone is used for volcaniclastic rocks composed of volcanic particles in the lapilli size range (Md 2 – 64 mm) while volcaniclastic rocks with a median of < 2 mm are called tuffs. The term lapillus is used for volcanic particles 2-64 mm irrespective of whether they are vesicular and have primary shapes such as found in scoria cones and onland fall-out deposits from lava fountain activity, or whether they are angular and owe their origin to different fragmentation processes. Lapillistones with primary shapes were surprisingly common on La Palma as well as the El Hierro submarine ridges. The term breccia is used for coarser-grained rocks made up of larger angular fragments. A common rock variety dredged consists of biogenic debris with variable amounts of volcanic particles ranging from <1 to >50 vol.%. These rocks were called calcarenite with volcanic clasts or calcareous tuffs. The term tube or pillow was used for sections of tube lava and the term sheet flow for flat slabs of basalt showing one or more glassy rinds and having evidently been emplaced as a sheet-like lava.

Most of the rocks dredged are volcaniclastic, especially in the older seamounts. Very simply, three types of volcaniclastic rocks were distinguished from each other.
(a) Classic basaltic hyaloclastites with angular clasts and vesicularities generally <50 vol.% were dredged e.g. from South La Palma and South El Hierro Ridges and Tropic, Paps and Endeavour Seamounts. In the older seamounts they are completely altered, dominantly to layer silicates. They very much resemble the hyaloclastites from the deeper parts of the 1200 m deep drill hole 953C (ODP Leg 157) (SCHMINCKE AND SEGSCHNEIDER, 1998). They are interpreted to have formed dominantly by quench-fragmentation of slightly vesiculated basaltic lava.
(b) A second major group, common on both the La Palma and El Hierro submarine ridges, consists of highly vesicular (generally >50 vol.%), dominantly lapilli-sized clasts. The deposits are generally well-sorted like the hyaloclastites discussed above. They are generally much fresher, however, than those from the older seamounts and most of them have some fresh glass left, even though much or most of their glass has been altered to reddish palagonite and its crystalline transformations to layer silicates. Their shape resembles that of lapilli formed subaerially but their thick, in many rocks still fresh, glass septa clearly indicates their formation under water.
(c) The third, more heterogeneous group comprises a variety of volcaniclastic deposits ranging from well-bedded basaltic tuffs as dredged on Tropic Seamount, poorly consolidated phonolitic ash from La Palma and somewhat pumiceous lapillistones of intermediate to evolved composition dredged at several places on South El Hierro Ridge.

The roughly breadcrust-shaped lapilli to bomb-shaped clasts that were dredged from the flanks of Hijo de Tenerife Seamount are unconsolidated deposits resembling scoriaceous bomb deposits from subaerial scoria cones except for their low vesicularity (<20 vol.%).

Groups a and b are interpreted to roughly represent a stratigraphic succession from deeper to shallower level. Those from group c comprise assemblages composed of highly vesicular particles owing to the high volatile contents of the parent magmas erupted in relatively deep water (1500 m bsl).

#### 5.1.2.3 Eruptive Depth and Island Subsidence

One of the aims of our study was to reconstruct the eruptive depth of lavas and pyroclastic/hydroclastic particles and deposits in order to better understand the growth and possibly subsidence history of the islands and seamounts. In principle, highly vesicular materials dredged at depths greater than a few hundred meters could have formed (a) at the depth of recovery more or less in situ, (b) subaerially or at shallow depth and been transported downslope into deeper water by slumps or debris flows or (c) subaerially or at shallow depth with subsequent transport into deeper water by bulk subsidence of the entire volcanic edifice or parts of it.

We have no positive evidence that any of the material dredged formed originally under subaerial conditions and was subsequently transferred into deeper water. Our evidence includes common glassy rinds on basalts, either fresh as on the La Palma and El Hierro Ridges and the flanks off Tenerife and Gran Canaria, or completely altered as on the older seamounts. Vesicles in the lava fragments are partly filled with matrix liquid (now glass or tachylite), typical of submarine basalts. Many fragments are associated and intermixed with nanno-foram ooze, and pillow and sheet flow morphologies and structures are common in several dredge hauls. While the volcaniclastic rocks composed of vesicular small lapilli and ash-sized shards could be explained by fallout from eruption on land, the highly vesicular pillow lavas have definitely formed under water. The basaltic lapilli dredged along both La Palma and El Hierro Ridges have commonly fresh sideromelane septa preserved between the vesicles, a sure sign that they were erupted under water and not in air. The pumiceous material of trachytic composition dredged at the South El Hierro Ridge was clearly erupted in situ and not in shallow water. Evidence includes

firstly the large abundance of felsic material at two dredge sites of differing depth; secondly the quenched rim of lapilli up to 10 cm in diameter with a change in vesicle size from fine-grained to coarser-grained in the interior and, thirdly, the abundance of denser to completely non-vesiculated and slightly crystallized, felsic rocks. An exception are the felsic rocks dredged on La Palma Ridge, Las Hijas Seamounts and Tropic Seamount which are non-vesicular, but are associated with pumiceous deposits of the same composition in which vesicularity exceeds 50 vol.%. While the vesicular, basaltic lapilli could conceivably have been derived from shallow water eruptive sites, their common association with highly vesicular lavas of the same compositional group does suggest that they formed at similar water depths and were not transported there by debris flows etc. The most compelling evidence comes from the vesicular nature (up to 20 vol.% vesicles) of the bomb to lapilli-sized clasts dredged on Hijo de Tenerife Seamount, many of which show a rough concentric texture with vesicle size increasing inwards and/or large rock fragments in the center of small round lapilli.

In the absence of positive evidence for transport of vesicular lapillistones from shallow to deeper water, their approximately in-situ-origin is based chiefly on their compositional similarity with basaltic lavas recovered in the same dredges and on the petrographic similarity among the lapilli in a particular lapillistone. Rocks were either emplaced at the approximate depth from which they were dredged or were transported to greater depths by subsidence of the island. There is no evidence for major subsidence of either El Hierro or La Palma. Evidence that Tropic Seamount had once been an island is strong (conglomerates, guyot-like flat top, shallow water calcarenite). The large amount of subsidence required by the flat top of the island now being 1000 m bsl is still an enigma unless the island is very old. This will be analyzed by single crystal laser dating of the feldspars in the trachytes dredged on Tropic Seamount.

We are thus left with two scenarios: either the unusually - at least with respect to our expectations - vesicular lavas and lapilli formed at the approximate water depth they were dredged from or the ridges represent bulk subsidence. Subsidence of this colossal amount of the probably very young volcanic ridges off La Palma and El Hierro is considered unlikely, especially if, as seems likely here, the amount of pyroclastic material is large, although the number of samples on which this interpretation is based is small. This means that the magmas erupted along the ridge were unusually volatile-rich. It also means that the use of lava vesicularity as a geobarometer has to be recalibrated drastically. For example, the depth estimate of STAUDIGEL AND SSCHMINCKE (1984) for the 700 m water depth for vesiculation of alkali basaltic lavas must be extended to much greater depths, perhaps as much as 1500 m. Vesicular glass shards of basaltic compositions with up to 40% vesicles are generated at depths of at least 1300 m bsl. In other words, the vesicularity of glass shards must be used with caution as a geobarometer. The pumiceous nature of the mafic phonolite bombs covering the top and surface of Hijo de Tenerife Volcano indicates that only moderately evolved magmas vesiculate significantly at water depths in excess of 2000 m. A more detailed discussion of this question is beyond the scope of this preliminary report.

### 5.1.3 Rosette-Water Sampling

The Rosette system includes a 6-position pylon with 30 l Niskin-type water sample bottles interconnected with a deck unit via conductive cable. In addition, the system is equipped with a single electronic pinger in order to measure the distance between pinger/pylon and sea floor. After deployment of the pylon down to a known water depth, a release was given from the deck unit to the motor unit to close the sample bottles at their top and bottom by an additional weight and a release spring. During the recovery of the Rosette system, water samples were taken at different water depths. After recovery, the water samples were sealed immediately into copper tubings. The Rosette system used had a maximum deployment depth of 3000 m.

The aim of sampling water was to locate sites of active submarine hydrothermal venting on the sea floor and above seamounts by measuring the flux of $^3$He in the water column. Since $^3$He is a primordial component derived from the Earth's mantle rather than from the atmosphere or sediments, it is an unambiguous indicator of hydrothermal injection. Tritium will also be measured in order to correct for atmospheric helium input caused by fusion bomb testings. Water samples were taken at different water depths above the young volcano Hijo de Tenerife and at the drill Site 954 (ODP Leg 157).

### 5.1.4 Areas Studied

#### 5.1.4.1 Submarine Ridges South of La Palma and El Hierro

The purpose of studying the submarine ridges extending away from two very young oceanic islands was to compare and contrast eruptive mechanisms and rock composition during the submarine stages of the evolution. The ridges are apparently built above fissures and are not tectonic features. Their strike is given independently by the total ridge and much smaller volcanic features that dot the ridges (Figs. 5, 6). The possibility that the ridges represent a successive propagation of volcanism towards the south seems unlikely because of the apparent younging of volcanism from the tip of the ridges towards the island. This possibly does not represent a gradual younging, but a more pronounced temporal and structural break associated with a change in direction of major fissure systems, evident along both ridges. The northern direction of La Palma is not common in the central, but dominates the eastern Canary Islands. The southeast-northwest direction is prominent in younger Gran Canaria. The presence of the well-developed NW/SE and less strongly developed NE/SW directions in the southern part of the South La Palma Ridge, the occurrence of such directions in the 20 km subaerial Cumbre Vieja, the onland continuation of the submarine ridge (a direction also characterizing the southern half of the South El Hierro Ridge), and several rows of newly discovered small seamounts, are all considered significant. These preferred directions are likely to reflect a deep-seated control of the stress field of the lithosphere rather than the direction of the stress field of the volcanic edifice itself, or directions imposed by fractures of large slumps as exemplified in other oceanic islands by the orientation of the SW and E rift on Hawaii.

*South La Palma Ridge*

Our combined bathymetric and dredge study of the submarine ridge south of La Palma is the first such study for a ridge-like extension in the Canary Island Archipelago (Fig. 5). This ridge resembles the Reykjanes Ridge south of Iceland in some ways, although the dimensions are very much smaller and this is a ridge extending from an oceanic island rather than along a mid-ocean ridge. Both ridges show gradually diminishing eruptive rates from mantle sources that release most magmas beneath the highest elevation of the volcanic edifice or platform.

South of Punta Fuencaliente, the southern tip of La Palma Island, the submarine ridge extends for about 22 km measured straight North to South. This ridge is just a little bit longer than the 20 km long, active, southern subaerial ridge of La Palma. The southern ridge of La Palma shows three main directions: N/S, NW/SE and NE/SW. These same directions can be recognized in the submarine ridge. The eruptive centers in the southernmost half of the submarine ridge show dominantly NW/SE direction and less pronounced NE/SW directions, while the northern half corresponds in direction with the main direction in the Cumbre Vieja.

The northern 5 km slopes relatively quickly from 0 to 1000 m bsl. The remainder of the ridge between 15 and 20 km in length slopes much more gently until the southwestern edge at about 1800 m bsl. From there on the ridge becomes very steep and drops quickly within about 3 km to a depth of 3000 m bsl (Fig. 5b). The blunt termination of the submarine ridge is about 10 km

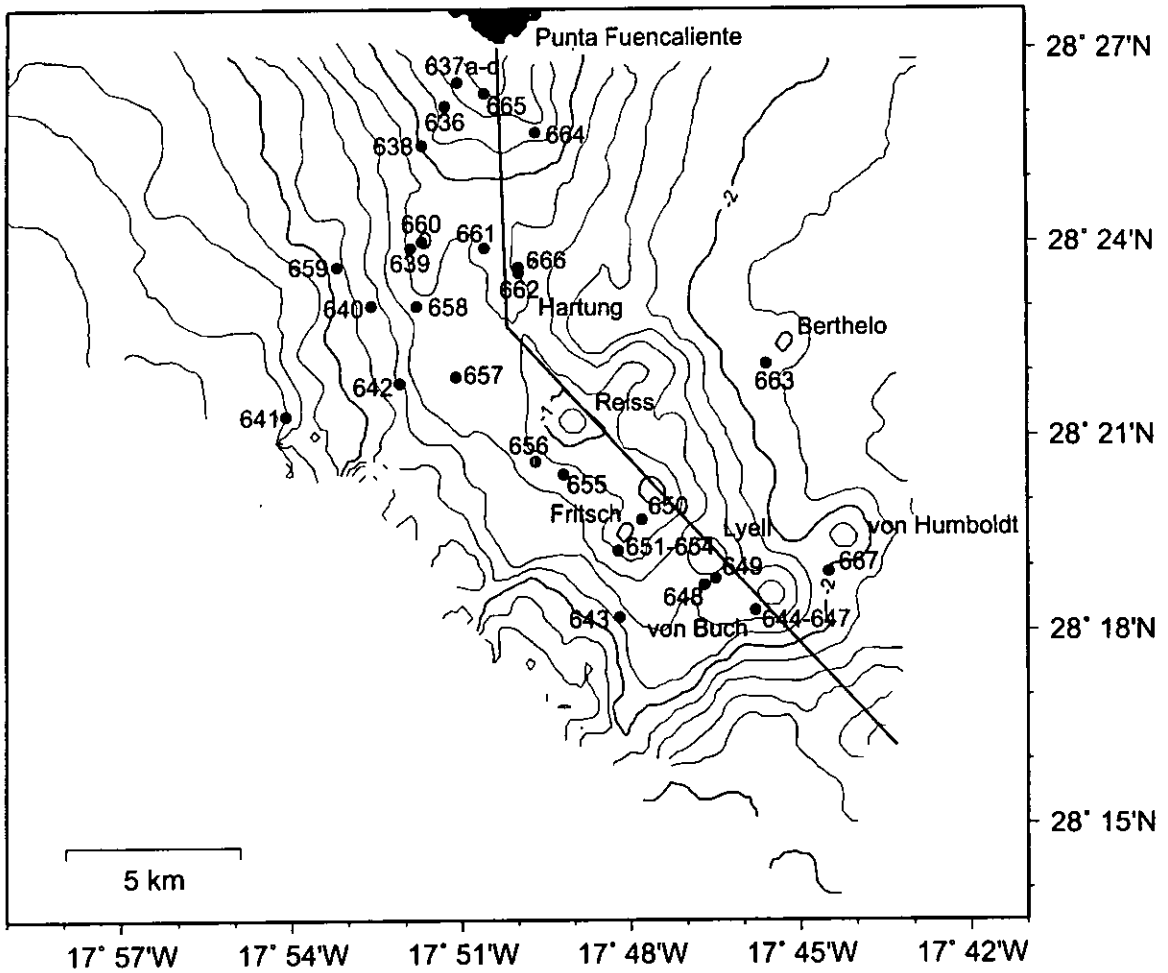


**Figure 5a:** Bathymetric multibeam map of the submarine south La Palma Ridge with 200 m contour lines and locations of dredge stations. The ridge is subdivided morphologically into a southern half trending SE-NW with prominent volcanic cones named provisionally after 18th century geologists who worked in the Canary Islands: Alexander von Humboldt, Berthelo, Leopold von Buch, Charles Lyell, Fritsch, Reiss and Hartung. The N-S trending northern half of the ridge merges into subaerial Cumbre Vieja at Punta Fuencaliente.

wide at the 2500 m bsl contour-line (Fig. 5a). The southern half of the ridge may be older than the northern part.

The broad ridge is dotted with a number of prominent volcanic structures which are dominantly sub-circular in the SE/NW-trending southern ridge and more elongate and north-south orientated at the southern end of the northern ridge. These structures are mostly 200-400 m, some less than 200 m high. They are about 1 km in diameter on average. We have provisionally named the cones in the south-eastern part of the ridge, from south to north: Leopold von Buch, Charles Lyell, Fritsch, Reiss, and Hartung and two other prominent cones Alexander von Humboldt and Berthelo (Fig. 5a). These are similar, evenly spaced structures about 2-3 km away from each other. The surface of the cones from the foot region to the top is covered by forests of coral-like animals and by calcareous and manganese crusts.

The rocks dredged range widely in composition from dominantly olivine-rich, through pyroxene-rich basalts to trachytes (Fig. 7). Intermediate rocks are rare. Both compositional groups

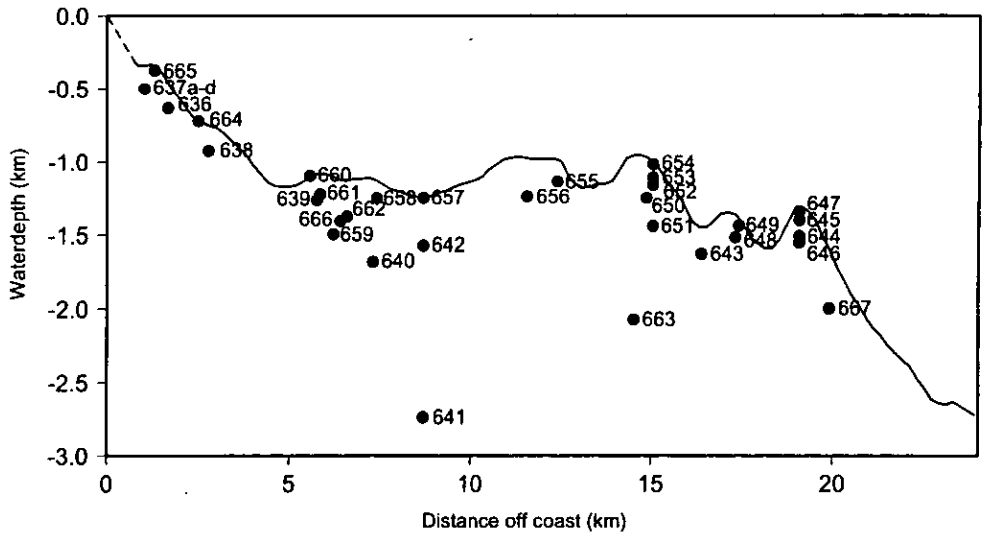


**Figure 5b:** Cross section (solid line of Fig. 5a) of the south La Palma Ridge from Punta Fuencaliente at the southern tip of the island of La Palma to the blunt end of the ca. 22-km-long ridge. The approximate depth of the dredge stations is shown.

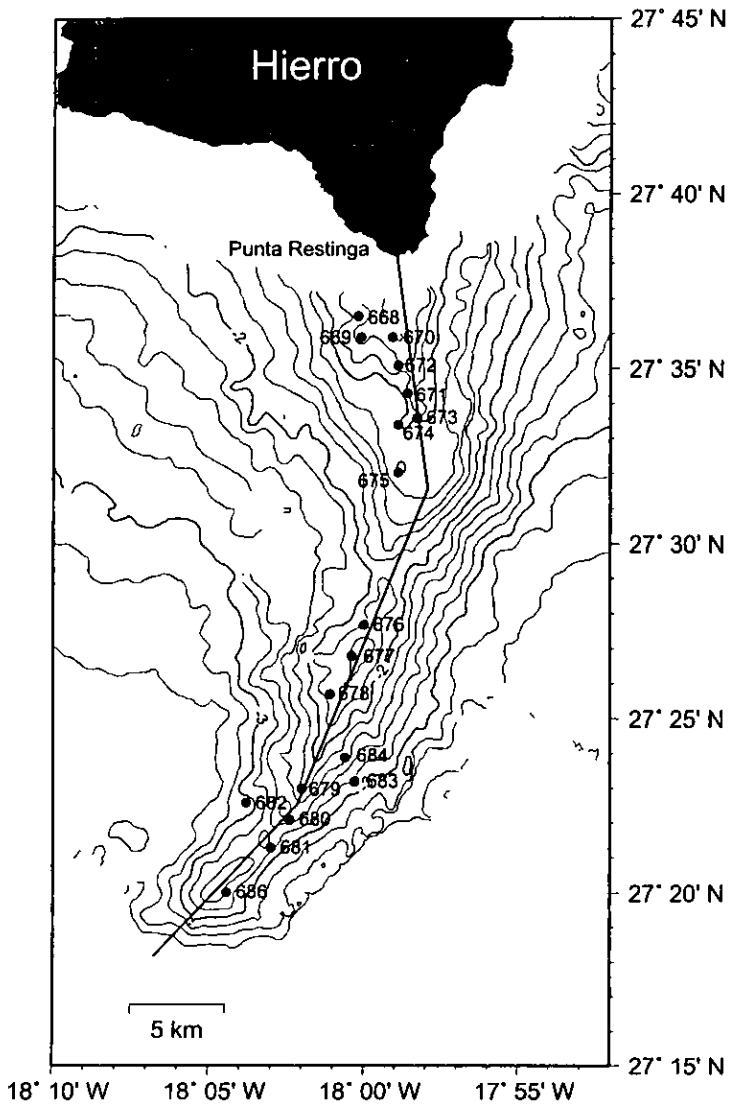


**Figure 6a:** Bathymetric multibeam map of the ca. 40-km-long submarine south El Hierro Ridge with 200 m contour lines and locations of dredge stations. The southern half of the ridge trends NE-SW. The NW-SE trending northern half merges into subaerial El Hierro at Punta Restinga.

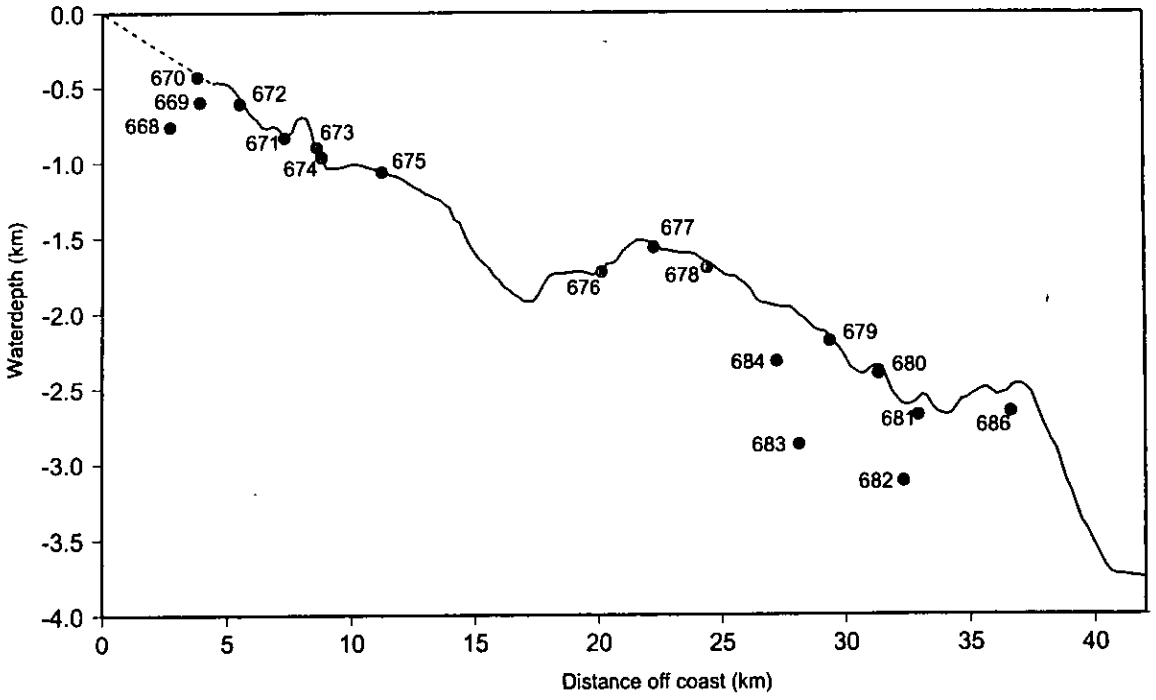


**Figure 6b:** Cross section (solid line of Fig. 6a) of the South El Hierro Ridge from Punta Restinga at the southeastern tip of the island to the blunt end of the ca. 40-km-long ridge. The approximate depth of the dredge stations is shown.

occur as solid lavas as well as abundant clastic rocks. The freshness of both basaltic and evolved rocks allows the study of their mineralogy and geochemistry in detail, including glass inclusions in olivine and clinopyroxene phenocrysts.

In summary, we interpret the southern submarine ridge off La Palma as part of the Cumbre Vieja system which evolved as activity concentrated in time beneath the central part of the Cumbre Vieja which grew to elevations that have reached nearly 2000 m above sea level at present. We speculate that the southern submarine ridge extends beneath the Cumbre Vieja and that its lavas represent an early stage of the Cumbre Vieja magmatic system. Whether or not magmas rose beneath the Cumbre Vieja and intruded southward, as along the east rift of Kilauea volcano is difficult to say. In any case, magma reservoirs did develop, at least beneath the north-

**Figure 7:** (right page) Photographs of volcanic rocks from dredges along the South La Palma Ridge. **1.** Sample 638-2. Reddish basaltic lapilli with >50% vesicles set in strongly indurated calcarenite matrix. **2.** Sample 657-1. Roundish pebble-like pieces of angular, highly altered calcarenite surrounded by manganese crusts. **3.** Sample 657-2. Roundish pebble-like piece of irregular, highly altered calcarenite surrounded by manganese crusts. **4.** Sample 658-2. Fresh piece of vesicular basalt. **5.** Sample 664-1. Basaltic lapillistone mixed with macrofossils. **6.** Sample 664-3. Moderately well sorted basaltic lapillistone **7.** Sample 664-4. Basaltic lapillistone with reddish, highly vesicular lapilli, mostly between 2 and 10 mm across with some larger fragments up to 4 cm across, set in nanno-foram matrix. **8.** Sample 667-1. Basaltic lapillistone with highly vesicular lapilli set in nanno-foram matrix.


1
10 cm


2
5 cm


3
5 cm


4
10 cm

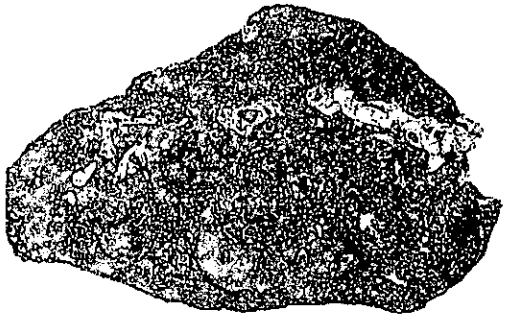
5
10 cm


6
5 cm

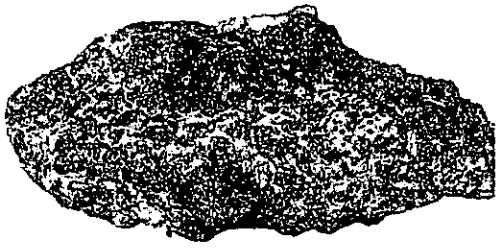
7
5 cm


8
5 cm

ern part of the southern submarine ridge, as reflected in the occurrence of trachyte lava and phonolitic pyroclastics.

*South El Hierro Ridge*

A 42-km-long submarine ridge starts at Punta Restinga at the southeast point of three-pronged star-shaped El Hierro, the youngest island in the Canarian Archipelago (Fig. 6). This ridge is a continuation of a subaerial ridge on the island dotted with numerous youthful scoria cones. Very young lava flows on the island with well-preserved surface forms, not yet covered by vegetation, entered the sea opposite the dredge sites.

The ridge is subdivided into a northern half showing a NW-SE orientation and a southern half showing SW-NE orientation. The elevation of the ridge drops to 1000 m bsl in the first 10 km and shows an elevation of 2800 m at its southwestern end. From there on the ridge becomes very steep and drops quickly within about 2 km to a depth of 3600 m bsl (Fig. 6b).

An important question concerns the evolution of El Hierro. The southwestern part of the submarine ridge shows an interesting curvature (Fig. 6a). Is this submarine ridge structure part of the El Hierro edifice? Or is it a separate volcano or caldera on the sea floor that became attached to El Hierro by the more proximal part of the submarine ridge? In any case, the surface morphology of the ridge is more irregular compared to the morphologically distinct cones on the southern part of the La Palma submarine ridge. As on La Palma, the youngest rocks dredged occur along the proximal northern part of the ridge, as reflected in their freshness and absence of significant manganese coating (Fig. 8).

### 5.1.4.2 Saharan Seamounts

Seamounts are a prominent morphological feature SW of the Canary Islands and extend the archipelago by some 500 km. We chose to study four larger and two smaller seamounts. While Las Hijas Seamounts had already been mapped by a Simrad EM12 multibeam system (RIHMET AL., 1998), topographic mapping by Hydrosweep was completed on Paps Seamount. A detailed bathymetric map was available for Tropic Seamount (HALBACH, 1993). We did not carry out detailed Hydrosweep mapping of Endeavour, El Hierro and Kiel Seamounts for lack of time, and restricted our work on these to dredging.

The most common rock type dredged on the older seamounts (Tropic, Paps, El Hierro, Endeavour, Kiel) are moderately vesicular, ash to lapilli-sized hyaloclastites and more vesicular lapillistones. All these rocks are strongly altered to layer silicate and carbonate but fresh glass was found in some volcaniclastic rock tightly cemented by carbonate. Clinopyroxene is the

**Figure 8:** (right page) Photographs of volcanic rocks from dredges along the South El Hierro Ridge. **1.** Sample 669-1. Basaltic lapillistone with highly vesicular basalt lapilli set in nanno-foram matrix. **2.** Sample 669-1. Close-up view of same sample showing good sorting of lapilli. **3.** Sample 676-1. Knobby manganese crust. **4.** Sample 676-3. Cross-section through basalt pillow (?) with glassy crust. **5.** Sample 678-1. Knobby manganese crust. **6.** Sample 678-2. Trachytic lapillstone with minor nanno-foram matrix. **7.** Sample 679-1. Relatively well sorted, pumiceous lapillistone. Flatter pumice fragment showing pronounced gradation in vesicle size, with smaller vesicles at the margin and larger vesicles towards the interior. The lapilli are held together by a matrix or cement but there is open pore space. The lapillistone is surrounded by a thick manganese crust. **8.** Sample 681-1. Pumiceous lapillistone showing graded bedding.

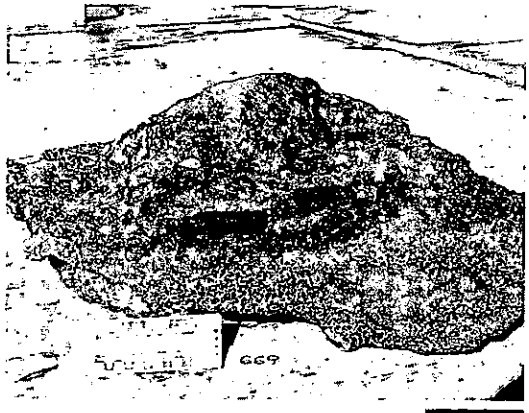
1 10 cm


2 5 cm

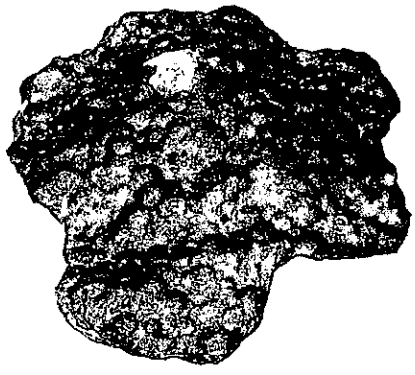
3 10 cm

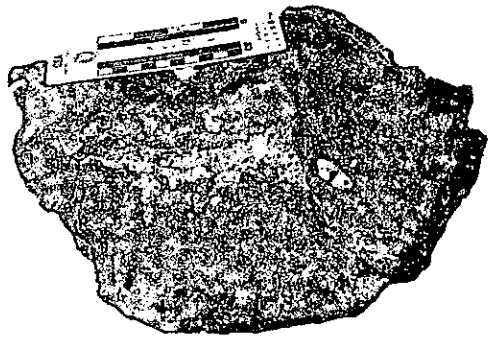
4 10 cm

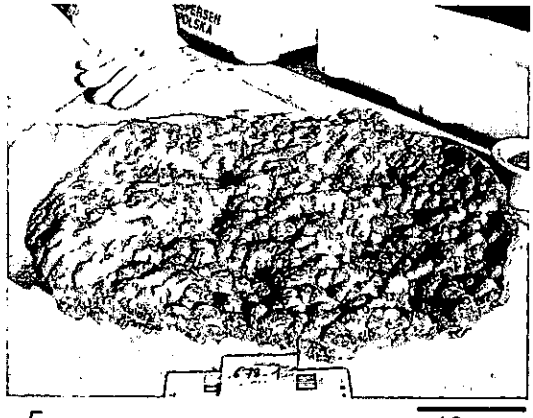
5 10 cm

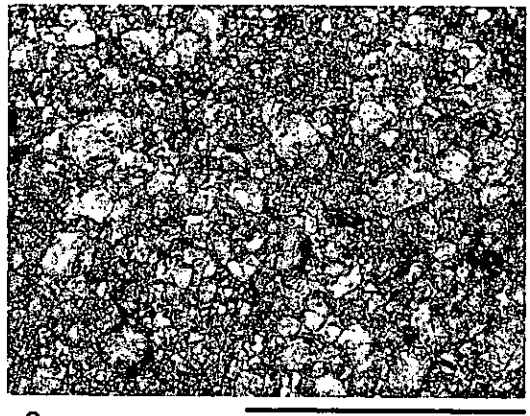
6 5 cm


7 5 cm

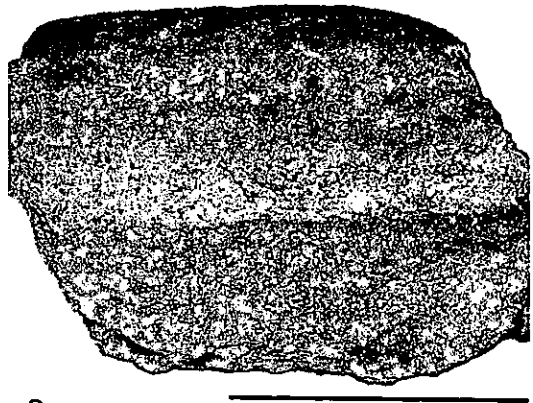
8 10 cm

phase that has survived the strong alteration in most rocks, while olivine is invariably replaced. Feldspar is moderately fresh in some trachytes.

*Las Hijas de Hierro*

A group of three seamounts 70 km SE of the island of El Hierro was discovered by RIHM ET AL. (1998). The northern and southern seamounts rise some 500 m above the seafloor while the central seamount rises as much as 1600 m from a depth of 3800 m bsl to 2200 m bsl with basal dimensions of 8 x 10 km. We dredged two stations on the western flank at 3000 and 2600 m bsl (Fig. 9) where we recovered abundant, non-vesicular, platy felsite rocks, probably trachyte.

*Tropic Seamount*

Tropic Seamount is the southernmost and most isolated of the Saharan Seamount group (Fig. 10). It lies about 100 km S/SW of the main group. It rises from a depth of about 4300 m and is cut by a plateau at about 1000 m bsl. The seamount has a diameter at the 4100 m contour line from N to S of 40 km and from E to W of 37 km. The plateau measures 15 km N/S and 11 km E/W. K-Ar dating of alkali basalts from the top of the seamount yielded an age of 101-95 Ma (BLUM ET AL., 1996).

Tropic Seamount is basically a four-pronged star resembling the NATO star with four slopes: SW, NW, NE and SE. In the Canary Islands, especially the younger ones, such scars are invariably associated with a hummocky terrain, which represents the debris avalanche that sourced along the island flanks. The evidence for such debris avalanche fans is not pronounced seaward of the four main scar-like slopes of Tropic Seamount. Considering the probable advanced age of the seamount, such avalanche deposits would long have become buried by 100's of meters of sediment.

Tropic Seamount was mapped and partly dredged by HALBACH (1993). Because of the NE wind, we dredged several profiles on the SW and W slopes and ridges (Fig. 10). Up to four stations were dredged along each profile from about 3000 to about 1200 m. We recovered mostly limestone with some manganese coating but also pebbles up to 15 cm in diameter and small pebble conglomerates. The trachytes dredged by us occur on the opposite side of the seamount on the SW flanks of the S ridge, some 15 km S of the main areas of trachyte recovery by HALBACH ET AL. (1993). This indicates that trachyte forms a significant part of Tropic Seamount, at least at depths of approximately 2000 m. The conglomerates and the flat top suggest that Tropic Seamount was once an oceanic island, became eroded and sank 1000 m.

Following recovery in three dredges of some reasonably fresh trachytes at the southern edge (Fig. 11) which contain alkali feldspar phenocrysts, we hope by dating these rocks by single crystal laser $^{40}Ar/^{39}Ar$ methods, to obtain ages that will allow to contribute to an understanding of the inception of volcanism in the southernmost outpost of the East Atlantic Volcanic Province.

*Paps Seamount*

The Paps Seamount is a curious structure differing significantly from other seamounts in its morphology. Its main part is a slightly pear-shaped structure which rises from a depth of 4300 m to 1600 m bsl (Fig. 12). The lower flanks are characterized by pronounced ridges and cones. A ridge, also with youthful volcanic cone morphology, extends S from the broader, blunter slope of the main structure for 35 km. This ridge is 2000 m bsl at its highest point rising from a depth of ca. 4000 m. No previous dredge results are known from Paps Seamount. Recovered rocks include alkali basaltic lava fragments and lapillistones, and more scarce felsic lapillistones.

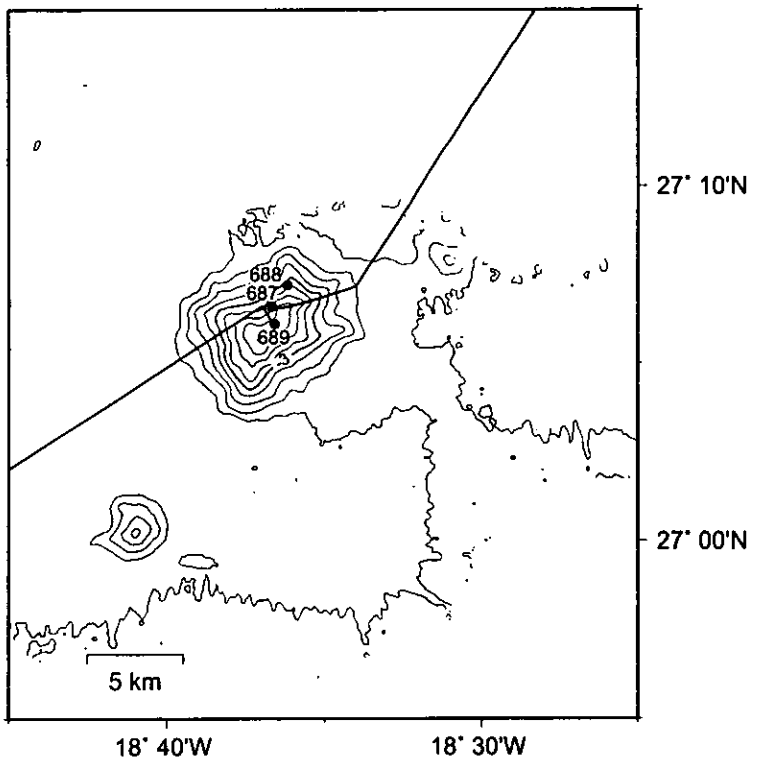


**Figure 9:**
Bathymetric multibeam map of Las Hijas Seamounts with 200 m contour-lines, locations of dredge stations and tracks.

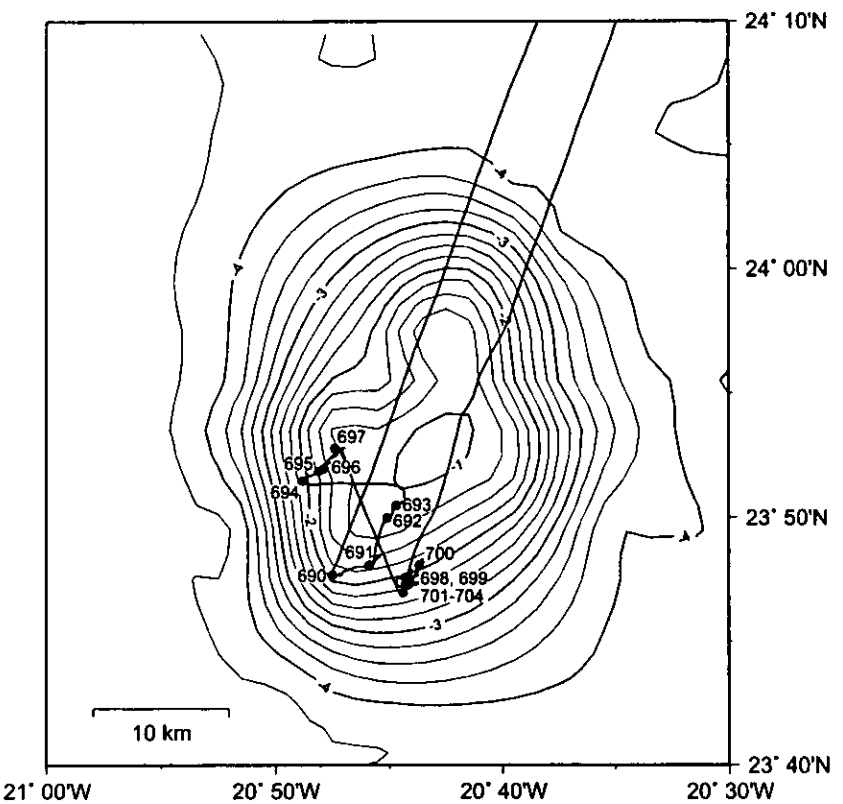


**Figure 10:** Simplified bathymetric map of Tropic Seamount with 250 m contour lines, locations of dredge stations and tracks. Bathymetry is taken from SMITH AND SANDWELL (1997).

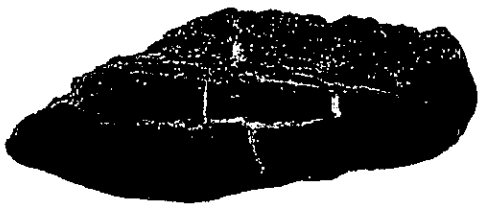

1 5 cm

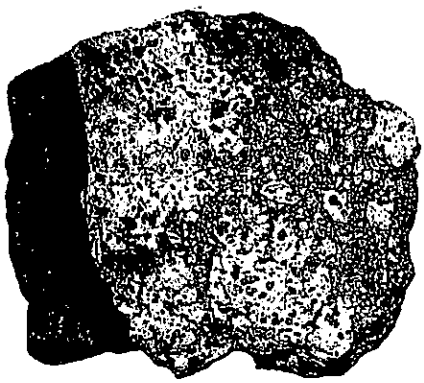

2 2 cm

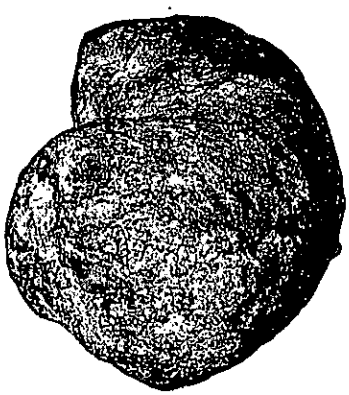

3 10 cm

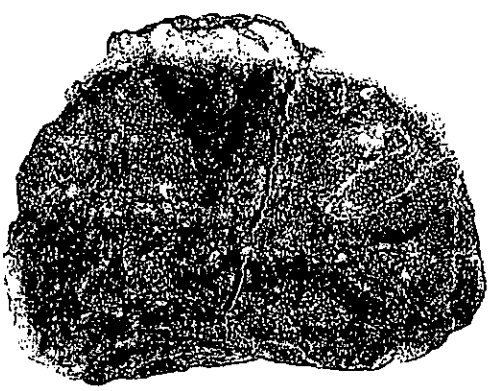

4 10 cm

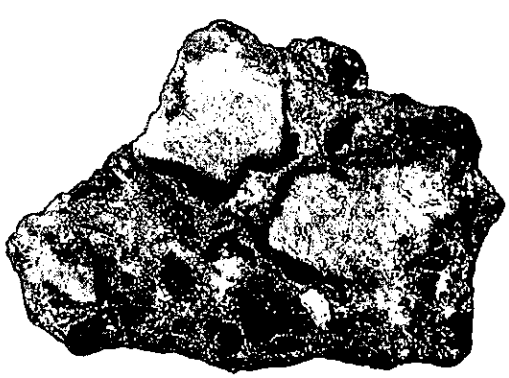

5 2 cm

6 5 cm

7 2 cm

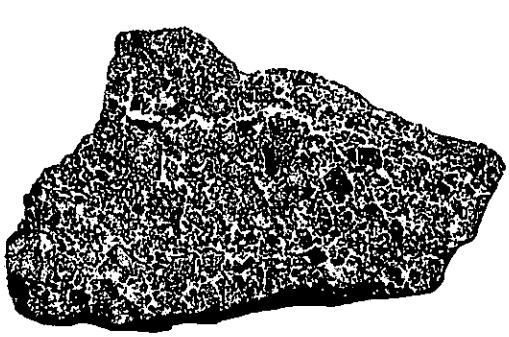

8 2 cm

**Figure 11:** (left page) Photographs of volcanic rocks from dredges along the southern slope of Tropic Seamount. **1.** Sample 693-1. Thick (1-1.5 cm) banded manganese crust surrounding brown, altered, moderately vesicular basalt fragments. **2.** Sample 694-1. Strongly altered tachylitic vesicular basalt fragments, now mostly replaced by carbonate which replaced former phillipsite filling. Many vesicles are partly filled by matrix. Thick banded manganese crust. **3.** Sample 694-4. Large round basalt fragment. **4.** Sample 694-6. Highly vesicular and strongly altered basalt with light colored former glassy rim. **5.** Sample 699-1c. Trachyte breccia. **6.** Sample 703-1. Bedded to graded bedded tuff/lapillistone with yellow/brown altered clasts cemented by carbonate. **7.** Sample 703-3. Well-sorted basaltic lapillistone to coarse tuff with carbonate cement and Mn encrustation. **8.** Sample 703-4. Well-sorted, coarse-grained basaltic lapillistone, strongly cemented by carbonate. Particles 50% vesicular.

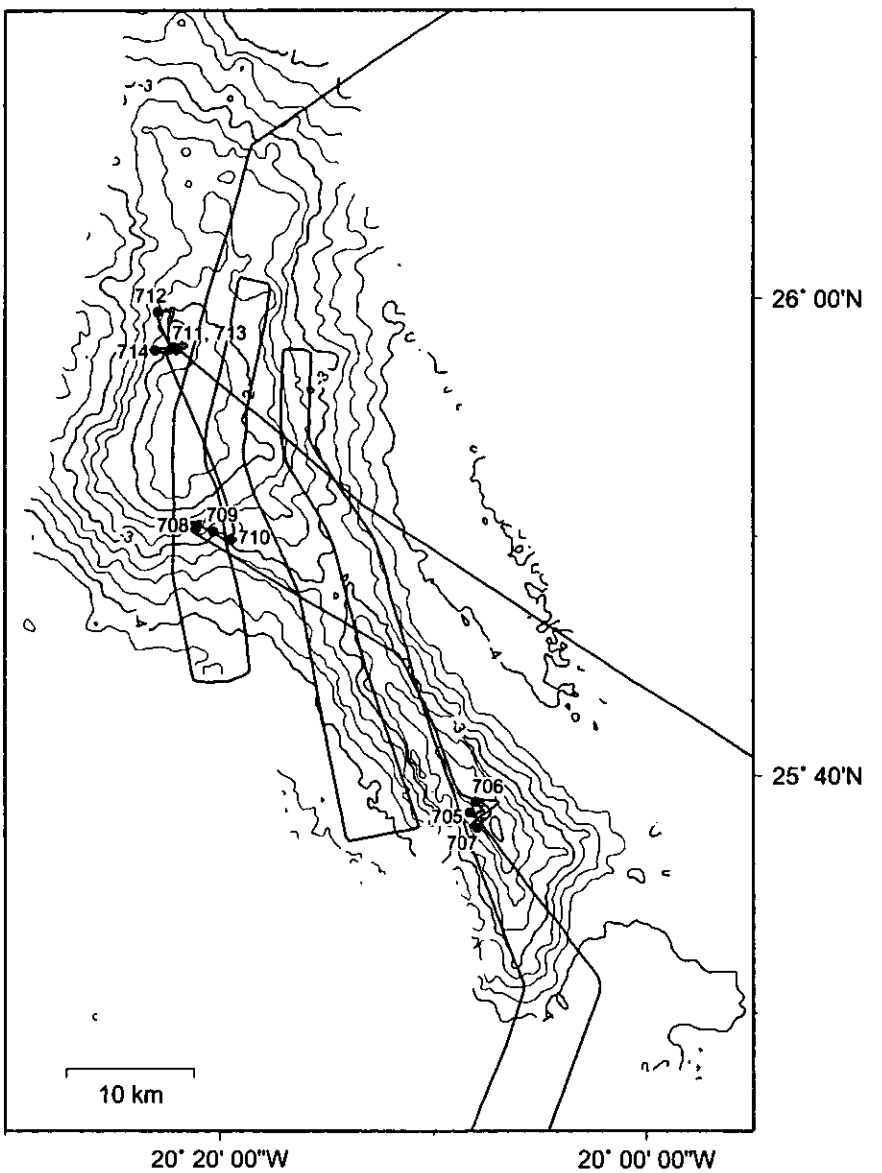


**Figure 12:** Bathymetric multibeam map of Paps Seamount with 250 m contour-lines, locations of dredge stations and tracks.

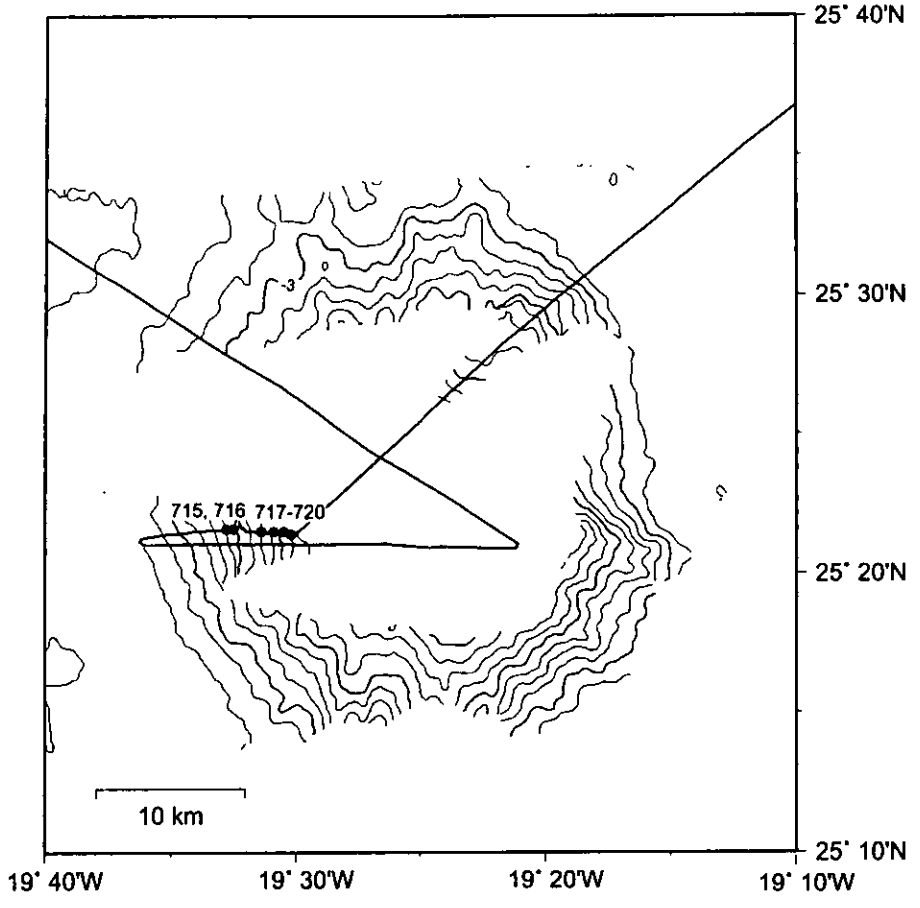


**Figure 13:** Bathymetric multibeam map of Endeavour Seamount with 250 m contour-lines, locations of dredge stations and tracks.

*Endeavour Seamount*

Endeavour Seamount, 90 km SE of Paps Seamount and 200 km N/NE of Tropic Seamount, rises to a height of 350 m bsl from a depth of 3500 m (Fig. 13). The diameters at the base and top are 40 km and 15 km, respectively. No previous dredge studies of Endeavour Seamount are known.

Because of its flat top, Endeavour Seamount is also a guyot, but we did not find additional evidence for the former island origin of this volcano because dredging at shallow depths was unsuccessful. Volcanic rocks comprise clinopyroxene-phyric basalt and basaltic lapillistone and scarce amphibole-bearing intermediate samples.

*El Hierro Seamount*

El Hierro Seamount, 100 km N of Endeavour Seamount, rises from a depth of 3300 m to a height of 1100 m bsl. The basal dimensions are 40 x 20 km. No previous dredge studies are known. Growth of El Hierro Seamount has probably terminated before it reached an island stage. Four dredges were carried out on the western flank of the El Hierro Seamount (Fig. 14), and contained mostly vesicular, coarse-graind basaltic rocks.

*Kiel Seamount*

An unnamed seamount 45 km SW of El Hierro rises 600 m above the surrounding seafloor from 3650 to 3050 m bsl (Fig. 1). We carried out 2 dredges and recovered aphyric vesicular basalt.

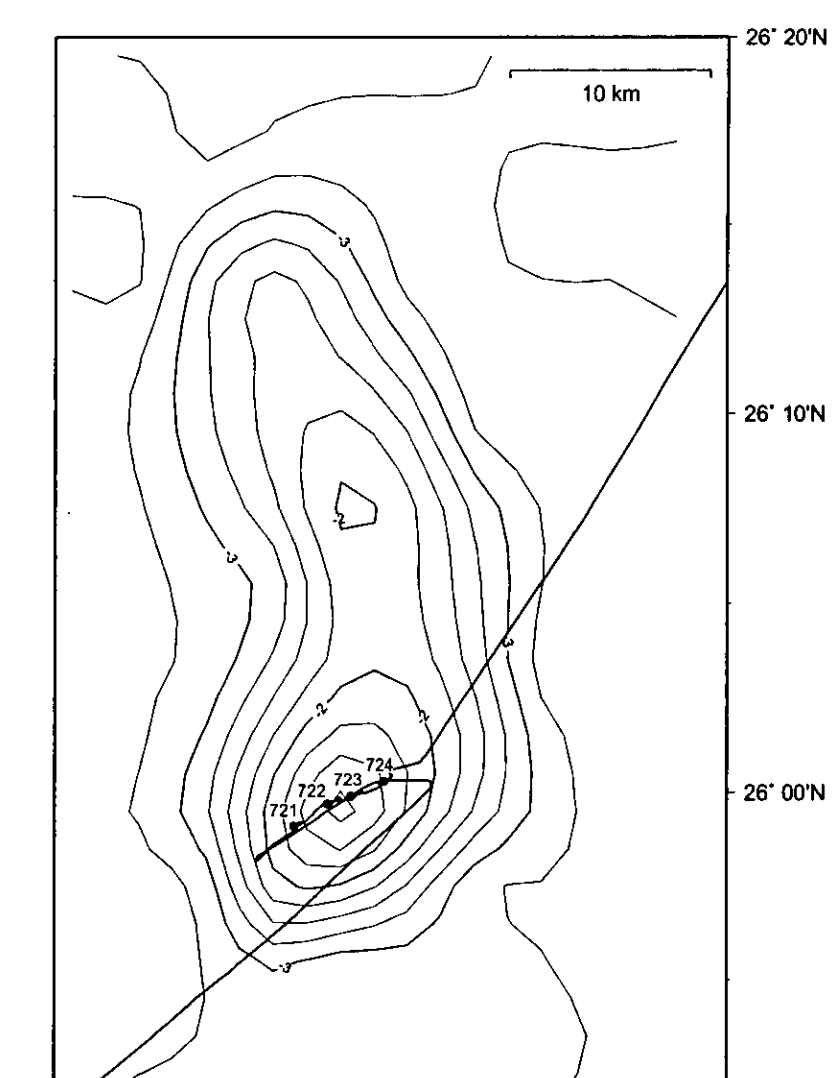


**Figure 14:** Simplified bathymetric map of El Hierro Seamount with 250 m contour-lines, locations of dredge stations and tracks. Bathymetry is taken from Smith and Sandwell (1997).

### 5.1.4.3 Flanks of Tenerife and Gran Canaria

A major goal of the M43/1 cruise was to study the submarine flanks of large oceanic islands in order to find the boundary between submarine and subaerial rocks. Identification of such a boundary helps to reconstruct the subsidence history of an island, to monitor the nature of deposits of the submarine structure, to have calibrated barometers of volatile contents of lava, and to monitor a change or otherwise in chemical and mineralogical composition of the submarine compared to the subaerial lavas. The main target areas for the study of these problems were Gran Canaria and Tenerife (Fig. 15).

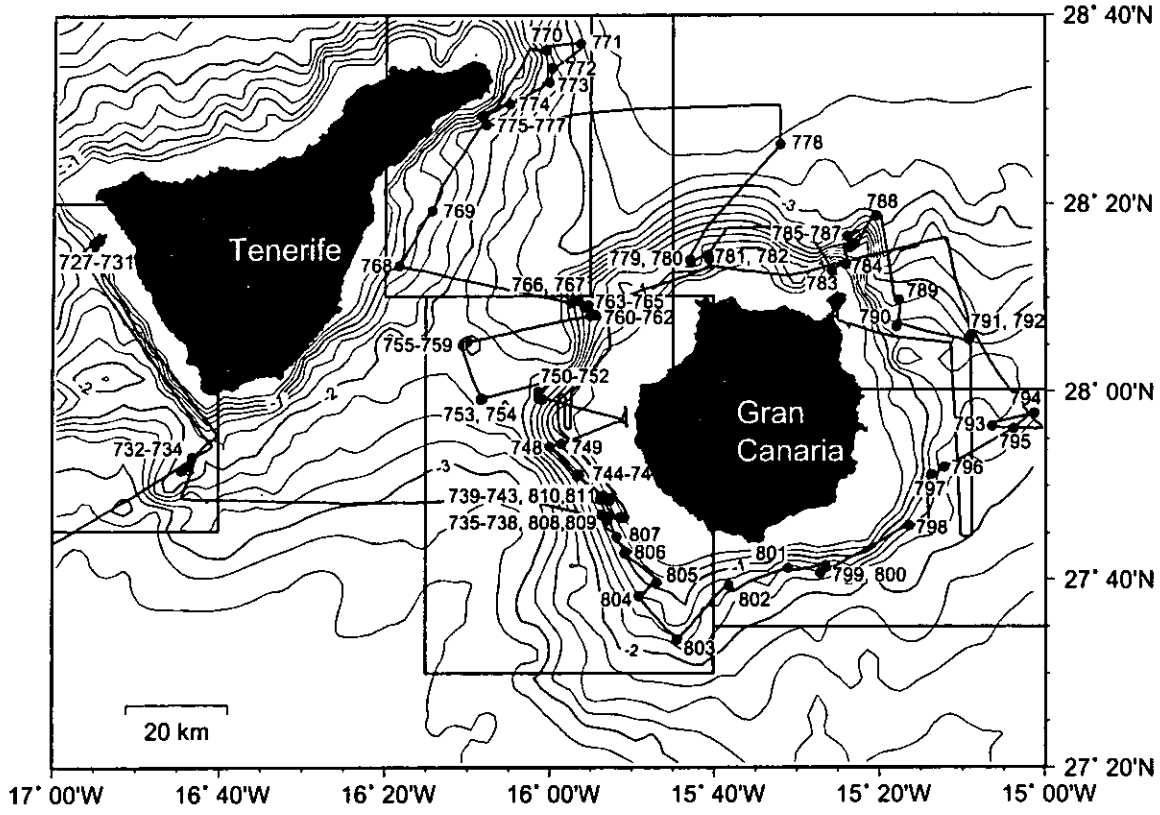


**Figure 15:** Overview map of working areas around Tenerife and Gran Canaria

*Tenerife*

We chose Tenerife to address three problems. For one, it is the island postulated to have sunk some 2500 m during its post-shield history (WATTS AND MASSON, 1995). Secondly, it is dissected by many large landslide scars. Some morphological hummocks off Güimar, possibly huge landslide blocks, were another aim. Thirdly, we wanted to find out if some morphological textbook-like features on the submarine flanks of the island suggestive of submarine volcanoes were young or even active.

To address question (1) we dredged at three areas around Tenerife. Dredging the northwest corner of the island northwest of Los Gigantes was of moderate success (Fig. 16). More clear-cut evidence for submarine eruptions at depths as low as 600 m was found off the southwestern Punta de la Rasca and southeast of the Miocene shield basalt area of Anaga (Figs. 16 - 18). Fresh, evidently quenched basalts, some with glassy crusts are excellent samples for detailed study of their ages and chemical composition. They represent additional important evidence that the boundary between subaerial and shallow water eruptions has to be sought in the upper 500 m or so below sea level rather than at 2500 m depth. One submarine hill dredged off Güimar turned out to be a submarine scoria/lapilli cone rather than a landslide block. This discovery contributed to help answer question two.

Hijo de Tenerife (Fig. 19) was our main goal. The conical volcano, rising some 600 m from a depth of 2300 m, its top being at a depth of 1700 m below sea level, seems to be covered (four dredges) largely of microvesicular mafic phonolite bombs (Fig. 20). We cannot exclude that the eruptions took place in historic or pre-historic times. While the material dredged consists of bombs, their moderate vesicularity (<20 vol.%) is important for calibrating the vesicle barometer. For this tephri-phonolitic composition, significant vesiculation starts as deep as 2000 m or more. Most striking is the large abundance of mostly fine-grained, partly digested xenoliths in

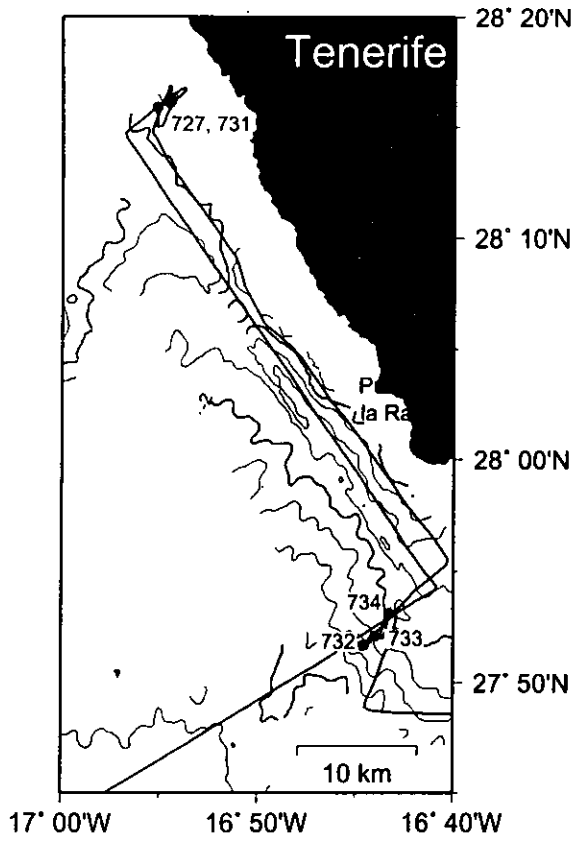


**Fig. 16**: Bathymetric multibeam map of the submarine flank southwest of Tenerife with 200 m contour-lines, locations of dredge stations and tracks.

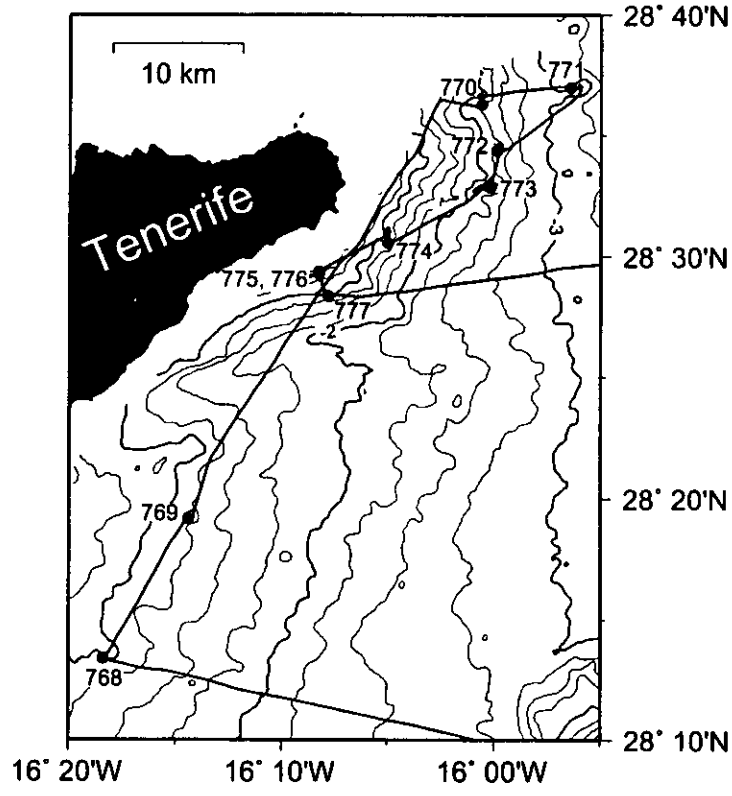


**Figure 17:** Bathymetric multibeam map of the submarine flank northeast of Tenerife with 250 m contour-lines, locations of dredge stations and tracks.

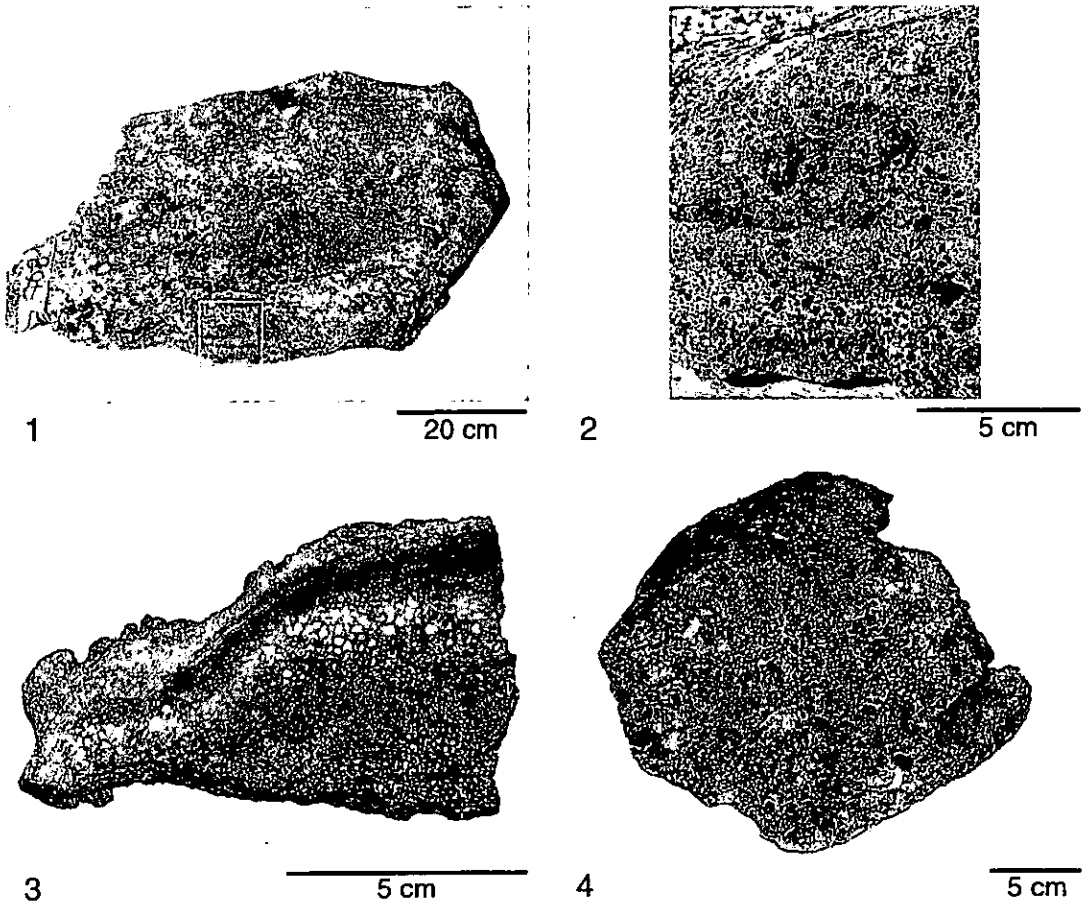


**Figure 18:** Photograph of volcanic rocks from dredges along the submarine flank of Tenerife. **1.** Sample 768-1. Well-sorted basaltic lapillistone, clasts ranging from 1-12 mm in diameter. Lapilli are brown and highly vesicular. **2.** Sample 768-1. Close-up. **3.** Sample 771-1. Fragment of highly vesicular (> 50 vol.%) basalt, vesicles decreasing strongly in diameter from outer surface to center of specimen. Vesicles in the outer rind are filled with carbonate sediments, and in the middle part are lined with zeolite, some globular, possibly phillipsite while the vesicles in the center of the piece are lined with light-brown material being a coating on zeolite which in term is a coating of the vesicle interiors. Well-developed 1 cm banded manganese crust. **4.** Sample 774-1. Unconsolidated brownish altered basaltic lapillistone and a few ash-sized fragments surrounded by manganese crust.

this rock. We think that, as the viscous magma slowly moves up through the thick sedimentary cover, it is slowly expanding but at the same time becomes quenched along the contact with the water-saturated sediments. This must inevitably lead to cracking and intake of all sorts of sediments, some of which becomes incorporated, partially digested and carried upward until the magma batch erupts at the surface. The ribbon-like structure on the surface of many of these bombs dredged suggest to us that the magma is squeezed through small openings like viscous dow when making Christmas cookies. Such an extrusion process is supported by the extreme alignment of vesicles, phenocrysts and microlites in these rocks.

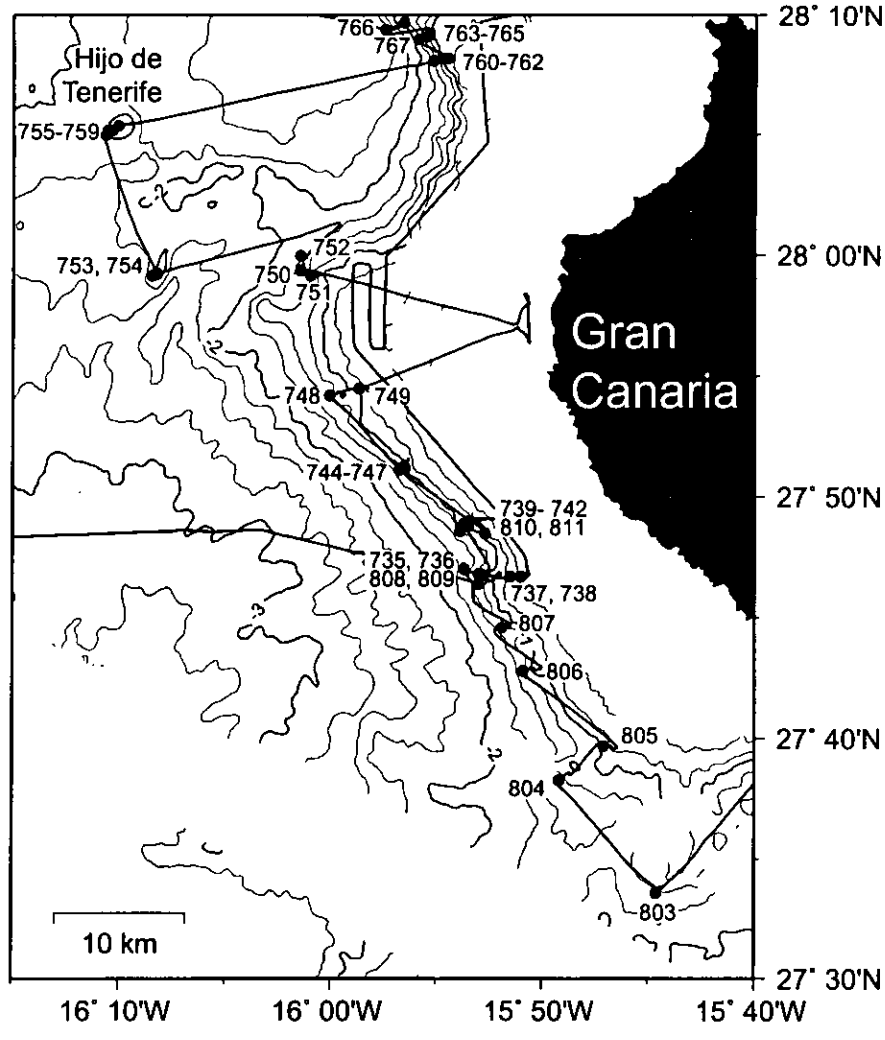


**Figure 19:** Bathymetric multibeam map of the submarine flank West of Gran Canaria with 250 m contour-lines, locations of dredge stations and tracks.

*Gran Canaria*

We dredged the submarine flank areas off southern, western, northern and eastern Gran Canaria as well as within the channel between Gran Canaria and Tenerife which is defined as the area enclosed approximately by the 3000 m contour-line (Figs. 19, 21, 22). The submarine flanks of the island are quite variable in shape and gradients, steep gradients characterizing scalloped zones in the southwest, west, northwest and north-northeast. It is not clear whether these are true scallops, caused e.g. by large landslides or are due to sediment fans or lines of submarine volcanoes enclosing embayments but the interpretation as landslide scars seems most plausible at present. The submarine flanks of Gran Canaria extend about 40 km both to the north and south to the edge of sedimentary basins sloping extremely gently between ca. 3400 and 3650 m, the northern basin being slightly deeper than the southern one, possibly due to higher sediment influx from the continental slope into the latter.

The stratigraphic continuity of the rocks dredged off SW and W Gran Canaria with the land stratigraphy is impressive. Around 1000 m bsl, very clinopyroxene and olivine-rich basalt, some picrites, corresponds to the Miocene Güigüi Formation on land (Fig. 23). They are overlain by

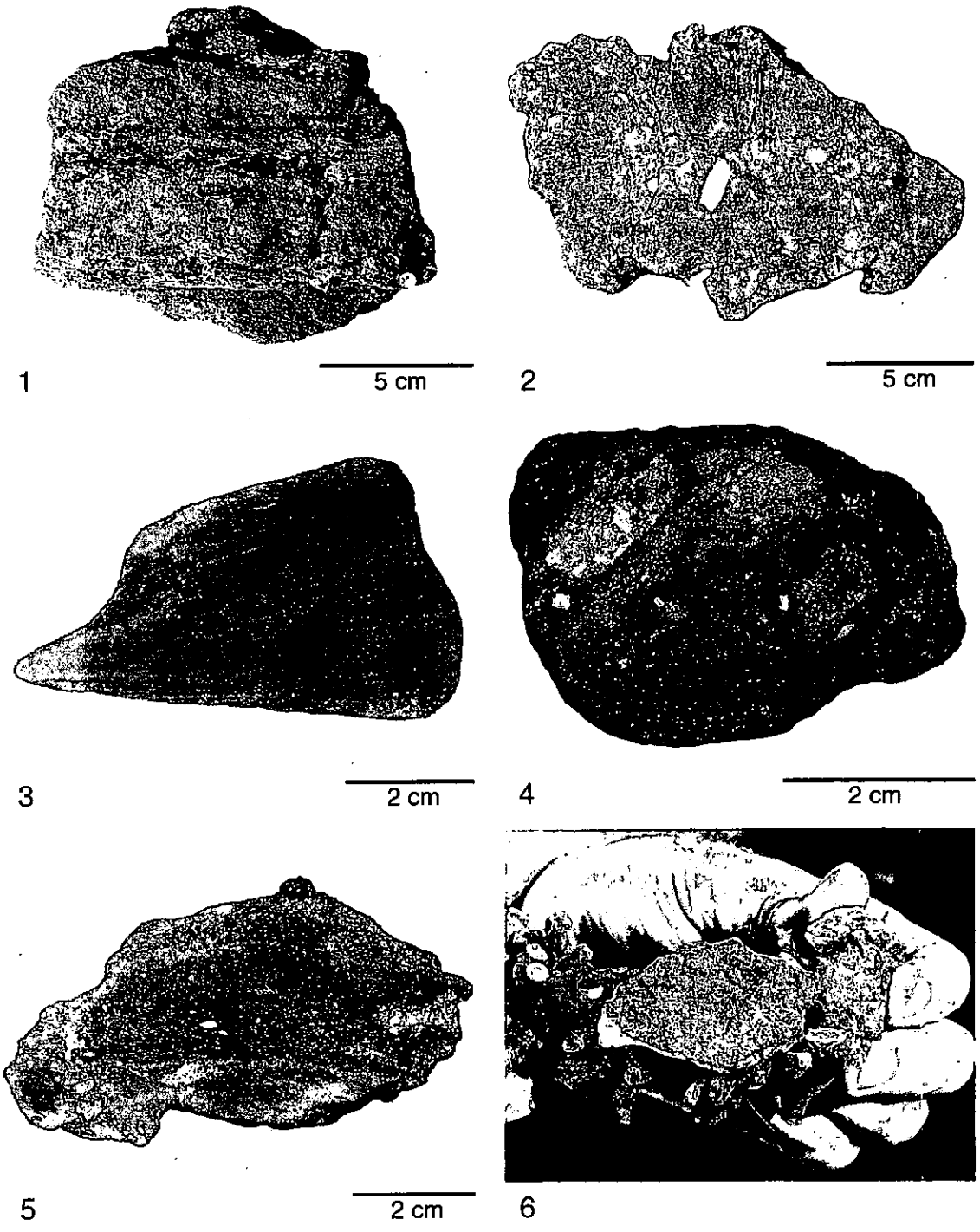


**Figure 20:** Photographs of mostly volcanic rocks from dredges on Hijo de Tenerife. **1.** Sample 755-6. Bread-crusted ribbon bomb. **2.** Sample 755-7. Cross-section through bread-crusted bomb showing abundant inclusions characteristic for rocks from Hijo de Tenerife (metasediments, basanite schlieren and peridotite fragments). **3.** Sample 755-1. Contact-metamorphosed quartzite, possibly piece of Mesozoic sediment. **4.** Sample 755-7. Breadcrusted bomb with metasediment inclusions. **5.** Sample 755-8. Cross-section through bread-crusted bomb showing elongate vesicles (ca. 20 vol.%) and inclusions. **6.** Peridotite xenolith overgrown by coral.

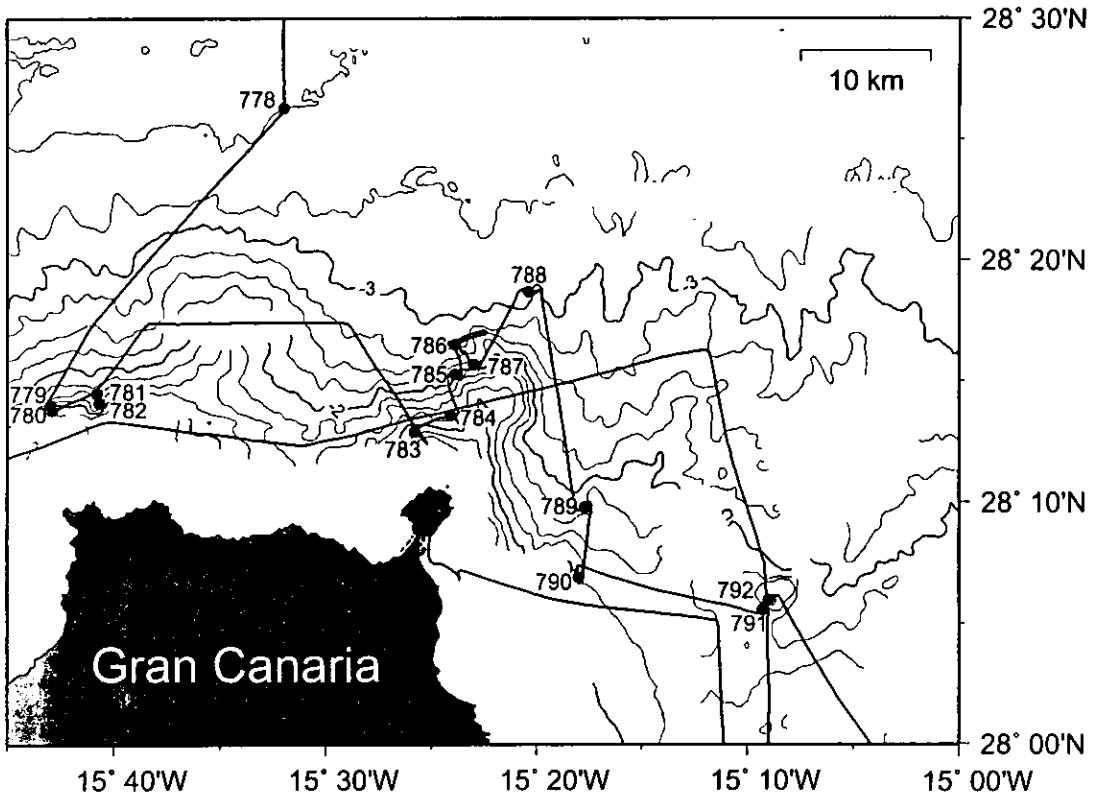


**Figure 21:** Bathymetric multibeam map of the submarine flank north of Gran Canaria with 250 m contour-lines, locations of dredge stations and tracks.

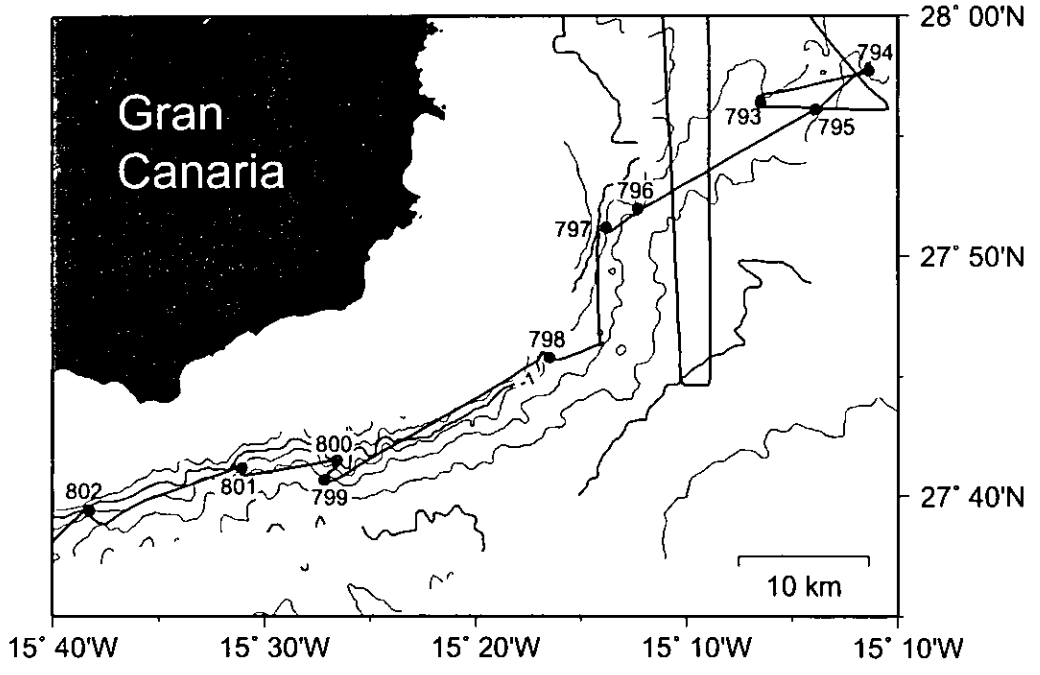


**Figure 22:** Bathymetric multibeam map of the submarine flank southeast of Gran Canaria with 250 m contour-lines, locations of dredge stations and tracks.

either almost aphyric basaltic rocks or by those devoid of olivine but with abundant plagioclase and small clinopyroxene crystals. These compositionally more evolved rocks that were dredged at higher elevations than the picrites correspond both compositionally and stratigraphically to the lavas of the Horgazales formation on land. At still higher elevation, the glassy rhyolite lava flow VL (Mogán Formation on land) and glassy phonolite lavas (Fataga Formation on land) were dredged. All the three rock types are in their stratigraphic continuity and were emplaced beneath water as shown by a variety of textural and structural characteristics, such as glassiness or very fine grain size and vesicles with sucked-in matrix. Most basalts are dense to very poorly vesicular, possibly indicating that they flowed from land into the sea. This strongly contrasts with the true submarine rocks dredged from both La Palma and El Hierro submarine ridges.

### 5.1.5 Conclusions

1. Continental rocks were not found on any of the flanks of the Canary Islands nor on the seamounts. The islands and seamounts have grown as independent volcanic complexes from the seafloor.

2. A recently postulated model implying sinking of Tenerife by 2.5 km during the past three million years was not corroborated. All the rocks dredged to water depths as shallow as 600 m – the minimum depth for dredging during the cruise – were erupted in water, implying that Tenerife could not have sunk more than a few hundred meters.

3. The abundance of highly evolved volcanic rocks is extremely high on the submarine ridges south of La Palma and Hierro as well as the southern seamounts (Las Hijas de Hierro and Tropic Seamount). These magmas have probably evolved from basaltic parent magmas and do not represent partial melting products of the lower ocean crust (confirmation by trace element analysis and isotope ratios pending) implying larger magma reservoirs probably at the base of the oceanic crust.

4. More than 30 new volcanic cones more than 100 m high were discovered and mapped in detail by Hydrosweep. Most rise between 100 - 200 m above the surrounding seafloor and have basal diameters of 1 - 3 km.

5. The seamount density south of El Hierro is very high. Volcanic activity along the northwest African volcanic belt is even higher than previously estimated and contradicts the model of

**Figure 23:** (right page) Photograph of volcanic rocks from dredges along the southern and northern flanks of Gran Canaria. **1.** Sample 736-1. Breadcrusted glassy crust of rhyolite lava resembling 14.0 Ma old rhyolite lava VL on land. **2.** Sample 736-4. Cross-section through very fine-grained to glassy, quenched rhyolite lava showing scattered phenocrysts of sodic anorthoclase and minor mafic phenocrysts. **3.** Sample 750-1. Mixed glassy lava with abundant feldspar and minor olivine phenocrysts. **4.** Sample 790-1. Largely fresh 3-phase basalt fragments with at least 10 vol.% phenocrysts mostly fresh olivine and small amounts of clinopyroxene. **5.** Sample 800-3. Ryolithe with largely fresh dark centers to altered bulk of roc k. **6.** Sample 800-1. Altered VL rhyolite breccia. Some fresh mineralogy, but there are also phenocrysts of alkali-amphibole, pieces of phonolitic lava etc. as well as fossils suggesting formation post-Fataga. Former perlitic cracks are well shown.

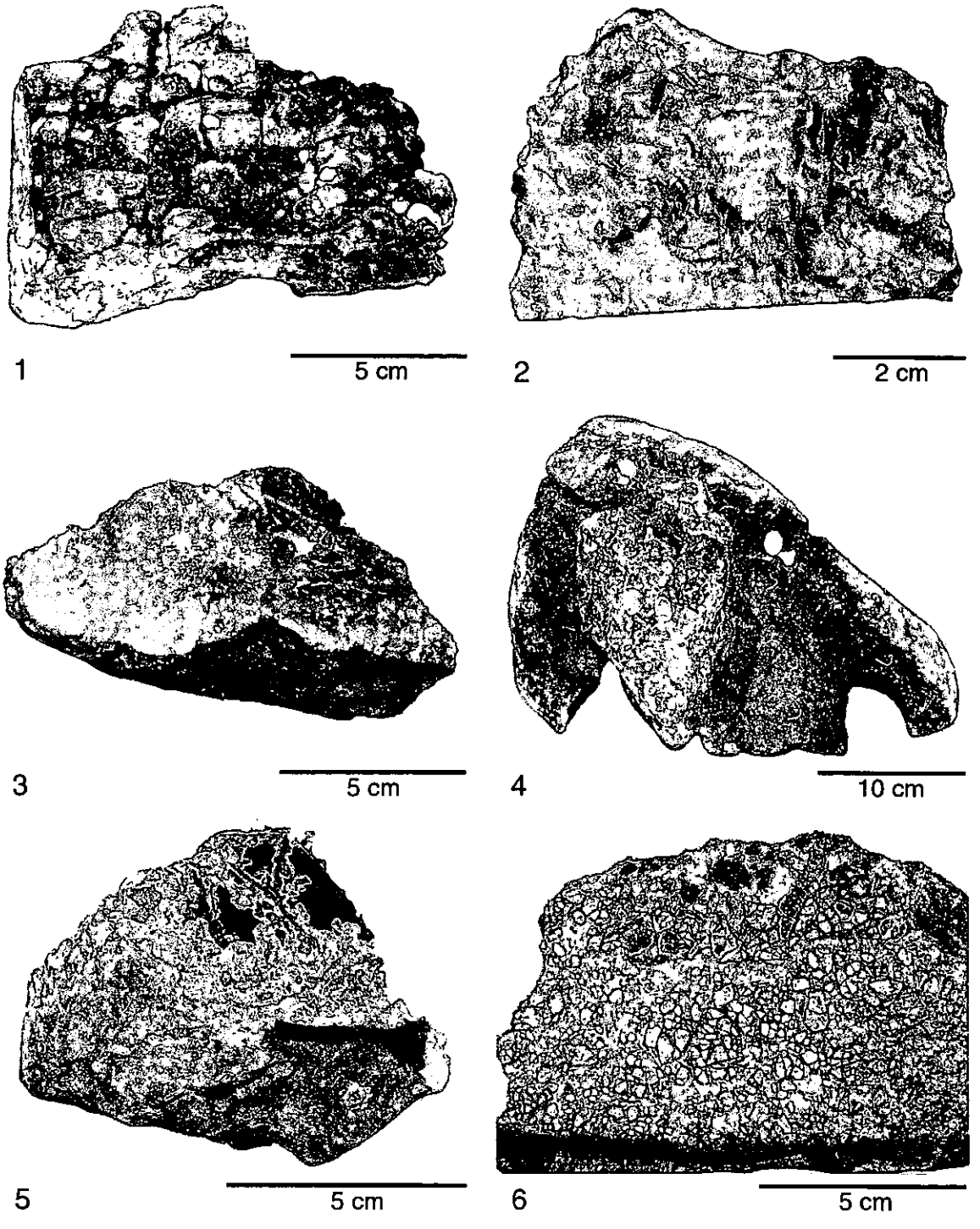


a single well-defined mantle plume. We are developing the model of a leaky continental-oceanic lithosphere boundary.

6. Most rocks dredged from the flanks of the Canary Islands are surprisingly fresh and allow a detailed compositional analysis. Rocks from the seamounts of the Saharan Seamount group are more strongly altered.

7. Alkali feldspar phenocrysts in trachytic, phonolitic and rhyolitic rocks dredged from the Canary Islands and the southern seamounts will allow precise single-crystal age dating.

8. Lapilli-stones and submarine lavas dredged from the submarine ridges south of La Palma and El Hierro between 1000 and 2000 m bsl commonly contain 50% or more vesicles, interpreted as indicating high volatile concentrations in the magmas of the western Canary Islands. These findings necessitate re-calibration of barometers based on the abundance of vesicles in lavas erupted under water.

9. On the south-western and south-eastern flanks of Gran Canaria, phonolitic, rhyolitic and basaltic lavas of contrasting compositions (picrites, alkali basalts, mugearites) were dredged in a stratigraphic sequence corresponding to that known from land. These lavas are relatively dense and we interpret them as lavas that flowed from land into the sea and were degassed during subaerial transport.

10. We dredged debris avalanche deposits in the channel between Gran Canaria and Fuerteventura and tentatively interpret them as being part of the ca. 3.5 Ma old Roque Nublo debris avalanche events.

11. Some 30 $km^2$ of a debris avalanche area south of El Hierro were mapped by HYDROSWEEP.

12. The submarine ridges south of La Palma and El Hierro are 3 - 5 km wide and up to 40 km long with steep lateral and terminal slopes. They are interpreted as discrete rift zones. Abundant seamounts on the ridges suggest locally developed conduit systems.

13. One of the most interesting volcanoes dredged is Hijo de Tenerife, about 600 m high (2300-1700 m bsl) discovered by us during METEOR Cruise M24. It has a basal diameter of about 5 km. Several dredges contained entirely bomb-shaped breadcrusted volcanic particles up to 20 cm in diameter. These very fresh rocks are of intermediate composition but contain both entire and fragmented peridotite xenoliths as well as slightly metamorphosed sandstones of possibly Mesozoic age. The volcano is speculated to be still active.

## 5.2 Leg M43/2 (OMEX)

### 5.2.1 Physical Oceanography

#### 5.2.1.1 CTD Methodology

(Roy Lowry, Ricardo Torres, Holger Pielenz)

The CTD system used on the cruise was a Sea Bird SBE-9+ underwater unit fitted with a Sea Bird SBE-33 12-bottle rosette. A Beckman oxygen sensor and a SeaTech 25 cm path length 661 nm wavelength transmissometer were fitted to the package. The system was driven by a Sea Bird SBE-11+ deck unit. Data were logged by a laptop PC running Seasoft version 4.214. Twelve rubber-sprung 10-litre Niskin bottles were mounted on the rosette.

The temperature, oxygen and salinity sensors were recalibrated in November 1998. No reversing thermometers were available but previous experience with SBE-9+ sensors give confidence in the accuracy of data based on such a recent calibration. Water samples were taken for post-cruise salinity determination to check the CTD salinity calibration. The oxygen sensor will be recalibrated against water bottle data from the University of Liège.

The pressure calibration was checked by comparing the sum of the CTD depth plus altimeter height against PARASOUND water depth measurements. Good agreement was obtained.

The CTD transmissiometer (SN 104D) calibration was based on air reading data taken in September 1997. Careful measurements during the cruise indicated that the light source had deteriorated and that the voltage reading in air was now 4.597 V (blocked path reading 0.001 V).

The data will be further worked up, including spike editing and recalibration of the oxygen, transmissometer and (if necessary) salinity data after the cruise by the British Oceanographic Data Centre.

#### 5.2.1.2 ADCP and ARGOS Drifters

(Ricardo Torres , Siân Clement)

Our main interest is focused on the poleward flow that develops seasonally along the slope of Eastern Iberia. During winter, the OMEX II region is generally under the influence of south-westerly winds. The upper layer circulation in this season is characterised by the presence of a narrow northward slope current which settles in November and disappears around May. This structure appears as a warm and saline intrusion (temperature 1-3°C and salinity 0.2-0.3 psu higher than surrounding values), trapped within about 50km of the shelf break, about 200-600m deep, and flowing along the slope with characteristic velocities of 0.2-0.3 $ms^{-1}$, extending more than 1500 km.

The poleward flow has been poorly surveyed so far but is a general feature of most eastern boundaries around the world. Repeated transects across the slope (with ADCP and CTD) and satellite images in conjunction with ARGOS drifter data will provide information about the spatial and short temporal variability of the flow.

*Method*

Our group is responsible for the operation of the vessel mounted ADCP and the launch of 4 ARGOS tracked drifters as well as being involved in the operation of the CTD, all of which will help to achieve our objectives.

The VM 75kHz Broad Band RDI ADCP (installed in the moon pool of the ship) has been used throughout most of the cruise. The depth range has been the full nominal range of the instrument (500-600m) when conditions were favourable and the ship was not sailing against the prevailing sea. The software used for the acquisition of the data was RDI DAS. The settings

were optimised during the first day of cruise and several parameters have been regularly checked for acquiring the best quality data (i.e. number of bins, automatic bottom tracking, etc..). The ADCP was set to average profiles over 5 minutes giving a dense spatial resolution with a vertical resolution of 16m. It was noticed that the transducer temperature sensor was consistently giving temperature readings 1.1°C less than the thermosalinograph.

On the 5th of January the 75 kHz ADCP was replaced by the 150 kHz Narrow Band RDI ADCP (permanently fixed to the hull of ship) due to a failure on the communication cable. The second ADCP also experienced problems with the ADCP deck unit and the PC used to run the acquisition software which meant gaps in the data collection while it was being repaired by the electronics engineers. The depth range of the 150 kHz ADCP was 200 m, recording 5 minute averages with a vertical resolution of 8 m.

During postprocessing a heading correction from the ASHTECH system onboard will be implemented as well as a calibration for the amplitude and phase offset.

Four SC40 ARGOS tracked drifters from SERPE-IESM® were released during the cruise. They are spherical (40 cm of diameter) mixed layer drifters equipped with a cylindrical HOLEY SOCK drogue (8 m length, 1.5 m of diameter) located at a depth of 15 m. The SC40 also measures the water temperature with an accuracy of ±0.3°C which is transmitted with every positioning message.

*Preliminary Results*

One of our main objectives for this cruise has been successfully achieved by the launch of the four drifters in a square cluster of 2nm on the 2nd of January of 1999. The positions are summarised under station 2 in chapter 7.2. Identification numbers of the 4 drifters are 4010, 3924, 4558 and 3923.

These 4 drifters have an expected life of 8 months and will be tracked for as long as they remain operational. Its data will contribute not only to the lagrangian knowledge of the poleward flow but also to estimate its statistical characteristics in terms of Mean and Eddy Kinetic Energy and Taylor mixing parameters (lateral diffusivity and lagrangian Time and Length scales).

The distribution in a square cluster will also enables us to calculate the vertical vorticity of the flow and particle dispersion. We expect them to follow the poleward flow along the eastern Iberian margin and continue along the slope into the Bay of Biscay unless they are driven offshore by mesoscale eddies associated with the slope current.

The ADCP has been continually recording data but several cross-shelf sections (station 3,) were requested by our group.

A cross-slope CTD section (Stations 18, 19, 21 and 24) along 42° 09'N was carried out to determine the width and vertical scale of the poleward flow over the slope. The station positions are given in chapter 7.2.

During the station number 24 the ADCP showed the passing of an inertial oscillation (long period wave of ~18 hours). The upper 200 m of CTD and ADCP data will be used in the description of such oscillations.

The ADCP and CTD sections have shown the poleward flow to be a slope process extending to a depth of 700 m with a characteristic velocity of 20 $cms^{-1}$. The drifter trajectories moved northward following the bathymetry in good agreement with the CTD and ADCP data.

## 5.2.2 Marine Chemistry

### 5.2.2.1 $pCO_2$ - Measurements

(Alberto Borges)

The role in the global inorganic carbon cycle of continental shelf seas influenced by seasonal upwelling remains controversial because they are sites of processes that have antagonist effects on the flux of carbon dioxide across the air-sea interface. Upwelling brings to the shelf water oversaturated in $pCO_2$ in respect to the atmosphere. This water has also an important nutrient content which enhances primary production that in turn reverses the air-sea gadient of $pCO_2$. To improve our understanding of these regions more field data are needed with an adequate resolution both in time and in space. To meet this goal, two approaches are used: the mapping of surface $pCO_2$ and the description of the vertical distribution of inorganic carbon.

*Method*

The determination of $pCO_2$ is carried out using both direct and indirect methods. The direct one consists to equilibrate seawater with air and then measure $CO_2$ using an IR analyser. The indirect one relies on the calculation of $pCO_2$ from experimental determinations of pH and Total Alkalinity (TAlk). These measurements can also be used to calculated the dissolved inorganic carbon (DIC) which can be used together with dissolved oxygen (Winkler method) to discuss $CO_2$ dynamics with linked biological, physical and chemical processes.

*Preliminary Results*

The underway measurement of $pCO_2$, pH and dissolved oxygen were carried out throughout the cruise. Discrete samples for pH, TAlk (total alkalinity) and dissolved oxygen were obtained from the rosette at 12 stations (1,8,10,11,12,13,15,17,21,24,25,28) and 169 dephts:

Fig. 24 shows preliminary results of underway partial pressure of $CO_2$ ($pCO_2$) and pH measurements carried out during the OMEX cruise on board of the Meteor (January 1999). The plot corresponds to the transect along 42°09N (OMEX S-line) obtained during the 8th January. There is a marked gradient in $pCO_2$ values between the continental shelf and the offshore oceanic region. The higher $pCO_2$ values on the continental shelf can be related to a relatively weak upwelling event revealed by SST satellite images (available at http://www.pol.ac.uk/bodc/omex.html). From the water temperature distribution the influence of the warm poleward slope current ('Navidad') is not apparent. This can be explained by the fact that the northerly winds observed prior and during the cruise inhibited significantly the Navidad.

These observations are quite different from those obtained in the same area during the CHARLES DARWIN 110B cruise in January 1998 when the influence of the Navidad and the fresh water inputs from the rias were the dominant features influencing the subsurface distribution of $pCO_2$ (refer to: M. FRANKIGNOULLE, A. BORGES & K.T. DOTANSI (1998) Preliminary results of the distribution of the partial pressure of $CO_2$ ($pCO_2$) and related parameters off the Galician coast, in summer 1997 and winter 1998. OMEX first annual report. Available at http://www.pol.ac.uk/bodc/omex.html)

### 5.2.2.2 Methane Measurements

(Robin Keir, Gregor Rehder)

During Meteor Cruise 43/2, measurements of dissolved methane in the water column were made in order to assist in identifying water masses and their ages. Samples for stable carbon isotope ratio measurements on dissolved inorganic carbon were also collected. These provide informa-

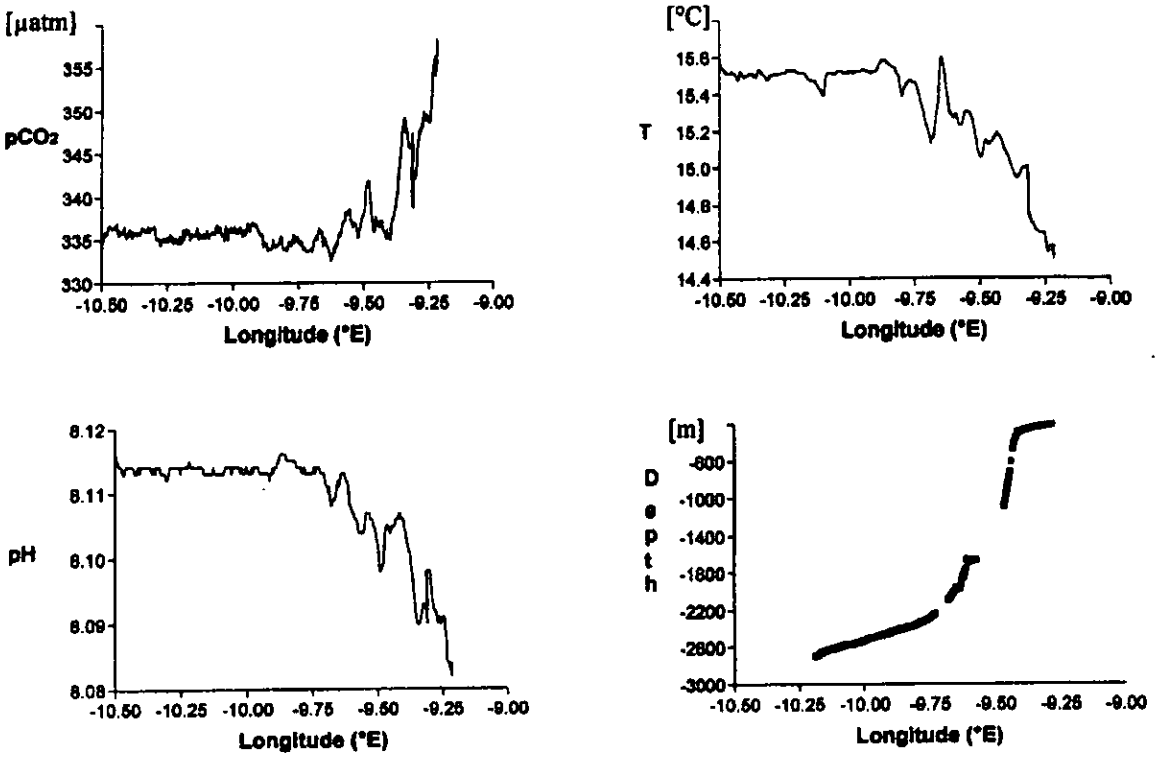


**Figure 24:** $pCO_2$, temperature and pH on a transect across the continental slope at 42°09N corresponding to the OMEX S-line.

tion on the biogeochemical cycling as well as penetration of anthropogenic $CO_2$ into the waters of the Iberian margin. Partial pressures of $CO_2$ and methane in surface waters were continuously measured underway with a dual equilibrator system for the purpose of intercalibrating with the $p(CO_2)$ (5.2.2.1) and providing addition information on the methane distribution.

*Methods*

Analysis of the dissolved methane concentration was carried out on board using a partial degassing extraction method. Water samples are drawn into a previously evacuated bottle that is then filled about half-way. During this process, the gas and water phases separate in the bottle. The gas phase is then transferred into a gas burette and recompressed to atmospheric pressure using a saturated salt solution. At this point a gas sample is taken into a gas syringe and injected into a gas chromatograph, where the methane is analyzed using a flame ionization detector.

The equilibrator consists of bubble exchange with seawater in a lower chamber followed by further exchange of the air as it continues upward into a glass column with the counter current flow of seawater down the inner wall of column. A small volume of air is periodically shunted out of the loop into a gas chromatograph, where the $CO_2$ is catalytically converted to methane that is measured by flame-ionization detection. A mixture of 361.1 ppmV $CO_2$ in natural air (Deuste Steiniger GmbH) was used for calibration. The gas chromatograph cycles automatically through a series of gas inputs from the equilibrator, the standard gas, and air from outside the ship for atmospheric measurements.

Dissolved inorganic carbon is acidified to $CO_2$ that is subsequently analyzed for its $^{13}C/^{12}C$ ratio in an automated mass spectrometer system at the Leibniz Labor, University of Kiel.

*Preliminary Results*

The dissolved methane concentration was analyzed from CTD stations 1, 7, 8, 10, 12, 14, 24, 25, 27 and 28. At 42°09N and 39°N, the vertical distribution of methane reflects the water mass structure, with concentrations generally decreasing from surface to bottom. However, the vertical methane distribution in the Sea of Cadiz shows a strong maximum at the depth of the lower branch of the Mediterannean Overflow Water (MOW). This indicates that there is a methane source within the intermediate waters of the Mediterannean Sea. It was also observed that at about 600 meters depth in the Sea of Cadiz, methane shows a relatively low concentration. This may support the recent hypothesis of van Aken, that remnant Antarctic Intermediate Water (AIW) is circulating into the region and rising over the MOW, assuming that AIW has depleted methane concentrations.

Isotope samples were collected at the stations listed above, and samples from stations 11 and 19 were taken as well. From the results of the shore-based measurements, the $\delta^{13}C$ of dissolved inorganic carbon off the Iberian Peninsula is observed to exhibit a functional relationship with dissolved phosphate. However, this relationship is not linear, as would be expected from a simple two box model of biological recycling. As at the Goban Spur, upper waters appear to exhibit a shift towards lower $\delta^{13}C$ than expected from expected due to new production alone, which is likely to invasion of isotopically light anthropogenic $CO_2$. At phosphate concentrations less than about 0.5 µmol/L, i.e. in the upper 200 meters or so, the relationship of $\delta^{13}C$ versus phosphate does follow the expected biological fractionation slope of about 1‰ in $\delta^{13}C$ per µmol/L decrease in phosphate. This may be because biological fixation of the upwelling carbon occurs on a much shorter timescale than the isotopic re-equilibration of the DIC with the atmosphere.

The partial pressure of methane in surface waters was observed from the equilibrator to be close to equilibration with the atmospheric mixing ratio. The $CO_2$ partial pressure was generally undersaturated. Our $CO_2$ results compare well with those of Borges and Frankignoulle's equilibrator, being within a few µatm of the values they measured with an infrared analyzer.

### 5.2.2.3 Spectrophotometric pH Measurement on Discrete Water Samples

(Karsten Friis)

A newly designed fully automated spectrophotometric pH-system for high accuracy pH measurement has been tested for 'at sea conditions'. 167 discrete water samples were analysed from 12 hydrocasts of 8 hydrographic stations (1, 7, 8, 10, 12, 14, 24, 25). 19 samples were stored for dissolved inorganic carbon (DIC) measurements.

The spectrophotometric pH determination is based on pH-dependent indicator dye spectra. For high accuracy pH-measurement in sea water, there are two indicators (thymolblue and metacresolpurple which have been calibrated on absolute methods within ± 0.002 pH-units on the total seawater scale ($\equiv pH_T$).

The first aim of the cruise participation was the precision and accuracy assessment of the pH-system. The precision assessment was done by replicate measurements. For accuracy assessment certified reference materials (CRM) from the Scripps Institution of Oceanography were used. For a thermodynamic consistency check pH- and Alkalinity values determined by A. Borges (see 5.2.2.1) will be used to calculate theoretical pH-values which will be compared with the spectrophotometrically determined pH. The additionally needed DIC will be determined at home.

The second aim was to check the consistency between the two indicator dyes through measurements on replicate samples with both indicators.

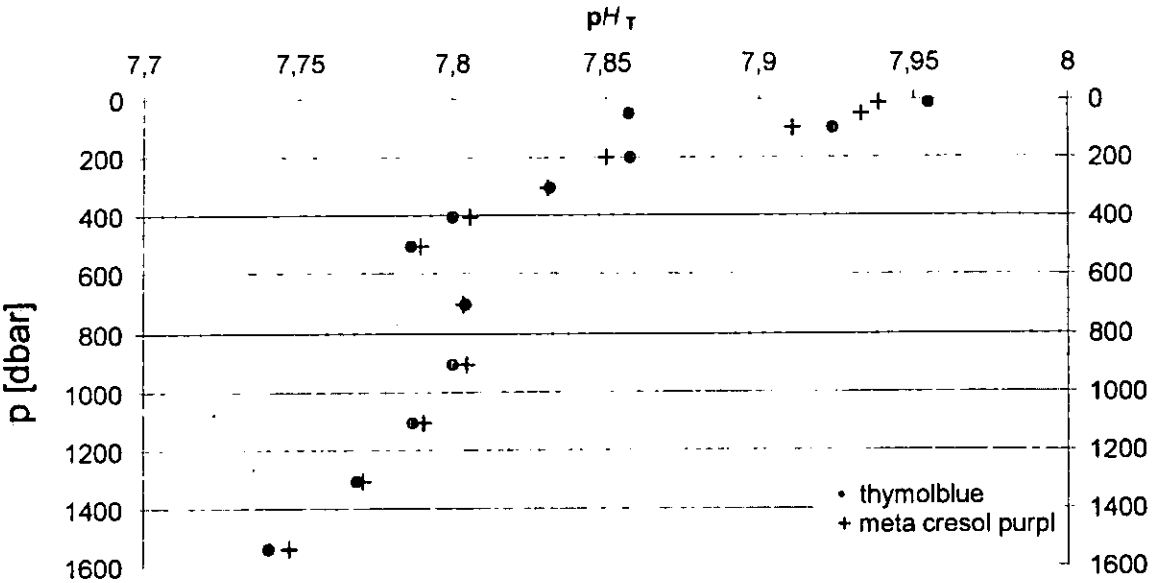


**Figure 25:** Vertical $pH_T$-profiles at station 12 measured on replicate samples with two different indicators. The profiles show in general a good agreement between both indicator series, although the pH values are not corrected for dye perturbation. - The indicator dye itself has acid-base properties, and therefore influences the sample pH.

Shipboard results depict a system precision of better than ± 0.002 pH-units for replicate samples. A first comparison of the pH-indicators meta-cresol purple and thymolblue show good agreements between both indicators (fig. 25).

### 5.2.2.4 Determination of DOC and DON Using High Temperature Catalytic Oxidation

(Georgina Spyres)

One of the key topics in the OMEX project (OMEX II-II Work Package II) is Dissolved Organic Carbon (DOC) and its impacts on the marine carbon cycle. Additional investigations on the processes that control the fluxes of organic carbon at the ocean margin will aid in the constructing and understanding the carbon cycle and its associated elements (eg. Dissolved Organic Nitrogen, DON). The analysis of DOC and DON involves the use of a rapid and precise technique, the high temperature catalytic oxidation (HTCO) technique.

Cruise M43/2 gave the opportunity to measure organic matter at the Iberian margin during the winter season. In addition it allowed an inter-annual investigation of DOC/DON results. Samples were collected from the CTD (stations 1, 7, 8, 10, 11, 12, 14, 16, 24, 25, 26, 27), the surface underway supply, and the bottom lander sampler (station 11).

*Method*

DOC/DON: The collection and preservation technique of sea water samples involved the 'clean' collection of water from the CTD rosette and subsequent filtration through GFF filters (Ø = 47 mm) into ashed (450°C, 4hr) 10 ml glass ampoules using a high-purity oxygen closed-

filtration system. The purpose of filtering is to exclude the particulate fraction from the final sample. Furthermore, each sample was acidified with orthophosphoric acid (30 µl) for preservation purposes. The ampoules were finally flame-sealed until analysis.

The HTCO technique involves the direct injection of aliquots of seawater samples that have been filtered, acidified and decarbonated, into the Shimadzu TOC-5000 analyser. The sample, carried by pure oxygen gas (99.999%), is passed through a catalyst (Al/Pt, 0.5%) at high temperatures (680°C) and converted to $CO_2$ gas. The latter is quantitatively measured by an Infrared Gas Analyser (IRGA) (i.e. LiCor). The data produced is recorded onto a PC-based integration system.

Through the use of an Antek 705D Nitrogen Specific Chemiluminescence Analyser, Total Dissolved Nitrogen (TDN) in the seawater sample can also be determined. The nitric oxide radicals produced from the combustion of nitrogenous compounds in the sample in an oxygen atmosphere at 680°C, react with ozone to produce excited nitrogen dioxide species, which emit quantifiable energy as they return to their ground state. Nitrogen based nutrient data is used to calculate the concetration of DON from the TDN measurements (DON = TDN- Inorganic Nitrogen).

NUTRIENTS: Seawater was collected from the CTD bottle into Nalgene plastic bottles (50ml) that were prewashed and acid-rinsed (5%HCl). Immediately after collection the bottles were stored in a freezer at -20°C. The samples will be analysed at the PML by Malcolm Woodward. There was not a chance to work up the preliminary data onboard.

### 5.2.2.5 Radionuclides

(Sabine Schmidt)

The aim of this investigation was to estimate particle residence time in intermediate nepheloid layers and in surface waters, using $^{234}Th$ ($t_{1/2}$= 24.1 d) / $^{238}U$ and $^{228}Th$ ($t_{1/2}$= 1.9y) / $^{228}Ra$ activity ratios. Furthermore $^{230}Th$ / $^{231}Pa$ were used to assess the importance of boundary scavenging and its variation in the vicinity of the continental margin.

For $^{234}Th$ and $^{228}Th$ measurements 40-liters seawater sample were filtered through a 0.45 µm filter. Due to the short half-life of $^{234}Th$ and to avoid significant ingrowth corrections, the separation of $^{234}Th$ from its $^{238}U$ parent is carried out on board within 24 hours after seawater collection. For analysis, $^{229}Th$ yield tracer and 120 mg Fe (as $FeCl_3$) were added to the dissolved sample after acidification to pH 2. After spike equilibration, $Fe(OH)_3$ was precipitated by adding $NH_4OH$ up to pH 7. After recovery of the precipitate, the separation of $^{234}Th$ and $^{238}U$ is obtained by passage through an anion exchange column (Dowex 1x8, 100-200 mesh) under 8N HCl conditions.

Within two months after the cruise, particulate $^{234}Th$ will be directly measured on the filter with a low background-high efficiency detector. Purification of dissolved $^{234}Th$ will be achieved prior to determination of chemical yield, derived from $^{229}Th$, and dissolved $^{234}Th$ activity by gamma-counting.

On board Radium is extracted from seawater by coprecipitation with $BaSO_4$. At the lab precipitates will be rinsed and dried, prior to measurements by gamma spectrometry within 6 months after the cruise. The following stations were sampled: 7, 10, 13, 16, 24 corresponding to the CTD-numbers 4, 10, 19, 22, 33.

For $^{230}Th$ / $^{231}Pa$ determination, $^{229}Th$ / $^{233}Pa$ yield tracers and 80 mg purified Fe are added to each total 20-liters seawater sample. The precipitate is recovered on board. Further measurements will be done by mass spectrometry at the Lamont laboratories, next autumn. The following stations were sampled: 8, 11, 24 corresponding to the CTD-numbers 7, 15, 33.

*Sediment*

By using selected isotopes with different half-lives we will focus on the characterisation of sedimentation pattern of the Iberian margin on short-time scale. With a multitracer approach (i.e. $^{234}Th_{xs}$ (24.1 d), $^{228}Th_{xs}$ (1.9 y), $^{210}Pb_{xs}$ (22.3 y) and $^{137}Cs$ (30 y)), we will better constrain the determination of the bioturbation rate coefficient, and in particular test the assumption of steady state at the sea-sediment interface. The occurrence of $^{234}Th_{xs}$, when observed in the uppermost layer of cores will indicate recently deposited particles.

Box-corer samples were taken from Station 9, multicorer samples from stations 9, 20, 24, 25 and 26.

On board, each core is sub-sampled. The top 5 cm were cut into 0.5 cm slices, deeper in the core into 1 cm slices and sealed into plastic bags. At the laboratory, sediments will be dryed at 60°C, then aliquots of 2-12 g will be measured by gamma spectrometry. The top of each core (2-3cm) will be measured within 1 month after the cruise in order to detect $^{234}Th$ in excess. The detectors in use are two well-type high efficiency germanium crystals (215 and 430 $cm^3$). Measured radionuclides will be: $^{210}Pb$, $^{226}Ra$, $^{234}Th$, $^{228}Th$, , $^{228}Ra$, $^{137}Cs$ and $^{40}K$ (expressed in %K).

### 5.2.3 Fluxes as Measured by Moored Sediment Traps and Suspended Particle Inventories

(Rolf Peinert, Kerstin Nachtigall)

In the framework of OMEX we determine the flux of particles at the northern Iberian Margin and interpret these fluxes in relation to the productivity and physical regime, also in comparison to the differing region at the Goban Spur. The main objective of our work during METEOR cruise 43/2, thus, was to gather information on winter non-upwelling conditions off NW Spain, and in detail:

- to obtain time-series recordings of sediment trap and current data to characterise vertical and horizontal fluxes of particulates at and across the continental margin. For this purpose deep-sea moorings fitted with automated sediment traps, current meters and transmissiometers had been deployed during a cruise with R/V PELAGIA in summer 1997 and recovered & redeployed (fitted additionally with *in situ* pumps) during the POSEIDON 327/1 cruise in late winter 1997. Final recovery of these mooring was planned for this cruise .
- to characterize suspended particle inventories in upper ocean layers off NW Spain for comparison with trap and in situ pump samples and as a contribution to describing seasonality of sources for particle flux. Particle load and composition in Intermediate Nepheloid Layers were sampled for a better assessment of their relative impact on fluxes measured by sediment traps at the continental slope.

*Sediment trap moorings*

Two moorings (IM 2-2 and IM 3-2) had been deployed along a transect at 42°38'N at water depths of 1500 and 2245 m in March 1998 (positions in table 5). The upper part of mooring IM 2-2 had been found adrift and had been retrieved by a fishing vessel far to the north of the initial mooring position in October 1997. The sediment trap, in situ pump and current meter deployed at ~600 m depth had functioned well. The in situ pump (Baltec GmbH, Germany) had been programmed to filter sea water onto 47mm diameter polycarbonate filters at the mid-time of the trap collection interval. Samples were poisoned in situ with mercuric chloride and stored water-tight until recovery. The respective trap and pump samples were handed over to IFM and are processed currently. Data from the also recovered current meter precisely indicated the date

when the mooring had been fished. Trap collections from prior to October are evaluated as reliable since the samples were sealed and poisoned. An almost complete set of trap samples, thus, is at hand for the upper (~600 m) horizon from mooring IM 2-2. During the METEOR cruise the remaining (deeper) part of this mooring (sediment trap, pump, current meter/transmissiometer) was searched and found at its original position on 4th January. Release was successful according to responses by both acoustic releasers. The array, however, failed to ascend to the surface, possibly due to a lack of buoyancy, and at a scale of hours upon release there were no signs for any horizontal drifting of the array. It has to be considered as a loss.

Recovery of mooring IM 3-2 took place under quite unfavorable weather conditions and state of the sea on 4th January. The whole array including all instruments could be recovered safely, however, due to the expert assistance of the crew of R/V METEOR. The deepest trap had malfunctioned, and flooding of the pressure housing was to be noted for the deepest current meter. The *in situ* pump deployed at 645 m provided 5 filters as pre-programmed but had failed to continue operation thereafter, and corrosion of the steel pressure housing was noted. A full set of 40 sediment trap samples and current meter/transmissiometer data from the two shallower depth horizons (~600 m and ~1000 m depth, see table below) was obtained from this mooring. First visual inspections of the trap samples revealed that fluxes at the mooring site had been substantial during selected sampling intervals and that variability is coupled to seasonal changes in the export regimes in the overlaying waters (related to seasonality in upwelling).

**Table 5:** Details of sediment trap moorings

| **Mooring** | **Water depth** | **Position** | **Instrument depth** | **Instrument** |
|---|---|---|---|---|
| IM 2-2 | 1500 m | 42°38'N, 009°42'W | 580 m | Sediment trap |
| | | | 600 m | Current meter |
| | | | 650 m | In situ pump |
| | | | 1050 m | Sediment trap |
| | | | 1070 m | Current meter |
| | | | 1120 m | In situ pump |
| **Mooring** | **Water depth** | **Position** | **Instrument depth** | **Instrument** |
| IM 3-2 | 2245 m | 42°38'N, 010°02'W | 570 m | Sediment trap |
| | | | 590 m | Current meter |
| | | | 645 m | In situ pump |
| | | | 1050 m | Sediment trap |
| | | | 1070 m | Current meter |
| | | | 1750 m | Sediment trap |
| | | | 1770 m | Current meter |

*Suspended particle inventories*

Hampered by foul weather and time constraints a reduced water column sampling programme was conducted at stations 7, 8, 10, 11, 13, 17, and 24 in the OMEX Box off NW Spain. Stations covered the shelf regime as well as those of the slope and of the adjacent deeper waters. 50 samples were taken *in toto* predominantly from the productive upper 200 m layer using the CTD rosette,. Between 2 and 12 l were filtered onto GF/F or Cellulosis Nitrate filters and stored at – 20 °C for later land-based determinations of dry weight, carbonate, POC, PON, Opal and $\delta^{15}N$. These samples will contribute to the basis for seasonal comparisons of suspended matter with sinking particles at the Iberian Margin. For the same reason suspended particles in intermediate nepheloid layers (INL) were sampled for analyzing possible differences in particle composition relative to waters above and beneath.

## 5.2.4 Benthic Ecology

### 5.2.4.1 The Benthic Resuspension Loop

(Laurenz Thomsen, Volker Karpen)

One of the aims of the benthic subproject within OMEX is to evaluate the role of biological processes in cycling of particulate organic matter within the benthic boundary layer (BBL). Our hypothesis is that lateral mass fluxes of particulate matter exceed the vertical fluxes, byepass the vertical transport pathway and that aggregates in the BBL play an important role in these fluxes. To understand and quantify these transport processes, both laboratory and field studies are required to link hydrodynamics with particle and bed formation. Advective near-bed fluid flow imports both particles and solutes from sources upstream (in addition to those arriving from above) that can serve as food (and fuel) for benthic communities. Through the coupling to the local ecosystem, more or less nutrient-rich, reprocessed or remoulded particles such as faecal wastes or detritus, and dissolved metabolites are subsequently exported (moved downstream). For a model as well as calculations of the mass fluxes associated with this bed-flow-biology interaction, several important particle and hydrodynamic parameters need to be determined: the bottom stress (t), expressed as friction velocity ($u_*$), the turbulence intensities and the mean local horizontal speed together with the controlling variables of sediment transport: the critical erosion stress ($t_c$) and the particle settling velocity ($w_s$).

The goal of this Meteor cruise was to determine these key parameters at the Vigo transect. In order to determine the horizontal particle fluxes, bottom water samples in the lowermost watercolumn (0-100 cm) were taken with the BIOPROBE system and the erosion resistance of slope sediments was determined. On a total of 6 stations between 200 and 4000 m water depth, onboard measurements with an erosion chamber were carried out and sediment samples were taken for laboratory flume experiments on biodeposition and bioerosion of slope sediments. Priliminary results showed that flow velocities at 40 cm height above bottom at the slope varied between approximately 2 and 15 cm/s and were either directed downslope or along slope. Benthic boundary layer (BBL) aggregates > 100 µm in diameter were resuspended under flow conditions > 8 cm/s and the critical shear velocity of the cohesive slope sediments increased with depth to $u_*$ of 1.4 cm/s. First deployments of a calibrated sediment trap, connected to BIOPROBE at 1.5 m height (in cooperation with the Technical University Hamburg-Harburg) will allow the determination of in situ particle size/ settling velocity relationship in the BBL. With a newly developed particle camera/Laser - Schlieren optic, near bed flow conditions and effluxes of dissolved substances were measured.

### 5.2.4.2 Phytopigments in the Sediment

(Marc Lavaleye)

The objective to participate the cruise was to collect sediment samples for the (HPLC) analysis of algal pigments. Because algal pigments, and specifically free chlorophyll-a, belongs to the category of very labile organic compounds it serves as a tracer for the fresh organic matter. Analysis by means of HPLC not only allows detection of chlorophyll and its degradation products but also of accessory carotenoid pigments. Because several carotenoids are highly specific for algal taxa they provide a clue on the source of the phytodetritus present near the sea floor. Also the short term mixing by benthic fauna can be resolved by means of the downcore distribution of pigments. For this purpose we have sectioned the sediment samples down to 10 cm.

*Method*

Sediment samples for study of the vertical pigment profiles were collected with a multi-corer. Two cores (Ø 10 cm) from as many multicores as possible were sliced in a cold lab (4°C) into the following layers: 0-1 mm, 1-5 mm, 5-10 mm, 10-15 mm, 15-20 mm, 20-25 mm, 25-30 mm, 30-35 mm, 35-40 mm, 40-45 mm, 45-50 mm, 50-60 mm, 60-70 mm, 70-80 mm, 80-90 mm and 90-100 mm. Cores were sliced as acurate as possible with the help of adjustable piston and 5 and 10 mm ring. The fluid upper one millimeter of the sediment was partly sampled with a syringe. All phytopigment samples were stored at -20°C and are taken to the NIOZ on dry ice for HPLC analysis. The analyses will be compared with the fluorometric determinations of Chlorophyll-a determined by Kähler et al. (5.2.4.3).

The first three stations sampled (stations 11, 20, 24) are situated on the OMEX S-transect along 42° 09' N, while the last two were taken in the Nazaré Canyon (stations 25, 26). The cores from the first two station were shared with Sabine Schmidt. At two other stations the multicore failed to bring up any samples or did not yield enough samples.

### 5.2.4.3 Bioturbating Macrofauna, Sediment Oxygen Demand, ATP and Food Quality

(Anja Kähler, Uli Franke, Florian Peine, Gerhard Graf)

Downslope transport of organic particles across the shelf edge is a major factor to determine benthic biomass and activity in continental slope habitats. The major objective during this cruise was to investigate a transect off Vigo as an example for a very narrow shelf and to compare the results with measurements in the Nazaré-Canyon, where an intensive focusing of downslope transport can be expected.

Benthic activity was described in terms of sediment oxygen demand, whereas biomass was measured as macrofauna and ATP-biomass. To characterise food quality C/N ratios and Chlorophyll-a were measured in the sediment. The latter will later also be used as natural tracer for the modelling of bioturbation. On the Vigo transect stations 11, 20, 24 and on the Nazaré-Canyon stations 25, 26 and 27 were sampled.

*Method*

The sediment samples were taken with a multiple-corer for Chl.a, C/N, POC, ATP, water content of the sediment, and core-incubation for SOD, or with a box-corer for macro-fauna and grain-size analysis. Macrofauna was sieved with a 0.5 mm sieve and fixed with buffered formaldehyde (4%). Special emphasis will be given to bioturbating fauna. The data will be combined with the analysis by João Luís da Silva Cúrdia (cf. 5.2.4.4)

All sediment samples (for: C/N, Chl.a, POC) are from the upper most 9cm of the sediment. The cores (Ø 10cm) were sliced in the cold lab (4°C) into 7 horizons: 0-0,5cm, 0,5-1cm, 1-2cm, 2-

3cm, 3-5cm, 5-7cm and 7-9cm. After slicing the sediment was homogenised by stirring and stored frozen (-20°C). All samples were taken home on dry ice for later analysis, only Chl. a measurements were carried out on board using a fluorometer after extraction with 90% acetone. The sediment for ATP-measurement was stabilised in phosphate-buffer and boiled in glycine-buffer for 30 min. at 90°C. The samples were kept frozen (-20°C). ATP-measurement will be done at home using the luciferine-luciferase assay.
Oxygen consumption was measured on board by Winkler-titration after whole core incubation for at least 12h in an incubation-box at in situ temperature.

*Preliminary Results*

Fig. 26 depicts high chlorophyll a concentrations in the Nazaré-canyon, reaching more than 0.4 µg $cm^{-3}$ in the deepest station investigated. All values were significant higher as compared to the Vigo transect suggesting that the canyon concentrates the downslope transport and works as a huge sediment trap. The shape of the profiles indicate intensive bioturbation which will not be explainable by diffusion analogy, but will need a significant non-local contribution.

Fig. 27 shows the sediment oxygen demand at the Vigo-transect at Stations 11, 20 and 24. The highest values of 4,4 mmol $O_2m^{-2}d^{-1}$ are observed at the shelf station (20) at a depth of 217m, at Station 24 the oxygen demand is 2,3mmol $O_2m^{-2}d^{-1}$ (2765m) and at Station 11 it is 1,9mmol $O_2m^{-2}d^{-1}$ at a depth of 1952m.

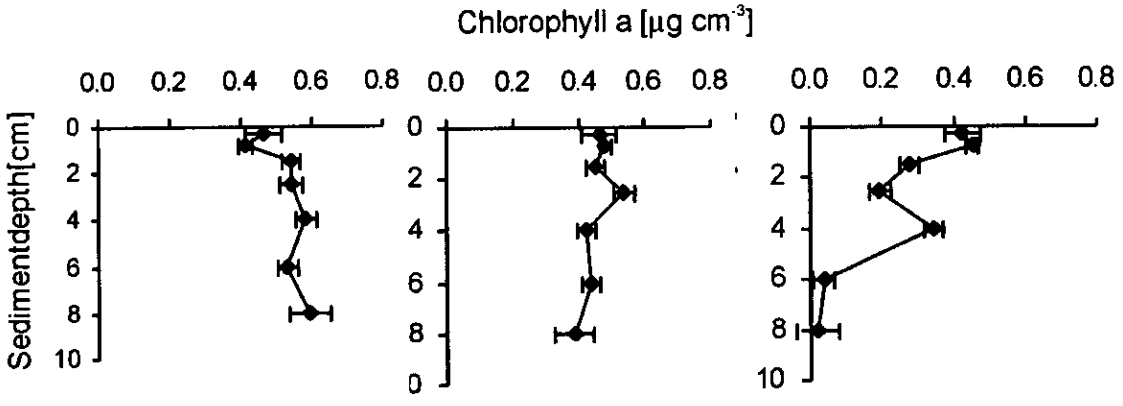


**Figure 26:** Chlorophyll a in sediments of the Nazaré-canyon

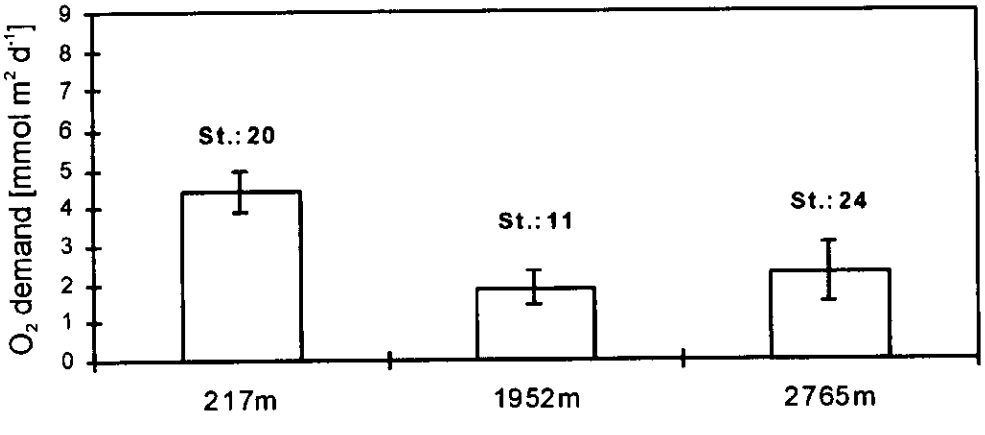


**Figure 27:** Sediment Oxygen Demand on the Vigo transect. Error bars give the standard deviation.

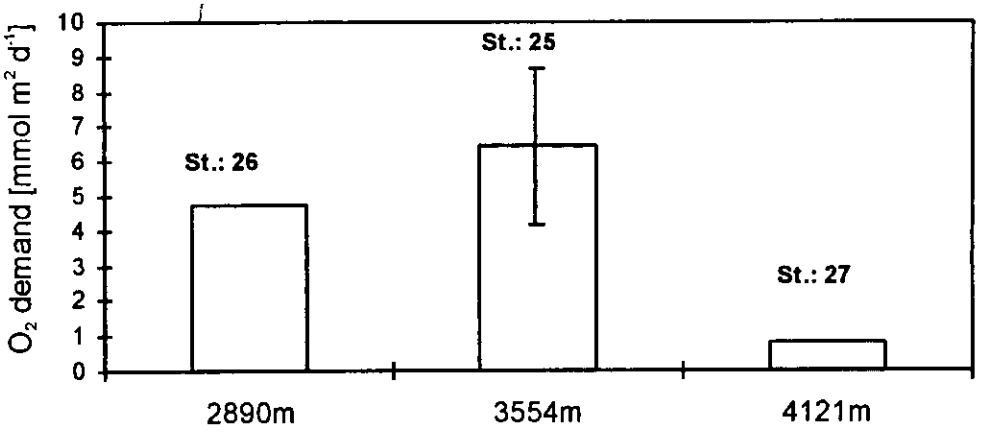


**Figure 28:** Sediment Oxygen Demand on the Nazaré-Canyon. Error bars give the standard deviation. For station 26 and 27 the mean of two measurements is given.

Fig. 28 depicts that the sediment oxygen demand in the canyon is extremely high. Especially at station 25 one of the highest values ever reported for such a water depth was measured.

### 5.2.4.4 Macrofauna and Meiofauna

(João Luís da Silva Cúrdia)

The study of the structure of benthic macrofauna communities is very important to understand the carbon and nutrient cycles. As an OMEX II project objective, benthic comunities are to be studied, aiming a better knowledge of the role of some characteristic parameters regarding the development of deep sea benthic animal communities. The main objective of this work is to collect winter data from the Vigo transect in order to establish a seasonal pattern in biodiversity and community structure, comparing winter data with summer data (previously sampled in another OMEX II cruise). In addition to this, we are looking forward to compare the composition and structure of benthic communities from Vigo (Spain) and the Nazaré canyon (Portugal). Since the depth seems to be the major factor affecting benthic comunities, two transects were established, one in Vigo and the other in Nazaré. Four stations at different depths on the continental slope (stations 9, 11, 24) and one on the shelf (Station 20) were analised on the Vigo transect. In Nazaré canyon, three stations (25, 26, 27) at different depths were sampled.

In order to study the different types of benthic macrofauna communities a boxcore of 50 x 50 cm was used. In each boxcore a sediment sample was collected in a small box for future determination of Total Organic Matter and grain size analysis. This small box was frozen immediately at -20°C. The redox potential of the boxcore was measured after 2 minutes at a sediment depth of about 4 cm. The upper 15 cm of the boxcore were sliced into 5 layers, 0-1cm, 1-3 cm, 3-5 cm, 5-10 cm and 10-15 cm. These layers were then sieved with a 500 µm sieve for macrofauna which was stored in a buffered 4 % formalin solution.

A subcore (from the boxcore) of 10 cm diameter was used for meiofauna determination. Whenever possible, another subcore of 10 cm diameter was taken from another boxcorer as a replicate for meiofauna (in the Nazaré canyon this second subcore was not possible to take).The subcores of 10 cm were also sliced in the 5 layers as previously specified and, in each layer, the redox potential was measured. The layers of meiofauna samples were stored in a buffered 4 % formalin solution without being sieved. All analyses will be carried out in our home institution.

### 5.2.4.5 Uptake and Mixing of Algal Carbon by Benthic Organisms

(Leon Moodley, Hilda Bouma)

The fate of phytodetritus shortly after its deposition is poorly understood in terms of which organisms have early access to it and the rates by which it is displaced and decomposed within the seabed. Understanding the fate of labile organic matter arriving at the seafloor is of great importance as it is the primary driving force of the benthic system. It has an impact on the magnitude and timing of various benthic fluxes and mineralisation and life strategies of the benthic organisms. In this cruise, we addressed this question by conducting short-term experiments (24-48 hrs), in which we added $^{13}C$ enriched algae to sediments in benthic chambers maintained on deck at bottom water temperature. The uptake or mineralization of the added algal carbon will be reflected either in the $\delta^{13}C$ of different faunal components or in the $\delta^{13}C$ of the $CO_2$ produced in the overlying waters. A detailed study was done only at station 20 having a water depth of 216 m. Less elaborate analysis were done at station 11 (1952 m watewr depth and at station 25 in the deeper part of the Nazaré Canyon (see Table 6).

*Method*

Upon addition of 15 mg of algal material and following a period of incubation, sediment or water samples were taken for the following analysis:

Benthic response: The response of the benthic system as a whole was examined by measuring sediment oxigen consumption SOC and $CO_2$ production in benthic chambers (14 cm inner diameter) fitted with oxygen probes and stirrers. The oxygen consumption was recorded on a data logger and the overlying water was sampled for $CO_2$ content. The overlying water was acidified in cap vials having a 3 ml nitrogen headspace. The $CO_2$ content in the headspace will be analyzed with a Carlo Erba high resolution MEGA 5340 gas chromatograph.

Faunal and bacterial uptake of algal carbon: The fauna > 300 µm were or will be isolated from different sediment intervals down to 6 cm. Sediment from these intervals were also collected for the isolation of bacterial biomarkers. The $\delta^{13}C$ of these components will allow us to determine the distribution of the labeled algal carbon over the different components of the benthic system.

Bioturbation: Transport of highly reactive organic matter from the sediment-water interface to the deeper layers will be examined through analysis of bulk $^{13}C_{org}$ in the different sediment intervals. Sediments were sampled in centimeter slices down to 12-14 cm. An attempt will also be made to measure the $\delta^{13}C$ of $CO_2$ produced in sediment slurry incubations (see below).

$CO_2$ production: In addition to this we sampled sediments down to 13 cm in centimeter intervals for long-term sediment slurry incubations; to measure $CO_2$ production in the headspace above sediment-water slurries. A volume of 10 ml sediment was transferred into 70 ml glass incubation bottles (Chrompack), diluted with 10 ml filtered seawater and sealed with screw caps provided with rubber septa. Headspaces were purged with $N_2$ for the anoxic incubtions and with synthetic air having no $CO_2$ for the oxic incubations. The $CO_2$ production in the head space of these long-term sediment slurry incubations will provide insight into the organic carbon mineralizatin rates (the amount of labile organic matter present in the sediment). The utility of this method in estimating carbon mineralization rates in deep-sea sediments can be assessed when results are compared to mineralization rates measured by Kähler et al. through SOD measurements (5.2.4.3).

*Preliminary Results*

The greatest concern with deck incubations is the effect of pressure changes on the benthic community. Organisms from both the 216 and 1952 m deep stations remained alive and active. However, although a few polychaetes were still alive after 2-3 days, organisms from the 3500 m deep canyon station showed clear signs of decay after 3 days. Whether organisms indeed continued normal activities will only be evident after isotope analysis.

Sediments from the canyon were distinctly different from the transect off Vigo that were characterized by presence of foraminifera and pteropod shells even more at the 1950 m station (11). Sediment from the canyon station (25) was composed mainly of plant debris and pieces of charcoal.

At the 216 m station, a clear difference in SOC was evident before and after the addition of algal material. This was evident following an incubation period of 24 hours and this suggests that the benthic response may be very rapid.

### 5.2.4.6 The Deep Water Coral Settlement Experiment

(Marc Lavaleye)

During the Dutch OMEX cruise in May-June 1998 with the RV Pelagia a settlement lander was deployed at a station G100 (780m) at the Galicia Bank in an area where the cold water corals *Lophelia pertusa, Madrepora oculata, Desmophyllum cristagalli* are abundant. The lander consists of a frame with 18 plates (45x45cm) and a large sediment trap. The plates are either from PVC, polypropyleen or ethyleen. To each plate, tiles (glazed and unglazed) and oyster shells are attached in a random order. This experiment is to investigate where (substrate preference) and when cold water corals settle, and how quick they grow. This study forms an addition to our current growth studies on *Lophelia* and *Madrepora* skeletons. It will also contribute to the discussion on how quick cold water corals can recover from damage caused by commercial fishing activities. In order to find out whether any bio-erosion by microborers occurs during the deployment period, two pieces of iceland spar had been attached to the lander (cooperation with John Wilson, Holloway University, London).

During a second expedition with the RV Pelagia in September 1998 the lander was succesfully recovered. After the replacement of 9 out of 18 plates the lander was re-deployed at the same location. An inspection of the plates and attached tiles and oyster at that time did not reveal an abundant growth of epifauna, though small white tubes of polychaetas were seen in small numbers at most of the tiles and oysters. There were, however, no macroscopical traces of coral settlement detectable.

During this Meteor cruise it was the objective to recover the frame and end the experiment. However, because of the bad weather, we refrained from recovering the settlement frame. The chances of loosing or damaging it during recovering and the risk for the deck crew were too great. The only thing done on 5 Jan. 1999 was checking if the frame was still there by waking up one of the releases. It responded without any problems. Immediately afterwards the ship sailed to a more southern transect to escape the bad weather condition. Another possibility has to be found to recover the frame this year.

### 5.2.5 Sedimentology

(Carla Garcia)

*Sediment surface*

Box corer (BC) and multicorer (MC) samples were used for the analysis of the sediment surface. The upper 3 cm were taken from each sample. They will be analysed regarding, among other sedimentological parameters, grain size, mineral composition and clay mineralogy. The aim of this work is to create a sedimentary map of the OMEX area including the shelf region. Furthermore, the results should lead to a better understanding of the diagenetic processes occurring in this area. Knowing more about the sediment dynamics will help identifying the main depocenters. Similar treatment for the samples from Nazaré Canyon will provide additional information, also for other partners within the project. Samples were taken according to the following station list:

| Station | Latitude | Longitude | Deep (m) | Description |
|---|---|---|---|---|
| 9 | 42° 08.5'N | 9° 46.6'W | 2323 | Mud |
| 11 | 42° 10.5'N | 9° 36.0'W | 1951 | Fine Mud |
| 20 | 42° 09.0'N | 9° 18.7'W | 216 | Sandy Mud |
| 21 | 42° 07.0'N | 9° 18.8'W | 206 | Sandy Mud |
| 221 | 42° 11.0'N | 9° 18.8'W | 222 | Sandy Mud |
| 24 | 42° 09.0'N | 10° 30.0'W | 2764 | Muddy Sand |
| 25 | 39° 29.7'N | 9° 55.4'W | 3510 | Fine Mud rich in organic matter. |
| 26 | 39° 29.0'N | 9° 45.1'W | 2894 | Fine Mud |
| 27 | 39° 34.0'N | 10° 10.3'W | 4141 | Silty-clay |

*Kasten Core*

During this leg of the cruise, two "Kasten" (KC) cores were taken, one in the Vigo transect and one in the Nazaré Canyon. Unfortunately, the latter sampling failed due to a bending of the core. The first one will be analysed for its record of small climatic changes. To do so, it will be X-rayed to identify sediment structures. Other works like grain sizes, clay mineralogy, mineralogical composition, heavy-minerals, heavy-metals, the study of foraminifera, and $^{14}C$ dating will also be performed.

| Station | Latitude | Longitude | Deep (m) | Length |
|---|---|---|---|---|
| 24 | 42° 09,0'N | 10° 30,0'W | 2761 | 2.16 m |
| 27 | 39° 33.9'N | 10° 09.9'W | 4121 | Failed |

The major part of the work on the sediment surface analysis as well as on the "Kasten" core will be carried-out in the lab. Preliminary conclusions are therefore difficult to draw.

*PARASOUND*

PARASOUND profiles provide precious additional information for the interpretaion of sediment studies. They can help to define sediment changes and rock outcrops, contributing to a more rigorous cartography. In return, the knowledge about the sampled surface sediments can be used to enhance the PARASOUND results. The data were stored digitally.

### 5.2.6 Determination of the Net Total Radiation and Atmospheric Turbidity at Sea

(Hein Dieter Behr)

Information about the spatial and temporal distribution of the net total radiation and its components at the sea surface as well as atmospheric turbidity are one of the most important parameters in resolving numerous meteorological and oceanographic questions. Therefore during the cruise the following radiation components were recorded: direct solar radiation, sunshine duration, global solar radiation and UV-B-portion of global solar radiation as well as longwave thermal radiation of the atmosphere. Additional components necessary to establish a radiation balance: reflected solar radiation and ocean surface radiation are computed using numerical models successfully tested on former research cruises in the Atlantic.

As atmospheric turbidity influences global solar radiation on its way through the atmosphere, the knowledge of this quantity is essential. The turbidity factor T is defined as the ratio of the optical depth $\bar{\delta}$ of the actually loaded atmosphere to the optical depth $\bar{\delta}_R$ of the pure and dry atmosphere (so-called Rayleigh atmosphere). Therefore T states how many Rayleigh atmospheres are equivalent to the actual atmosphere:

$$\bar{\delta} = T \cdot \bar{\delta}_R. \qquad (1)$$

The bar shall indicate that the optical depth is integrated over the entire solar spectrum. If the wavelength dependence of the optical depth is considered, an index $\lambda$ is added: $\delta_\lambda$ or $\delta_{R\lambda}$.

As optical depths $\bar{\delta}$ and $\delta_\lambda$ are not accessible to direct measurement, direct solar irradiance I recorded on the sea surface after penetrating the loaded atmosphere (measurement), was compared with the irradiance $I_R$ of a Rayleigh atmosphere (computed values). To evaluate the spectral turbidity factors, the corresponding spectral irradiances were used.

A Linke-Feussner-Actinometer (LFA) equipped with various filters is used for measuring different spectral direct solar irradiance. The so-called IGY-filters RG2 and OG1 are commonly used as standard-filters (IGY = International Geophysical Year).

Atmospheric turbidity is expressed by turbidity factors as follows:

- Total-turbidity factor $T_g$, identical with the Linke-turbidity-factor $T_L$, describing all radiative processes in the whole solar spectrum: $0 < \lambda < 8$,
- short-turbidity factor $T_s$, comprising the solar spectrum between: $0 < \lambda < 0.62$ µm. It is essentially determined by aerosol extinction within the atmosphere,
- red-turbidity factor $T_r$, comprising the solar spectrum between: $0.62\ \mu m < \lambda < 2.8\ \mu m$. This factor is essentially influenced by water-vapour absorption. The filter RG2 is designed to span over the significant absorption bands of water vapour (720 - 740 nm, 810 - 840 nm, 890 - 940 - 990 nm, and 1070 - 1110 - 1200 nm).

The factors $T_L$ ($\equiv T_g$), $T_s$, and $T_r \equiv T_x$ can be computed by:

$$I_x = I_{0x} \exp(-T_x \cdot m \cdot \delta) \quad (2)$$

with:

- $I_x$: direct solar radiation received from a surface normal to the beam of the sun, e.g. measured with a Linke-Feussner-Actinometer during the cruise.
- $I_{0x}$: extraterrestrial solar radiation received from a surface at the top of the atmosphere normal to the beam of the sun. Its quantity depends on the distance sun - earth only. The quantities $I_{0g}$ [total-solar constant], $I_{0r}$ [red-solar constant] and $I_{0s}$ [short-solar constant] are calculated from the data of the extraterrestrial spectrum. Their spectral integration according to the characteristics of the filters used results in:

$$I_{0g} = 1367.13 \text{ W/m}^2 \quad (3a)$$

$$I_{0r} = 818.52 \text{ W/m}^2 \quad (3b)$$

$$I_{0s} = 516.60 \text{ W/m}^2 \quad (3c)$$

- m: optical pathlength, dependent on the solar elevation angle.
- $\delta$: optical thickness of the atmosphere.

$m \cdot \delta$ are expressed in exact spelling:

$$-\delta_R\lambda \cdot m \equiv -[\delta_R(\lambda) \cdot m_R(\gamma) + \delta_Z(\lambda) \cdot m_Z(\gamma)] \quad (4)$$

with $\delta_R(\lambda)$ and $\delta_Z(\lambda)$ spectral vertical optical depths of the atmosphere related to:

R: Rayleigh scattering by air molecules

Z: ozone absorption

$m_R(\gamma)$ and $m_Z(\gamma)$ are the corresponding relative optical air mass and ozone mass, respectively, at solar elevation angle $\gamma$. The spectral optical depth $\delta_R(\lambda)$ due to Rayleigh scattering was calculated with help of an equation given by IQBAL (1983):

$$\delta_R(\lambda) = 0.008735 \, (\lambda/1000 \text{ nm})^{-4.08} \quad (5)$$

The spectral optical depth $\delta_Z(\lambda)$ was calculated by a formula of KASTEN (1996). He considered ozone absorption and additional absorptions by totally mixed gases (carbon dioxide and oxygen in particular). This absorption has to be considered because it shows considerable values in the UV up to 360 nm and in the Chappius-band between 410 nm and 850 nm.

Exact formulas to compute the air mass m passed by the radiation were published by KASTEN AND YOUNG (1989). As these formulas would overtax the accuracy of the LFA, a simpler formula is used which is valid for LFA-readings at solar elevation angles $\gamma = 10°$. In this case is

$$m(\gamma) \equiv m_R(\gamma) = m_Z(\gamma) = 1/\sin\gamma. \quad (6)$$

The data set of numerous measurements of direct solar radiation I done with a Linke-Feussner-Actinometer revealed the spatial and temporal variation of the atmospheric turbidity during the cruise. As a first result the daily courses of $T_L$, $T_s$, and $T_r$ along the transect from Las Palmas d. G. C. via the mooring stations at 42°N/9.5°W to Cádiz (Dec 28, 1998 to Jan 14, 1999) will be shown here. As R/V METEOR worked nearly the whole time in cold fresh air coming from the dust-free Northwestern Atlantic Ocean the Linke-turbidity factor was about 2.5 during sunrise and sunset and increased to 4.8 during noon, representing clear unloaded air. $T_s$ and $T_r$ correspond to this findings, they are low too: $T_s$=1.5 to 2.0 and $T_r$ = 7 to 12. But there was a short change in the airmasses reaching R/V METEOR during January 4 to 6: southwesterly winds transported airmasses with high humidity in all layers and loaded with dust particles from the Morocco-area. These particles swell and adhered together during their transport to the working area causing an increase of $T_L$ from 6,5 during sunrise and sunset and 8.5 during noon. $T_s$, and $T_r$ increased simultaneously: $T_s$ about 3.0 and $T_r$ = 30 to 37. These data characterise an industrial area.

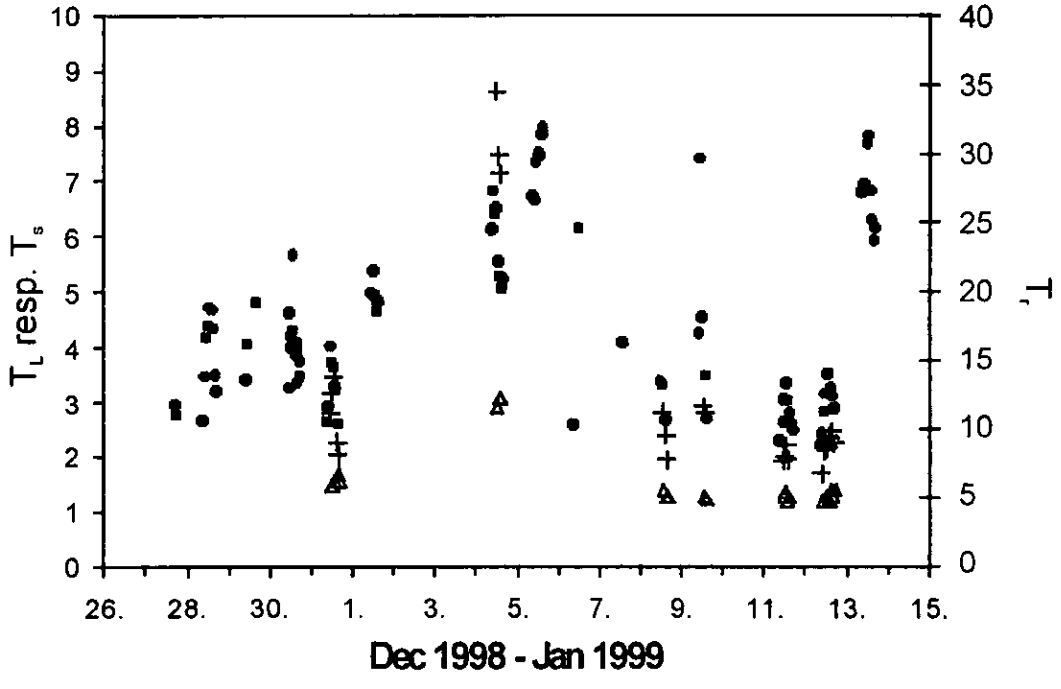


**Figure 29**: Daily cycles of the turbidity factors $T_L$ (•), $T_s$ (Δ), and $T_r$(+) during Dec 28, 1998 to Jan 14, 1999.

# 6 Ships Meteorological Station

## 6.1 Weather and Meteorological Conditions During Leg M43/1

(R. Strüfing)

During transit from Viana do Castelo to the Canary Islands a high near the Azores supplied METEOR with fine pushing trade winds around Beaufort (Bft) 5 to 6. The sun was sometimes hidden behind some low clouds. Whilst the first dredging took place on November 29th near the southern tip of La Palma the trade winds were locally intensified by mountains up to Bft 8. The wave height of 2 to 2.5 meter did not hamper progress. On December 1st a coldfront passage caused some showers. The high near the Azores had moved to Europe weakening the trade winds and giving way to the remainders of a cut-off low approaching from the west. The frontal system of this low passed on December 4th with moderate westerly winds and some showers. On December 5th a new high developed near the Azores causing the wind to back to northeasterly directions. At this time METEOR started exploring the seamounts south of the Canary Islands. During the next days a strong cyclogenesis evolved in the northern parts of the North Atlantic. Starting from a position south of New Foundland a series of severe gale lows moved into the Norwegian Sea. The high westerly to northwesterly windseas in the rear of these lows travelled the Atlantic Ocean to arrive south of the Canary Islands. This 2 to 2.5 meter northwesterly swell in conjunction with the up to 2.5 meter windsea of the trade winds caused some rolling movement of METEOR . However, research went on to schedule. From 12th until 23rd December METEOR operated near the islands of Tenerife and Gran Canaria. Due to the weaker high over Spain the trade winds blew at Bft 4 to 5 only. In the absence of any swell research could continue under ideal conditions. Whereas between December 12th and 18th sunshine added to the high spirits of crew and scientists the very last days passed under a layer of high clouds caused by a more northerly air flow originating from a new high west of the Azores. During cruise M43/1 METEOR has experienced winds slightly above the average climate conditions which are near Bft 4 with 70% northerly to easterly directions. Only the swell in the south of the Canary Islands seems to have been higher than normal but at no time research was significantly handicapped by the weather conditions.

## 6.2 Weather and Meteorological Conditions during Leg M43/2

(H.D. Behr)

R/V METEOR left the port of Las Palmas d. G. C. on December 28, 1998 noon steering on a northeasterly course to her first working position at 37°30'N/10°30'W. The first gale centre in the time of this cruise moved eastwards and deepened in the vicinity of the British Isles to a storm centre causing south-west 8 Bft with gusts of 10 Bft and a swell with heights of 6 m and more in our area. For the safety of the ship and the crew R/V METEOR reduced her velocity and reached her working position in the morning of January 1, 1999. The first tests with the CTD-sondes at this position failed because of the swell. In order to save time R/V METEOR sailed to the northern part of the OMEX-region, which is the expected main working area of this cruise. After reaching this area R/V METEOR picked up a mooring at 40°N/9.5°W and tried to do so with another one at 42°N/13.5°W. As this failed due to heavy sea R/V METEOR returned to 40°N/9.5°W processing PARASOUND observations meanwhile.

The series of storm centres ended in the morning of January 6. The last gale centre influencing the working area of R/V METEOR with southerly winds force 8 Bft and swell with 6 m moved southwards to the Canary Islands. The wind decreased to Southwest 4 Bft and the swell to 1 to 2 m at January 7. There was no weather-influence on station work for two days. A cold front

changed at the north-western corner of the Iberian Peninsula (Cape Finisterre) to a low within 12 hours causing northerly winds increasing to 8 Bft with gusts up to 10 Bft. R/V METEOR could put her bow in the wind easily in order to continue station work as wind, swell, and sea were coming from the same direction for the first time. As this low moved quickly to the Balearic Islands the wind calmed down with variable directions up to January, 11. The last low during this leg moved from the Central North-Atlantic towards the coast of Portugal and from here to Morocco causing north-easterly winds force 7 to 8 Bft at first, decreasing to 4 Bft until the end of the cruise. R/V METEOR reached Cádiz in the late afternoon of January 14, 1999.

# 7 Lists

## 7.1 Leg M43/1

### 7.1.1 Dredge Protocol With Brief Description of Rocks Dredged

Abbrevations
DD: drum dredge
CDBD: chain dredge-Burkhardt dredge
CDRD: chain dredge-Russian dredge
CDWS: chain dredge-white shark
RO: Rosette (water sampling system)
NR: no revovery
c.: circa
phc: phenocrysts
ol: olivine
cpx: clinopyroxene
opx: orthopyroxene
amph: amphibole
fsp: feldspar
alkfsp: alkalifeldspar
anor: anorthoclase
hau: hauyne
mt: magnetite
phl: phlogopite
tit: titanite
zr: zirkon
sideromelane = basaltic glass
felsite = highly evolved volcanic rock, probably mostly trachyte, in some cases possibly phonolite
Weight of dredge hauls crudely estimated: one fishbox measures 70x40x15 cm (around 15-30kg)

*1. South La Palma Ridge*

| Date/Station number | On bottom | Water depth | Off bottom | Water depth | Dredge type |
|---|---|---|---|---|---|
| *29.11.1998* | | | | | |
| **Station # 636** | 28°26,1 N, 17°51,3 W | 630m | 28°26,5 N, 17°51,0 W | 412,7m | DD |
| Weak link broken, NR | | | | | |
| **Station # 637** | 28°26,4 N, 17°51,0 W | 498m | 28°26,5 N, 17°51,0 W | 430m | DD |
| Weak link broken, NR | | | | | |
| **Station # 637b** | 28°26,5 N, 17°51,1 W | 510m | 28°26,5 N, 17°51,0 W | 441m | DD |
| NR | | | | | |
| **Station # 637c** | 28°26,5 N, 17°51,1 W | 472m | 28°26,5 N, 17°51,1 W | 390m | DD |
| NR | | | | | |
| **Station # 637d** | 28°26,5 N, 17°51,1 W | 513m | 28°26,5 N, 17°51,0 W | 411m | CDBD |
| NR, 6 teeth broken | | | | | |
| **Station # 638** | 28°25,5 N, 17°51,7 W | 924m | 28°25,6 N, 17°51,6 W | 780m | DD |

Around 20 pieces of irregularly shaped, ol- and cpx-phyric (<5 vol.%) basalt up to 20 cm in diameter, held together by a lithified calcilutitic to arenitic matrix. A few calcilutites with minor glassy clasts and possibly crystals. About 30 to 50% lapillistones. Lapilli (vesicularity 50-60 vol.%) are up to 4cm in diameter, most varying widely in morphology. Some red oxidized lapilli have round, others primary blocky shapes and glassy groundmass. The blocky-shaped lapillistones are dominantly clast-supported. Mixing of blocky-shaped lapillistones with fine-grained carbonates results in a typical salt and pepper structure. Dense basalts with glassy crusts are up to 5cm or more in diameter. Some grainstones and rudstones contain thick-shelled fossils (Lamellibranchiata, Gastropoda). Many fragments are coated by zeolite, possibly phillipsite.

**Dredge Protocol Leg M43/1 (continued)**

| | | | | | |
|---|---|---|---|---|---|
| **Station # 639** | 28°23,9 N, 17°51,9 W | 1091m | 28°24,0 N, 17°51,7 W | 868m | DD |

At least 30 kg of basically three rock types. One piece of half a metre and several up to 35cm in diameter. One fresh black tube-like vesicular (10-15 vol.%) basalt with a glassy crust. Groundmass very fine-grained to glassy. Vesicle size (1-3mm in diameter) and distribution uneven. Phc: cpx (c. 5 vol.%, <4mm in size) and probably some ol. Reddish, poorly consolidated basaltic lapillistones with lapilli (0.5-1mm in diameter) having thick walls of fresh sideromelane. They are set in a yellowish-brownish matrix composed of smaller, vesicular, more strongly altered lapilli. Fresh ol and cpx phc are abundant in the matrix and in the lapilli, probably totaling < 10 vol.%. The third lithology is a grey-green calcareous soft sediment, some with larger

| | | | | | |
|---|---|---|---|---|---|
| **Station # 640** | 28°23,0 N, 17°52,6 W | 1681m | 28°22,9 N, 17°52,6 W | 1681m | DD |

NR

| | | | | | |
|---|---|---|---|---|---|
| **Station # 641** | 28°21,52 N, 17°54,3 W | 2735m | 28°21,4 N, 17°54,2 W | 2550m | DD |

Grayish-brown hemipelagic sediment, bioturbated.

*30.11.1998*

| | | | | | |
|---|---|---|---|---|---|
| **Station # 642** | 28°21,8 N, 17°52,1 W | 1572m | 28°21,8 N, 17°52,0 W | 1422m | DD |

NR

| | | | | | |
|---|---|---|---|---|---|
| **Station # 643** | 28°18,2 N, 17°48,2 W | 1628m | 28°18,1 N, 17°48,2 W | 1709m | DD |

NR, 6 teeth broken

| | | | | | |
|---|---|---|---|---|---|
| **Station # 644** | 28°18,3 N, 17°45,8 W | 1505m | 28°18,3 N, 17°45,8 W | 1382m | DD |

Coral debris, altered glassy sediment.

| | | | | | |
|---|---|---|---|---|---|
| **Station # 645** | 28°18,3 N, 17°45,8 W | 1398m | 28°18,5 N, 17°45,9 W | 1260m | DD |

Carbonate crusts.

| | | | | | |
|---|---|---|---|---|---|
| **Station # 646** | 28°18,2 N, 17°45,8 W | 1550m | 28°18,2 N, 17°45,9 W | 1620m | CDBD |

Four pieces of basalt with manganese crusts, carbonate crusts and coral debris.

| | | | | | |
|---|---|---|---|---|---|
| **Station # 647** | 28°18,4 N, 17°45,8 W | 1340m | 28°18,5 N, 17°45,6 W | 1201m | CDBD |

Coral debris.

| | | | | | |
|---|---|---|---|---|---|
| **Station # 648** | 28°18,7 N, 17°46,7 W | 1443m | 28°18,8 N, 17°46,6 W | 1374m | CDBD |

Two vesicular pieces of basalt with manganese crusts and carbonate-filled vesicles. Coral debris.

| | | | | | |
|---|---|---|---|---|---|
| **Station # 649** | 28°18,8 N, 17°46,5 W | 1361m | 28°19,0 N, 17°46,5 W | 1225m | CDBD |

Coral debris.

*01.12.1998*

| | | | | | |
|---|---|---|---|---|---|
| **Station # 650** | 28°19,7 N, 17°47,8 W | 1142m | 28°20,0 N, 17°47,5 W | 870m | CDBD |

Coral debris, siliceous sponges.

| | | | | | |
|---|---|---|---|---|---|
| **Station # 651** | 28°19,2 N, 17°48,2 W | 1334m | 28°19,1 N, 17°48,4 W | 1245m | CDBD |

Minor carbonate sediments with volcaniclastic fragments.

| | | | | | |
|---|---|---|---|---|---|
| **Station # 652** | 28°19,2 N, 17°48,2 W | 1054m | 28°19,3 N, 17°48,1 W | 916m | CDRD |

NR

| | | | | | |
|---|---|---|---|---|---|
| **Station # 653** | 28°19,3 N, 17°48,3 W | 1002m | 28°19,3 N, 17°48,2 W | 919m | DD |

Two specimen of lapillistones, coral debris.

| | | | | | |
|---|---|---|---|---|---|
| **Station # 654** | 28°19,4 N, 17°48,1 W | 910m | 28°19,4 N, 17°48,1 W | 965m | CDRD |

Carbonate with manganese crusts.

| | | | | | |
|---|---|---|---|---|---|
| **Station # 655** | 28°20,4 N, 17°49,2 W | 1254m | 28°20,3 N, 17°49,1 W | 1266m | CDRD |

Coral debris.

| | | | | | |
|---|---|---|---|---|---|
| **Station # 656** | 28°20,6 N, 17°49,7 W | 1236m | 28°20,8 N, 17°49,4 W | 1019m | CDRD |

Carbonate crusts and coral debris.

| | | | | | |
|---|---|---|---|---|---|
| **Station # 657** | 28°21,9 N, 17°51,1 W | 1247m | 28°22,0 N, 17°50,8W | 1246m | CDRD |

At least 50 kg. Basically 2 rock types. Fresh, highly vesicular (70-80 vol.%, 0.5-10mm in diameter) cpx-phyric (1-2 vol.%) basalt with glassy to fine-grained groundmass. The second lithology is brownish scoria (vesicle volume 60->85 vol.%). Coral debris, manganese crusts, limestone breccias and calcarenites.

| | | | | | |
|---|---|---|---|---|---|
| **Station # 658** | 28°23,0 N, 17°51,8 W | 1251m | 28°23,2 N, 17°51,6 W | 1112m | CDRD |

Basaltic pillow lava fragments including one 30cm long pillow tube. Mostly dark, vesicular basalt with a fine-grained to glassy groundmass and a thin well-preserved glassy rind. Size and amount of vesicles (up to 50 vol.%) increase towards the glassy crust. Some rocks show two generations of vesicles: larger round ones (1-5mm) and smaller ones (< 0,5mm). Phc: ol and cpx (c. 5-15 vol.%) some intergrowth.

| | | | | | |
|---|---|---|---|---|---|
| **Station # 659** | 28°23,6 N, 17°53,2 W | 1325m | 28°23,4 N, 17°51,9 W | 1019m | CDRD |

NR

| | | | | | |
|---|---|---|---|---|---|
| **Station # 660** | 28°24,0 N, 17°51,7 W | 924m | 28°24,2 N, 17°51,6 W | 969m | CDRD |

Glassy to fine-grained, ol-, cpx- and fsp-phyric (c. 5-15 vol.%) tachylitic basalt with more than 50 vol.% vesicles of at least two generations, some up to 5mm in diameter and commonly unfilled. More altered, brownish basalts show large vesicles filled by clay minerals and/or carbonate or zeolites.

*02.12.1998*

| | | | | | |
|---|---|---|---|---|---|
| **Station # 661** | 28°23,9 N, 17°50,6 W | 1052m | 28°24,0 N, 17°50,4 W | 890m | CDRD |

Coral debris, sediments attached to corals.

## Dredge Protocol Leg M43/1 (continued)

| | | | | | |
|---|---|---|---|---|---|
| **Station # 662** | 28°23,5 N, 17°50,0 W | 1202m | 28°23,6 N, 17°49,8 W | 1079m | CDRD |

Gray green, medium-grained felsite with Mn-crust. Phc: c. 20 vol.% alkfsp (up to 1cm in length), 1-2 vol.% amph, mt and phl.

| | | | | | |
|---|---|---|---|---|---|
| **Station # 663** | 28°22,1 N, 17°45,6 W | 2072m | 28°22,2 N, 17°45,5 W | 1950m | CDRD |

Half a dozen pieces of volcaniclastic sediment. Relativly well-sorted calcareous tuffs. Dominantly small, round, vesicular, phonolitic lapilli, with abundant hau, clear fsp (anor?), phl, tit and amph mixed with ol, cpx and altered sideromelane.

| | | | | | |
|---|---|---|---|---|---|
| **Station # 664** | 28°25,7 N, 17°49,7 W | 719m | 28°25,9 N, 17°49,7 W | 469m | CDRD |

Mostly reddish, angular, cpx- and ol- phyric basaltic breccias. Vesicular lapilli and ash cemented by carbonate and zeolites. Vesicular basalt and fine-grained, cpx- and amph-phyric intermediate rocks minor. Some fine-grained, basaltic hyaloclastites contain biogenic fragments.

| | | | | | |
|---|---|---|---|---|---|
| **Station # 665** | 28°26,3 N, 017°50,8 W | 372m | 28°26,3 N, 017°50,6 W | 381m | CDRD |

Four pieces of dark-gray cpx-rich, ol-bearing vesicular basalt and one 30cm slab of a basaltic sheet flow with glassy crust.

| | | | | | |
|---|---|---|---|---|---|
| **Station # 666** | 28°23,6 N, 017°50,0 W | 1233m | 28°23,9 N, 17°49,9 W | 1245m | CDRD |

Basically three rock types. Six pieces of dense trachyte up to 15cm in diameter with fresh anor, phl and minor amph in a greenish groundmass. Three calcarenite pieces with volcanic particles. The third rock type is vesicular dark gray-brownish basalt. A dozen subround fragments (< 15cm) are ol- and cpx-phyric commonly glassy basalts. Pillow tubes about 20cm in diameter. Vesicularity in the centre up to 50 vol.%, decreasing towards the margin. The tube surface shows some ribbon-type structure lacking in a pronounced glassy crust.

| | | | | | |
|---|---|---|---|---|---|
| **Station # 667** | 28°18,9 N, 17°44,5 W | 1996m | 28°19,1 N, 17°44,4 W | 1892m | CDRD |

Vesicular (20 to >50 vol.%), cpx- and ol-phyric basalt clasts and lapilli cemented by carbonatic sediments. Vesicles and fractures commonly filled by clayey, lutitic sediments. All specimen coated by manganese crusts.

***2. South Hierro Ridge***

| Date/Station number | On bottom | Water depth | Off bottom | Water depth | Dredge type |
|---|---|---|---|---|---|
| *03.12.1998* | | | | | |
| **Station # 668** | 27°36,5 N, 18°00,2 W | 757m | 27°36,6 N, 18°00,1 W | 686m | CDRD |

Around ten pieces of basalt and sediment up to 20cm in diameter. Three fresh and vesicular (20-30 vol%) picrites (5-10 vol% ol), one fresh, black, fine-grained, very vesicular (70 vol%) basalt, one basaltic bomb, four specimen of fine- to medium-grained ol-phyric (traces) volcaniclastic sediment (one with carbonate crust) and one large (20cm in diameter) piece of reddish brown lapillistone breccia.

| | | | | | |
|---|---|---|---|---|---|
| **Station # 669** | 27°35,9 N, 18°00,1 W | 595m | 27°35,9 N, 18°00,1 W | 429m | CDRD |

At least 50kg. Large blocks of basalt up to 60cm in diameter and 20-30cm high. Most of the matrial clastic, but also some basalt plates. Vesicular (<70 vol%, vesicles up to 5cm in diameter) basalt alternating with sometimes layered volcaniclastic breccia of coarse-grained lapilli and bombs set in a carbonate matrix.

| | | | | | |
|---|---|---|---|---|---|
| **Station # 670** | 27°35,9 N, 17°59,1 W | 346m | 27°36,0 N, 17°59,0 W | 281m | CDRD |

Basaltic, clast-supported lapillstones (25-40cm in size) cemented by carbonate.

| | | | | | |
|---|---|---|---|---|---|
| **Station # 671** | 27°34,3 N, 17°58,6 W | 902m | 27°34,5 N, 17°58,6 W | 660m | CDRD |

Five pieces of round, glassy, black/red oxidized, vesicular basalt up to 5cm. Some fine-grained tuffaceous sediments with calcareous crusts.

| | | | | | |
|---|---|---|---|---|---|
| **Station # 672** | 27°35,1 N, 17°58,9 W | 554m | 27°35,2 N, 17°58,8 W | 524m | CDRD |

One piece (diameter 10 cm) of clast-supported, volcaniclastic, calcareous sandstone. Many carbonate crust and unlithified micrites. Coral debris.

| | | | | | |
|---|---|---|---|---|---|
| **Station # 673** | 27°33,6 N, 17°58,3 W | 898m | 27°33,8 N, 17°58,2 W | 694m | CDRD |

One piece of glassy, vesicular basalt, brown carbonate crust with corals, and strongly altered volcanics.

| | | | | | |
|---|---|---|---|---|---|
| **Station # 674** | 27°33,4 N, 17°58,9 W | 964m | 27°33,6 N, 17°58,6 W | 960m | CDRD |

Black, vesicular ol-, px-phyric lapilli in a carbonate matrix and cream-colored carbonate crusts with borings containing fragments of shell debris and dark mafic volcanics.

| | | | | | |
|---|---|---|---|---|---|
| **Station # 675** | 27°32,0 N, 17°58,9 W | 975m | 27°32,1 N, 17°58,9 W | 879m | CDRD |

Mostly coral debris, two large pieces of fine-grained, vesicular, px-phyric basalt. Vesicles unfilled. Some highly altered volcanic rock.

| | | | | | |
|---|---|---|---|---|---|
| **Station # 676** | 27°27,7 N, 18°00,0 W | 1689m | 27°27,7 N, 18°59,8 W | 1620m | CDRD |

Mostly dark colored coral debris. Some large pieces (up to 30cm in diameter, altogether about 6kg) of reddish, vesicular, aphyric pillow basalt fragments with some fresh glassy crusts. Many pieces coated with up to 8cm thick manganese crusts.

| | | | | | |
|---|---|---|---|---|---|
| *04.12.1998* | | | | | |
| **Station # 677** | 27°26,8 N, 18°00,4 W | 1539m | 27°26,9 N, 18°00,2 W | 1495m | CDRD |

Manganese crust with globular surface texture on calcareous sediments. Coral debris.

**Dredge Protocol Leg M43/1 (continued)**

| | | | | | |
|---|---|---|---|---|---|
| **Station # 678** | 27°25,7 N, 18°01,1 W | 1694m | 27°25,8 N, 18°00,9 W | 1621m | CDRD |
| Fine-grained, pumice-rich lapillistones containing subround dense and pumiceous gray to pink felsite fragments. | | | | | |
| **Station # 679** | 27°23,0 N, 18°02,0 W | 2173m | 27°23,2 N, 18°01,9 W | 2033m | CDRD |
| Coarse-grained, pumice-rich lapillistones up to 15cm in diameter with subround dense and pumiceous felsite fragments. Some lapilli show dark, fine-grained rims and moderate vesicularity in the interior. | | | | | |
| **Station # 680** | 27°22,1 N, 18°02,4 W | 2403m | 27°22,3 N, 18°02,5 W | 2240m | CDRD |
| Twenty kg of pink, hemipelagic, clayey-calcareous sediment with manganese crusts. | | | | | |
| **Station # 681** | 27°21,3 N, 18°03,0 W | 2638m | 27°22,3 N, 18°02,5 W | 2520m | CDRD |
| Fifty kg of pink, hemipelagic, clayey-calcareous sediment with manganese crusts. | | | | | |
| **Station # 682** | 27°22,6 N, 18°03,8 W | 3120m | 27°22,8 N, 18°04,2 W | 3056m | CDRD |
| Two bedded, well- to moderately-sorted volcaniclastic sediments (40cm in diameter) with glass-rich, ol- and cpx-phyric layers and intercalations of carbonatic, foram-rich layers. Some moderately vesicular (c. 40 vol.%) basaltic lapilli. | | | | | |
| **Station # 683** | 27°23,2 N, 18°00,3 W | 2871m | 27°23,5 N, 18°00,5 W | 2586m | CDRD |
| Fifteen kg of pink, hemipelagic, clayey-calcareous sediment with manganese crusts. | | | | | |
| **Station # 684** | 27°23,9 N, 18°00,6 W | 2319m | 27°24,1 N, 18°00,6 W | 2213m | CDRD |
| Two pieces (40cm in diameter) of hemipelagic, clayey-calcareous sediments with 2-20 vol.% of greenish, irregularly shaped, mt-, amph-, and fsp-phyric (<1 vol.%) pumice clasts. One specimen of vesicular (30 vol.%), plag-phyric basalt. Vesicles partly filled with hydroxides and clayey-micrites. | | | | | |
| **Station # 685** | Dredge not on bottom. | | | | |
| **Station # 686** | 27°20,0 N, 18°04,3 W | 2654m | 27°20,0 N, 18°04,4 W | 2599m | CDRD |
| Ten specimen of manganese crusts with concentric layering. | | | | | |

***3. Las Hijas Seamount***

| Date/Station number *05.12.1998* | On bottom | Water depth | Off bottom | Water depth | Dredge type |
|---|---|---|---|---|---|
| **Station # 687** | 27°06,6 N, 18°36,7 W | 2631m | 27°06,9 N, 18°36,7 W | 2382m | CDRD |
| About 25 kg of fresh, relatively well-crystallised, alkfsp-phyric (<1 vol.%), volcanic to subvolcanic felsites up to 60cm in diameter. Some fsp-pyhric (+ minor mafic phc) felsites are more vesicular (10-15 vol.%). Some vesicles filled with secondary minerals. | | | | | |
| **Station # 688** | 27°07,2 N, 18°36,2 W | 2434m | 27°07,5 N, 17°36,5 W | 2278m | CDRD |
| One large (1m in length and 40cm thick) light-coloured, semi-consolidated, hemipelagic limestone with manganese crust. | | | | | |
| **Station # 689** | 27°06,1 N, 18°36,6 W | 2862m | 27°06,5 N, 18°36,9 W | 2400m | CDRD |
| More than 50 kg of pumiceous felsite up to 1m in length and 40cm thick. The rocks range from moderately vesicular (50 vol.%), alkfsp-phyric (+ minor mafic phc) felsites with trachytic textures to slightly vesicular (<5 vol.%), alkfsp- and mafic phc-phyric felsites. Some clast-supported breccias consist of angular, blueish clasts alternating with roundish, white to greenish, vesicular shards. Fine-grained, mt-, fsp-, amph- and hau-phyric (<1 vol.%) felsic rocks minor. | | | | | |

***4. Tropic Seamount***

| Date/Station number *07.12.1998* | On bottom | Water depth | Off bottom | Water depth | Dredge type |
|---|---|---|---|---|---|
| **Station # 690** | 23°47,7 N, 20°47,5 W | 3603m | 27°47,7 N, 20°47,2 W | 3596m | CDRD |
| NR | | | | | |
| **Station # 691** | 23°48,1 N, 20°45,9 W | 3077m | 27°48,4 N, 20°45,5 W | 2680m | CDRD |
| Fifteen kg of hemipelagic, light-coloured and semi-consolidated carbonates with minor manganese crust. | | | | | |
| **Station # 692** | 23°50,0 N, 20°45,1 W | 1875m | 23°50,3 N, 20°44,9 W | 1584m | CDRD |
| Twenty kg of mostly hemipelagic, light-coloured and semi-consolidated carbonates with thin manganese crust and three altered basalt pebbles. Two vesicular (c. 20 vol.%), cpx-phyric (c.3 vol.%) basalt pebbles with reddish, dark 'schlieren'. One pebble is an intermediate, alkfsp-, amph-, mica-, tit-, and cpx-phyric (c.2-3 vol.%) felsite with trachytic texture. | | | | | |
| **Station # 693** | 23°50,5 N, 20°44,7 W | 1339m | 23°50,6 N, 20°44,5 W | 1048m | CDRD |
| Several pieces of hemipelagic, light-coloured and semi-consolidated carbonates with thin manganese crust and two pieces (around 10 cm in diameter) of altered, vesicular (10 vol.%), cpx- and ol-phyric (c. 2 vol.%) basalt and conglomerate with fine-grained, amph-and fsp-phyric, felsic pebbles. | | | | | |
| **Station # 694** | 23°51,5 N, 20°48,8 W | 2770m | 27°51,6 N, 20°48,6 W | 2575m | CDRD |
| Several pieces (one around 50 cm in diameter) of vesicular (c. 25 vol.%), relatively well-crystallized, cpx- and ol-phyric (c. 2 vol.%) basalt, coated by thick manganese crust. | | | | | |
| **Station # 695** | 23°51,9 N, 20°48,1 W | 2000m | 23°52,0 N, 20°47,8 W | 1870m | CDRD |
| Coral debris with two internal generations of manganese coating. | | | | | |

**Dredge Protocol Leg M43/1 (continued)**

| | | | | | |
|---|---|---|---|---|---|
| **Station # 696** | 23°52,0 N, 20°47,9 W | 1872m | 23°52,2 N, 20°47,7 W | 1756m | CDRD |
| Coral debris and hemipelagic, clayey, light-coloured and semi-consolidated carbonates. | | | | | |
| *08.12.1998* | | | | | |
| **Station # 697** | 23°52,5 N, 20°47,4 W | 1477m | 27°52,8 N, 20°47,1 W | 1219m | CDRD |
| Fine-grained felsite breccia and dense limestone strongly coated by manganese crust. | | | | | |
| **Station # 698** | 23°47,0 N, 20°44,4 W | 2447m | 23°47,2 N, 20°44,3 W | 2226m | CDRD |
| Coral debris and hemipelagic, clayey, light-coloured and semi-consolidated carbonates. | | | | | |
| **Station # 699** | 23°47,3 N, 20°44,2 W | 2057m | 27°47,5 N, 20°44,1 W | 1953m | CDRD |
| Ten pieces (up to 40cm in diameter) of fine-grained, alkfsp- and amph-phyric felsites, brecciated felsite (up to 10cm in diameter), basalt, conglomerate, and hemipelagic limestones. | | | | | |
| **Station # 700** | 23°48,1 N, 20°43,7 W | 1454m | 23°48,2 N, 20°43,5 W | 1181m | CDRD |
| Fifty kg of coral debris and hemipelagic, light-coloured and semi-consolidated carbonates. | | | | | |
| **Station # 701** | 23°47,3 N, 20°44,3 W | 2010m | 23°47,5 N, 20°44,2 W | 2037m | CDRD |
| NR | | | | | |
| **Station # 702** | 23°47,4 N, 20°44,1 W | 2054m | 23°47,6 N, 20°44,0 W | 1947m | CDRD |
| 65m of rope cut. One fishbox of samples. Mostly limestone and manganese crust, three fist size pieces of trachyte. Fine-grained, cream-coloured alkfsp-phyric (1 vol%) felsite with traces of mafic phc. | | | | | |
| **Station # 703** | 23°47,4 N, 20°44,3 W | 2052m | 23°47,6 N, 20°44,0 W | 1880m | CDRD |
| Dredge completely full with some large rocks up to 1m, mostly manganese-encrusted limestones but also 1-2 boxes with trachytes (?) and moderately lithified tuffs. Carbonate-cemented, bedded to graded, well-sorted, fine to coarse-grained, vesicular (c. 50 vol%) tuff and lapillistone of intermediate-felsic composition. Clasts angular to round and strongly altered to yellowish layer silicate. Locally some fresh glass preserved. Phc: rare cpx, possibly some former ol and/or fsp. Gray-green, dense alkfsp-phyric (c. 1 vol%) felsite (trachyte?) | | | | | |
| **Station # 704** | 23°47,6 N, 20°44,3 W | 2077m | 23°47,8 N, 20°44,2 W | 1908m | CDRD |
| Two pieces of manganese-coated rock. | | | | | |

*5. Paps Seamount*

| Date/Station number | On bottom | Water depth | Off bottom | Water depth | Dredge type |
|---|---|---|---|---|---|
| *09.12.1998* | | | | | |
| **Station # 705** | 25°38,3 N, 20°08,0 W | 2297m | 25°38,5 N, 20°07,6 W | 2004m | CDRD |
| One block (c. 40cm in diameter) of layered manganese crust with some brecciated material. One fist-sized piece of greenish, highly vesicular lapillistone (hyaloclastite). Altered, yellowish, earthy zeolite-bearing tuff. Thick-stemmed coral debris. | | | | | |
| **Station # 706** | 25°38,9 N, 20°08,0 W | 2105m | 25°38,5 N, 20°07,6 W | 2004m | CDRD |
| Highly vesicular, green altered, alkfsp-bearing felsitic lapilli in a pink matrix. | | | | | |
| **Station # 707** | 25°37,8 N, 20°07,9 W | 2312m | 25°38,1 N, 20°07,7 W | 2113m | CDWS |
| Eight fishboxes. One with volcaniclastic rocks. Vesicular lapillistone and highly altered pillow basalt all coated with manganese crusts. Black material is not only manganese crusts but there are some very dense (Fe-rich) pieces. | | | | | |
| **Station # 708** | 25°50,4 N, 20°21,1 W | 2579m | 25°50,7 N, 20°21,0 W | 2340m | CDWS |
| NR | | | | | |
| **Station # 709** | 25°50,4 N, 20°21,1 W | 2582m | 25°50,6 N, 20°21,3 W | 2417m | CDWS |
| Light pinky clay with manganese crusts. | | | | | |
| *10.12.1998* | | | | | |
| **Station # 710** | 23°49,9 N, 20°19,5 W | 2991m | 23°49,7 N, 20°19,5 W | 2649m | CDWS |
| One piece of volcaniclastic sediment. | | | | | |
| **Station # 711** | 25°58,0 N, 20°22,1 W | 2038m | 25°57,99 N, 20°21,89 W | 1974m | CDWS |
| One piece of vesicular, extremely fresh, 'dark melt' with 'partially melted' material and one piece (2 cm thick, 15 cm long) of vesicular, glassy material (slags). | | | | | |
| **Station # 712** | 25°59,5 N, 20°22,9 W | 2321m | 25°59,6 N, 20°22,5 W | 2069m | CDWS |
| NR | | | | | |
| **Station # 713** | 25°58,0 N, 20°22,2 W | 2048m | 25°58,2 N, 20°21,7 W | 1903m | CDRD |
| Twenty kg of manganese crusts and some small pieces of bioclastic, well-sorted carbonates. | | | | | |
| **Station # 714** | 25°57,9 N, 20°23,0 W | 2168m | 27°57,9 N, 20°22,5 W | 2066m | CDRD |
| Seventy kg of hemipelagic, light-coloured and semi-consolidated carbonates with thin manganese crusts and one piece of vesicular lapillistone. | | | | | |

## Dredge Protocol Leg M43/1 (continued)

*6. Endeavour Seamount*

| Date/Station number | On bottom | Water depth | Off bottom | Water depth | Dredge type |
|---|---|---|---|---|---|
| 11.12.1998 | | | | | |
| **Station # 715** | 25°21,6 N, 19°32,8 W | 2077m | 25°21,6 N, 19°32,6 W | 1880m | CDRD |
| Three pieces (up to 20cm in diameter) of vesicular, cpx-pyric basalt, mixed volcaniclastic-calcarenitic sandstone and altered lapillistone. | | | | | |
| **Station # 716** | 25°21,6 N, 19°32,5 W | 1817m | 25°21,7 N, 19°32,2 W | 1796m | CDRD |
| Twentyfive kg of lapillistones with large clasts of cpx-phyric basalt (up to 10cm in diameter) and some pieces of thick manganese crusts. | | | | | |
| **Station # 717** | 25°21,5 N, 19°31,4 W | 1429m | 25°21,4 N, 19°31,1 W | 1214m | CDRD |
| One piece of vesicular intermediate rock with brown, cpx-phyric groundmass. | | | | | |
| **Station # 718** | 25°21,5 N, 19°30,9 W | 1000m | 27°21,5 N, 19°30,7 W | 910m | CDRD |
| One piece of vesicular basalt (up to 10cm in diameter), coral debris, manganese crusts and hemipelagic limestone. | | | | | |
| **Station # 719** | 25°21,5 N, 19°30,5 W | 698m | 25°21,5 N, 19°30,3 W | 609m | CDRD |
| Coral debris and hemipelagic limestone. | | | | | |
| **Station # 720** | 25°21,4 N, 19°30,2 W | 532m | 25°21,5 N, 19°29,9 W | 504m | CDRD |
| One piece of hemipelagic, light coloured and semi-consolidated carbonate with thin manganese crust. | | | | | |

*7. Hierro Seamount*

| Date/Station number | On bottom | Water depth | Off bottom | Water depth | Dredge type |
|---|---|---|---|---|---|
| *11.12.1998* | | | | | |
| **Station # 721** | 25°59,1 N, 18°42,9 W | 2440m | 25°59,2 N, 18°42,7 W | 2311m | CDRD |
| Some pieces of relatively well-crystallized, vesicular (10-20 vol.%) dolerite coated by manganese crusts. Vesicles filled with clay minerals. | | | | | |
| *12.12.1998* | | | | | |
| **Station # 722** | 25°59,7 N, 18°41,9 W | 1953m | 25°59,8 N, 18°41,6 W | 1798m | CDRD |
| Fifty kg of hemipelagic, light coloured and semi-consolidated carbonate rocks with thin manganese crust. | | | | | |
| **Station # 723** | 25°59,9 N, 18°41,2 W | 1574m | 26°00,0 N, 18°40,8 W | 1393m | CDRD |
| Thirty kg of manganese crusts | | | | | |
| **Station # 724** | 26°00,3 N, 18°40,2 W | 1138m | 26°00,5 N, 18°40,0 W | 1045m | CDRD |
| Fifty kg of hemipelagic, yellowish carbonate rocks, manganese crusts and coral debris. | | | | | |

*8. Kiel Seamount*

| Date/Station number | On bottom | Water depth | Off bottom | Water depth | Dredge type |
|---|---|---|---|---|---|
| *12.12.1999* | | | | | |
| **Station # 725** | 27°19,4 N, 17°48,1 W | 3525m | 27°19,6 N, 17°47,3 W | 3288m | CDRD |
| NR | | | | | |
| **Station # 726** | 27°18,4 N, 17°46,4 W | 3385m | 27°18,9 N, 17°46,1 W | 3214m | CDRD |
| Two pieces of aphyric, vesicular basalt coated by manganese crust. | | | | | |

*9. Los Gigantes*

| Date/Station number | On bottom | Water depth | Off bottom | Water depth | Dredge type |
|---|---|---|---|---|---|
| *13.12.1998* | | | | | |
| **Station # 727** | 28°15,9 N, 16°55,2 W | 818m | 28°16,1 N, 16°54,8 W | 693m | CDRD |
| Five kg of amph- and fsp-phyric, felsite, dense ol- and plag-phyric basalt and calcareous crusts. | | | | | |
| **Station # 728** | 28°16,2 N, 16°54,6 W | 700m | 28°16,2 N, 16°54,6 W | 499m | CDRD |
| Fifteen kg of coral debris, bioclastic carbonates and some pieces of pumiceous rocks. | | | | | |
| **Station # 729** | 28°16,1 N, 16°54,6 W | 617m | 28°16,2 N, 16°54,4 W | 501m | CDRD |
| Coral debris and sponges | | | | | |
| **Station # 730** | 28°16,2 N, 16°54,5 W | 520m | 28°16,3 N, 16°54,5 W | 415m | CDWS |
| Ten kg of lithified bioclastic carbonates and some sponges. | | | | | |
| **Station # 731** | 28°16,3 N, 16°54,5 W | 367m | 28°16,4 N, 16°54,6 W | 401m | CDWS |
| One piece of dense, cpx- and ol-phyric basalt. | | | | | |

## Dredge Protocol Leg M43/1 (continued)

*10. Punta de la Rasca*

| Date/Station number | On bottom | Water depth | Off bottom | Water depth | Dredge type |
|---|---|---|---|---|---|
| *13.12.1999* | | | | | |
| **Station # 732** | 27°51,7 N, 16°44,6 W | 2503m | 27°51,8 N, 16°44,3 W | 2339m | CDRD |
| Hemipelagic, clayey, calcareous sediment. | | | | | |
| *14.12.1998* | | | | | |
| **Station # 733** | 27°52,1 N, 16°43,6 W | 1932m | 27°52,0 N, 16°43,6 W | 1980m | CDRD |
| Fourty kg of manganese-coated basalt and volcaniclastics. Fresh, vesicular (c. 30-40 vol.%), fsp- (c. 2 vol.%), cpx- (c. 1 vol.%), ol- (c. 1 vol.%) phyric basalt with a glassy crust. Fine-grained cpx- (c. 1 vol.%), fsp- (c. 2 vol.% microphenocrysts) phyric basalt with irregular to elongate vesicles. Brownish bedded volcaniclastic sediment, probably felsic tuff layers with crystals of fsp, dark mica, lit. | | | | | |
| **Station # 734** | 27°53,1 N, 16°43,3 W | 1942m | 27°53,1 N, 16°42,9 W | 1742m | CDRD |
| Dark vesicular basalt (15cm in diameter) with thin manganese crust. | | | | | |

*11. Off Barranco de Veneguera and Tasartico*

| Date/Station number | On bottom | Water depth | Off bottom | Water depth | Dredge type |
|---|---|---|---|---|---|
| *14.12.1998* | | | | | |
| **Station # 735** | 27°47,0 N, 15°53,7 W | 1596m | 27°46,9 N, 15°53,4 W | 1390m | CDWS |
| Two fish boxes of brownish, hemipelagic sediment with some light coloured lenses, probably tuffaceous. | | | | | |
| **Station # 736** | 27°46,8 N, 15°52,9 W | 954m | 27°46,8 N, 15°52,6 W | 833m | CDRD |
| Four bread-crusted specimen of fresh, dense, glassy, quenched fsp-phyric rhyolite with minor cpx, opx, mt and zr. Also one slightly more crystallized piece. | | | | | |
| **Station # 737** | 27°46,7 N, 15°51,5 W | 593m | 27°46,7 N, 15°51,5 W | 566m | CDRD |
| Half a fishbox of carbonate crusts with some crystals, rock fragments, and probably glass shards. One piece of conglomerate with well-rounded types of 'lava', ignimbrites and carbonate. One piece of mini-walnut-sized, gray ignimbrite. | | | | | |
| **Station # 738** | 27°46,7 N, 15°51,0 W | 450m | 27°46,8 N, 15°50,8 W | 339m | CDRD |
| NR | | | | | |
| **Station # 739** | 27°48,9 N, 15°53,7 W | 1173m | 27°49,0 N, 15°53,5 W | 844m | CDRD |
| Two pieces of dark grey, cpx-, plag-phyric, poorly vesicular, mugearitic lava. | | | | | |
| **Station # 740** | 27°49,0 N, 15°53,5 W | 929m | 27°49,1 N, 15°53,4 W | 670m | CDRD |
| Three fishboxes of brown, hemipelagic, clayey-calcareous sediment. | | | | | |
| **Station # 741** | 27°48,8 N, 15°53,5 W | 1000m | 27°49,0 N, 15°53,2 W | 708m | CDRD |
| Three fishboxes of brown, hemipelagic, clayey-calcareous sediment with some bioclastic fragments. | | | | | |
| *15.12.1998* | | | | | |
| **Station # 742** | 27°48,5 N, 15°52,7 W | 973m | 27°48,6 N, 15°52,7 W | 783m | CDRD |
| NR | | | | | |
| **Station # 743** | 27°48,5 N, 15°52,7 W | 854m | 27°18,5 N, 15°52,7 W | 793m | CDRD |
| Two big pieces (30cm in diameter) of dark grey, non- to moderately vesicular, ol- and cpx-phyric (c. 5 vol.%) basalt. | | | | | |
| **Station # 744** | 27°51,1 N, 15°56,8 W | 1286m | 27°51,2 N, 15°56,7 W | 1104m | CDRD |
| One fishbox of dense, ol-, cpx- and fsp-phyric (c. 10-20 vol.%) basalts and some pieces of brecciated hyaloclastites. | | | | | |
| **Station # 745** | 27°51,2 N, 15°56,7 W | 1056m | 27°52,3 N, 15°56,6 W | 950m | CDRD |
| NR | | | | | |
| **Station # 746** | 27°51,2 N, 15°56,5 W | 881m | 27°51,2 N, 15°56,5 W | 880m | CDRD |
| NR | | | | | |
| **Station # 747** | 27°51,2 N, 15°56,6 W | 1008m | 27°51,5 N, 15°56,4 W | 928m | CDRD |
| One fishbox of coral debris | | | | | |
| **Station # 748** | 27°54,2 N, 16°00,1 W | 1247m | 27°54,3 N, 15°59,7 W | 992m | CDRD |
| One fishbox of poorly vesicular, cpx-phyric glassy basalts, calcareous crusts with volcaniclastic fragments, coral debris and probably some coal pieces. | | | | | |
| **Station # 749** | 27°54,5 N, 15°58,7 W | 974m | 27°54,6 N, 15°58,4 W | 646m | CDRD |
| Half a fishbox of round, greenish, aphyric basalts. Some basalts slightly more crystallized, ol-, cpx- and plag-pyhric. | | | | | |

## Dredge Protocol Leg M43/1 (continued)

*12. Off Barranco de Güigüi Grande and GüiGüi Chico*

| Date/Station number | On bottom | Water depth | Off bottom | Water depth | Dredge type |
|---|---|---|---|---|---|
| *15.12.1998* | | | | | |
| **Station # 750** | 27°59,4 N, 16°01,5 W | 1685m | 27°59,4 N, 16°01,1 W | 1494m | CDRD |
| One fishbox of quenched, dark and in part glassy ignimbrites, coral debris and white, bioclastic limestones. | | | | | |
| **Station # 751** | 27°59,2 N, 16°01,0 W | 1405m | 27°59,2 N, 16°00,7 W | 1138m | CDRD |
| One 20 cm sized piece of ignimbrite. Coral debris. | | | | | |
| *16.12.1998* | | | | | |
| **Station # 752** | 28°00,0 N, 16°01,5 W | 1706m | 27°59,9 N, 16°01,2 W | 1725m | CDRD |
| NR | | | | | |
| **Station # 753** | 27°59,2 N, 16°08,5 W | 2171m | 27°59,2 N, 16°08,4 W | 1788m | CDRD |
| NR | | | | | |
| **Station # 754** | 27°59,3 N, 16°08,3 W | 1901m | 27°59,3 N, 16°08,2 W | 1776m | CDRD |
| Three fishboxes of coral debris. | | | | | |

*13. Hijo de Tenerife*

| Date/Station number | On bottom | Water depth | Off bottom | Water depth | Dredge type |
|---|---|---|---|---|---|
| *16.12.1998* | | | | | |
| **Station # 755** | 28°05,0 N, 16°10,7 W | 2100m | 28°05,2 N, 16°10,6 W | 1980m | CDRD |
| Two fishboxes with gray-green bomb shaped, microvesicular (0-30 vol.%), fsp-, mica-, and amph-phyric (only traces) fragments (35-2cm in diameter) with thin manganese coatings. Large variety of angular rock fragments (e.g. pumice-lapilli, one ol-megacryst). | | | | | |
| **Station # 756** | 27°05,2 N, 16°10,4 W | 1966m | 27°05,2 N, 16°10,4 W | 1891m | CDRD |
| Two fishboxes of similar fragments as in the previous dredge. Coral debris. | | | | | |
| **Station # 757** | 27°05,2 N, 16°10,4 W | 1893m | 27°05,4 N, 16°10,1 W | 1631m | DD with net inside |
| Ten pieces of pumiceous volcaniclastics. | | | | | |
| **Station # 758** | 28°05,4 N, 16°10,1 W | 1667m | | | RO |
| Water sampling | | | | | |
| **Station # 759** | 28°05,4 N, 16°10,1 W | 1660m | 28°05,4 N, 16°10,1 W | 1630m | CDRD |
| Ten pieces of volcaniclastites, lapillistone and one fishbox of coral debris. | | | | | |

*14. Submarine flank Gran Canaria off Agaete*

| Date/Station number | On bottom | Water depth | Off bottom | Water depth | Dredge type |
|---|---|---|---|---|---|
| *16.12.1998* | | | | | |
| **Station # 760** | 28°08,1 N, 15°55,2 W | 1576m | 28°08,2 N, 15°54,8 W | 1332m | CDRD |
| Some fishboxes of brown, hemipelagic calcareous ooze. | | | | | |
| **Station # 761** | 28°08,2 N, 15°54,8 W | 1368m | 28°08,2 N, 15°54,5 W | 1136m | CDRD |
| Some fishboxes of brown, hemipelagic calcareous ooze. | | | | | |
| *17.12.1998* | | | | | |
| **Station # 762** | 28°08,2 N, 15°54,5 W | 1093m | 28°08,2 N, 15°54,3 W | 711m | CDRD |
| Two small pieces of round basalt. | | | | | |
| **Station # 763** | 28°09,0 N, 15°55,9 W | 1768m | 28°09,0 N, 15°55,6 W | 1535m | CDRD |
| Three fist-sized pieces of dense ol- and cpx-phyric basalt and some coral debris. | | | | | |
| **Station # 764** | 28°09,1 N, 15°55,6 W | 1378m | 28°09,1 N, 15°55,5 W | 1129m | CDRD |
| NR | | | | | |
| **Station # 765** | 28°09,2 N, 15°55,4 W | 1073m | 28°09,3 N, 15°55,3 W | 938m | CDRD |
| Two fishboxes of dense, cpx- and ol-phyric basalt, basalt breccia with angluar fragments up to 7cm and coral debris. | | | | | |
| **Station # 766** | 28°09,4 N, 15°57,5 W | 2548m | 28°09,5 N, 15°57,3 W | 2231m | CDRD |
| Only some corals. | | | | | |
| **Station # 767** | 28°09,7 N, 15°56,6 W | 1796m | 28°09,7 N, 15°56,6 W | 1659m | CDRD |
| One piece (c. 25 cm in diameter) of cpx- and ol-pyric (c. 5 vol.%) basalt coated by manganese crust and some coral debris. | | | | | |

## Dredge Protocol Leg M43/1 (continued)

*15. Submarine flank off Güimar and Anaga*

| Date/Station number | On bottom | Water depth | Off bottom | Water depth | Dredge type |
|---|---|---|---|---|---|
| *17.12.1998* | | | | | |
| **Station # 768** | 28°13,4 N, 16°18,4 W | 988m | 28°13,7 N, 16°18,1 W | 653m | CDRD |
| One large piece (c. 1m in diameter) and some smaller pieces (5-20cm in diameter) of gray, microvesicular, cpx- and ol-phyric basalt and some carbonate matrix-supported, vesicular (>50 vol.%) lapillistone. All samples coated by very thin manganese crust. | | | | | |
| **Station # 769** | 28°19,2 N, 16°44,4 W | 1153m | 28°19,3 N, 16°14,2 W | 952m | CDRD |
| Calcareous, ooze and one coral. | | | | | |
| **Station # 770** | 28°36,3 N, 16°00,6 W | 2305m | 28°36,7 N, 16°00,6 W | 1883m | CDRD |
| One fist-size piece of relatively heavy scoria with irregular surface and some consolidated mudstones with volcaniclastic particles. | | | | | |
| *18.12.1998* | | | | | |
| **Station # 771** | 28°37,0 N, 15°56,4 W | 2970m | 28°37,0 N, 15°56,1 W | 2705m | CDRD |
| One piece of vesicular, ol- and cpx-pyhric basalt coated with manganese crust. | | | | | |
| **Station # 772** | 28°34,4 N, 15°59,8 W | 2386m | 28°34,6 N, 15°59,8 W | 2161m | CDRD |
| Dredge full of brown, hemipelagic mud. | | | | | |
| **Station # 773** | 28°32,8 N, 16°00,8 W | 2176m | 28°33,0 N, 16°00,1 W | 1947m | CDRD |
| Half a fishbox with brown, round, vesicular (<10 vol.%) glassy lapillstone, two pieces of glassy, vesicular (up to 50 vol.%) clasts and some calcareous, lutitic sediments with round lapilli. | | | | | |
| **Station # 774** | 28°30,6 N, 16°05,0 W | 1273m | 28°31,1 N, 16°05,0 W | 1149m | CDRD |
| One large block of slightly vesicular basalt, some small lapillstones and some semi-consolidated lutites with volcaniclastic particles. | | | | | |
| **Station # 775** | 28°29,3 N, 16°08,3 W | 541m | 28°29,5 N, 16°08,3 W | 380m | CDRD |
| One kg of dark, dense, ol- and plag-phyric basalt with glassy rim and some arenitic sediments. | | | | | |
| **Station # 776** | 28°29,4 N, 16°08,3 W | 436m | 28°29,3 N, 16°08,2 W | 538m | CDRD |
| About two fishboxes of very fresh, dark, cavernous, non-vesicular, cpx-, ol-, amph- and fsp-phyric basalt. Some pieces of semi-consolidated, arenitic sediments. | | | | | |
| **Station # 777** | 28°28,2 N, 16°07,8 W | 1172m | 28°28,6 N, 16°07,8 W | 944m | CDRD |
| Dredge full of brown, hemipelagic ooze. | | | | | |

*16. ODP Site 954*

| Date/Station number | On bottom | Water depth | Off bottom | Water depth | Dredge type |
|---|---|---|---|---|---|
| *19.12.1998* | | | | | |
| **Station # 778** | 28°26,2 N, 15°31,9 W | 3486 | | | RO |

*17. Submarine flank Gran Canaria off Galdar*

| Date/Station number | On bottom | Water depth | Off bottom | Water depth | Dredge type |
|---|---|---|---|---|---|
| *19.12.1998* | | | | | |
| **Station # 779** | 28°14,0 N, 15°43,0 W | 1268m | 28°14,1 N, 15°42,8 W | 1142m | CDRD |
| Around three kg of mostly very fine-grained, quenched, non-vesicular, aphyric (< 1 vol.% cpx and ol) basalt and minor cpx-(10 vol.%) and ol-phyric (c. 2-3 vol.%) basalt. | | | | | |
| **Station # 780** | 28°13,8 N, 15°42,9 W | 965m | 28°13,7 N, 15°42,9 W | 1013m | CDRD |
| Around two kg of cpx-, amph-, ol- and plag-phyric basalt and one piece of cpx- and ol-phyric lapillistone. | | | | | |
| **Station # 781** | 28°14,5 N, 15°40,8 W | 1617m | 28°14,2 N, 15°40,8 W | 1440m | CDRD |
| Dredge full of brown, hemipelagic ooze. | | | | | |

## Dredge Protocol Leg M43/1 (continued)

*18. Gran Canaria off Isleta*

| Date/Station number | On bottom | Water depth | Off bottom | Water depth | Dredge type |
|---|---|---|---|---|---|
| *19.12.1998* | | | | | |
| **Station # 782** | 28°14,2 N, 15°40,8 W | 1446m | 28°14,1 N, 15°40,7 W | 1283m | CDRD |
| NR | | | | | |
| **Station # 783** | 28°12,9 N, 15°28,8 W | 772m | 28°12,8 N, 15°25,5 W | 666m | CDRD |
| About five pieces of carbonate matrix-supported, cpx- and ol-phyric (2-3 vol.%) lapillistone-breccia with rounded clasts. Some specimen coated by fine-grained lapillistone and tuffs. | | | | | |
| **Station # 784** | 28°13,6 N, 15°24,1 W | 1293m | 28°13,5 N, 15°24,0 W | 1289m | CDRD |
| Dredge full of brown, hemipelagic ooze. | | | | | |
| **Station # 785** | 28°15,3 N, 15°23,9 W | 1932m | 28°15,1 N, 15°23,7 W | 1805m | CDRD |
| Dredge full of brown, hemipelagic ooze. | | | | | |
| **Station # 786** | 28°16,5 N, 15°23,9 W | 2801m | 28°16,2 N, 15°23,6 W | 2692m | CDRD |
| Dredge full of brown, hemipelagic ooze. | | | | | |
| *20.12.1998* | | | | | |
| **Station # 787** | 28°15,7 N, 15°23,0 W | 2162m | 28°15,6 N, 15°22,8 W | 1967m | CDRD |
| Dredge full of brown, hemipelagic ooze. | | | | | |
| **Station # 788** | 28°18,7 N, 15°20,4 W | 3078m | 28°18,7 N, 15°20,1 W | 2883m | CDRD |
| Dredge full of brown, hemipelagic ooze. | | | | | |
| **Station # 789** | 28°09,8 N, 15°17,7 W | 1882m | 28°09,8 N, 15°17,4 W | 1677m | CDRD |
| One piece (c. 10cm in diameter) of red, ol- and cpx-phyric (traces) tachylitic lapillistone. | | | | | |
| **Station # 790** | 28°06,9 N, 15°18,0 W | 1228m | 28°07,2 N, 15°18,1 W | 1040m | CDRD |
| One fishbox of basalt and ol-cpx-phyric picrites with round bizarre shapes. Five fishboxes of coral debris. | | | | | |
| **Station # 791** | 28°05,6 N, 15°09,3 W | 1467m | 28°05,8 N, 15°09,1 W | 1226m | CDRD |
| One piece of limestone. Manganese crusts and coral debris. | | | | | |
| **Station # 792** | 28°05,8 N, 15°09,0 W | 1305m | 28°06,0 N, 15°08,8 W | 1127m | CDRD |
| Half a fishbox of coral debris. | | | | | |
| **Station # 793** | 27°56,4 N, 15°06,5 W | 1603m | 27°56,6 N, 15°06,4 W | 1463m | CDRD |
| Four pieces of vesicular, cpx-, ol-phyric, manganese-coated basalt with minor glass crusts. Some pieces of manganese crust. | | | | | |
| **Station # 794** | 27°57,7 N, 15°01,4 W | 1637m | 27°58,0 N, 15°01,4 W | 1434m | CDRD |
| Two fishboxes of manganese-coated fsp-phyric phonolite breccia (up to 40cm in diameter), several types of volcanic breccia, minor vesicular basalt, one fishbox of coral debris. | | | | | |
| *21.12.1998* | | | | | |
| **Station # 795** | 27°56,1 N, 15°03,9 W | 1606m | 27°56,3 N, 15°03,9 W | 1565m | CDRD |
| Half a fishbox of manganese crusts. | | | | | |
| **Station # 796** | 27°51,8 N, 15°12,3 W | 1413m | 27°51,9 N, 15°12,4 W | 1304m | CDRD |
| One fishbox with one big plate (0,6x0,1 m) of manganese-coated bioclastic sandstone with scattered alkfsp crystals and < 1vol.% volcanic clasts, some corals. | | | | | |
| **Station # 797** | 27°51,2 N, 15°13,8 W | 1214m | 27°51,1 N, 15°14,0 W | 1102m | CDRD |
| Brown hemipelagic ooze. | | | | | |
| **Station # 798** | 27°45,8 N, 15°16,5 W | 1275m | 27°46,0 N, 15°16,8 W | 1087m | CDRD |
| One fishbox, several pieces of dark, highly vesicular and reddish slag, some manganese-coated limestone crusts with fsp and cpx (2-3 vol.%). | | | | | |
| **Station # 799** | 27°40,7 N, 15°27,2 W | 1515m | 27°41,0 N, 15°27,0 W | 1406m | CDRD |
| Brown hemipelagic ooze. | | | | | |

*19. Gran Canaria off SE coast*

| Date/Station number | On bottom | Water depth | Off bottom | Water depth | Dredge type |
|---|---|---|---|---|---|
| *21.12.1999* | | | | | |
| **Station # 800** | 27°41,2 N, 15°26,2 W | 1144m | 27°41,6 N, 15°26,6 W | 855m | CDRD |
| One fishbox of manganese-coated glass-rich phonolite breccia (up to 50cm in diameter) and brown hemipelagic ooze. | | | | | |
| **Station # 801** | 27°41,1 N, 15°31,1 W | 1338m | 27°41,3 N, 15°31,4 W | 1042m | CDRD |
| Brown hemipelagic ooze. | | | | | |

## Dredge Protocol Leg M43/1 (continued)

| | | | | | |
|---|---|---|---|---|---|
| **Station # 802** | 27°39,4 N, 15°38,3 W | 1206m | 27°39,5 N, 15°38,5 W | 890m | CDRD |
| NR | | | | | |
| **Station # 803** | 27°33,6 N, 15°44,6 W | 1455m | 27°33,8 N, 15°44,4 W | 1289m | CDRD |
| Two fishboxes with pumice altered glass lapilli (up to 4cm in diameter) in carbonate sediment, one piece of vesicular aphyric basalt, one piece of brownish scoria, one piece of light-colored volcaniclastic (?) sediment with lenticular texture, one fishbox of coral debris, all rocks manganese-coated | | | | | |
| **Station # 804** | 27°38,3 N, 15°49,2 W | 1330m | 27°38,6 N, 15°48,7 W | 1097m | CDRD |
| Brown hemipelagic ooze. | | | | | |
| *22.12.1998* | | | | | |
| **Station # 805** | 27°39,7 N, 15°47,1 W | 882m | 27°39,7 N, 15°46,7 W | 676m | CDRD |
| Brown hemipelagic ooze. | | | | | |
| **Station # 806** | 27°42,8 N, 15°50,9 W | 1227m | 27°42,8 N, 15°50,3 W | 900m | CDRD |
| Brown hemipelagic ooze. | | | | | |
| **Station # 807** | 27°44,6 N, 15°51,9 W | 1327m | 27°44,6 N, 15°51,6 W | 1128m | CDRD |
| NR | | | | | |
| **Station # 808** | 27°46,3 N, 15°53,0 W | 1261m | 27°46,5 N, 15°52,5 W | 968m | CDRD |
| Half a fishbox with fist-sized pieces of fresh glassy lava. Grayish, crystallized specimen, glassy specimen and brecciated rhyolite, all manganese-coated. Some manganese crusts. | | | | | |
| **Station # 809** | 27°46,8 N, 15°53,0 W | 1052m | 27°46,9 N, 15°52,6 W | 1005m | CDRD |
| Half a fishbox with three pieces of obsidian, one slightly crystallized, manganese crusts, carbonate sediment and corals. | | | | | |
| **Station # 810** | 27°48,9 N, 15°53,6 W | 1051m | 27°49,0 N, 15°53,4 W | 860m | CDRD |
| NR | | | | | |
| **Station # 811** | 27°48,6 N, 15°53,9 W | 1290m | 27°48,9 N, 15°53,6 W | 1039m | CDRD |
| Brown hemipelagic ooze. | | | | | |

### 7.1.1 On-board thin section petrography

The following table gives a summary of thin sections made on board (see chpater 5.1.2.1) and a brief description of their petrography.

Abbreviations used in this table are:

**Textures:**

anh: anhedral
euh: euhedral
subh: subhedral
glcr: glomerocryst
gm: groundmass
skel: skeletal
vf: vesicle filling
mfv: matrix-filled vesicles

**Minerals:**

ab: albite
alkfsp: alkali feldspar
amph: amphibole
aug: augite
bio: biotite
cpx: clinopyroxene
phl: phlogopite
pl: plagioclase.

**Glass alteration:**

strong: > 90 vol%
P: palagonite
PA: altered into sheet silicates/Fe-hydroxides

**Olivine alteration:**

O=Fresh
1=partly iddingsitic
2=pseudomorphs. Olivine pseudomorphs consist of sheet silicates, carbonate, Fe-hydroxides.

| Station no. /rock | Rock type | Vesicles vol | Fresh | Glass alteration | Olivine vol% | Ol alteratio | Cpx vol% | Pl vol% | Alkfsp | Amph vol% | Phl/Bio | Fe-Ti oxides | Mfv: x | Comment |
|---|---|---|---|---|---|---|---|---|---|---|---|---|---|---|
| ***1. South La Palma Ridge*** | | | | | | | | | | | | | | |
| 638-5 | Alkali basalt | > 50 | x | Minor(?): P, PA | < 2, euh/anh | 0 | <1, subh-euh | | | | | | x | Tachylite. Glassy rim (palagonite). Vf: partly zeolites |
| 638-12 | Alkali basalt, lapillistone | 80...90 | | P: strong, PA: minor | < 2, subh | 0 | <1, subh/anh, glcr | | | <1, subh/anh | | | x | Calcarous matrix with components of more evolved composition. Vf: partly zeolites |
| 638-14 | Carbonate sediment with volcanic clasts | | | Strong: P, PA | <<1 | 0 | <1, subh/anh | | | <<1, euh-subh-anh | | | | Biogenic components. cpx: aug, aegirine-aug, green-core cpx |
| 639-1 | Alkali basalt | 5...20 | x | None | <1, euh | 0 | 5-10, glcr, euh-subh; gm | | | | | | x | Tachylite. Spherulitic cpx aggregates in gm. Vf: partly Fe-hydroxides |
| 639-2 | Basaltic hyaloclastite | 80...90 | x | Minor: P, PA | <1, euh-anh, gm | 0 | <1, anh, gm | | | | | | | Spherulitic cpx aggregates in gm |
| 639-3 | Grain mount: hauyne-bearing felsic and basaltic components | 30-90 | x | Minor: P, PA | <1, subh-anh | 0 | <1, subh-anh, glcr | <1, subh-anh | <1, subh | | | | | Two major types of shards (a) glassy (b) tachylite. Shards with cpx spherulites. Hauyne: <<1, subh. Biogenic clasts |
| 645-1 | Carbonate sediment with volcanic clasts | | | Strong: PA | <1, anh | 0,1 | <1, subh/anh | | | <1, anh | | | | Crystals in calcareous matrix, rare lapilli. Titanite: <<1, anh. Biogenic components. cpx: aug, aegirine-aug, green-core cpx |
| 646-1a | Alkali basalt | <30 | x (?) | Minor(?): P, PA | <10; gm | 1,2 | <10%; glcr | <10%, gm | | | | | x | Tachylite. Vf: clay and carbonate, microfossils |
| 646-1b | Alkali basalt | <50 | | Strong: P, PA | <10; gm | 1,2 | <10%; glcr | <10%, gm | | | | | x | Tachylite. Vf: clay and carbonate, microfossils |
| 646-1c | Alkali basalt | <20 | x | Strong: P | <10, subh, glcr | 0,1 | Gm | <10, euh, gm | | | | | x | Tachylite. Gm olivine |
| 646-4 | Calcarenite with volcanic clasts | | | Strong: PA | <<1, anh | 0,1 | <<1, anh | | | <1, sub/anh | | | | |
| 648-1a | Alkali basalt | <60 | x | Strong: P | 5, subh /euh, glcr | 1,2 | <<1 euh | 2, gm | | | | | x | Tachylite. Glassy rim (palagonite). Vf: partly: zeolites, sheet silicates |
| 648-1b | Alkali basalt | <60 | | Strong: P, PA | <2, euh | 1 | <1, euh; gm: aug | 5...10, euh; gm: Pl | | | | | x | Tachylite. Vf: clay and carbonate, microfossils |
| 648-2 | Alkali basalt | <30 | x | Minor-strong (?): P, PA | <3, euh-subh | 1 | <1, euh/anh, glcr; gm: aug | 15, euh-subh/anh | | | | | x | Tachylite. Spherulitic cpx in gm |

| Station no. /rock | Rock type | Vesicles vol | Fresh | Glass alteration | Olivine vol% | Ol alteratio | Cpx vol% | Pl vol% | Alkfsp | Amph vol% | Phl/Bio | Fe-Ti oxides | Mfv: x | Comment |
|---|---|---|---|---|---|---|---|---|---|---|---|---|---|---|
| 651-1 | Carbonate sediment with minor volcanic clasts | >20 | | Strong: PA | <<1, subh | 0;1 | <1, euh/anh | <3, euh-subh | | | | | | Manganese crust |
| 654-1 | Carbonate sediment with volcanic clasts | | | Strong: PA | Gm | 0 | <<1, gm | | | | | | | |
| 656-1 | Carbonate sediment with alkali basaltic clasts | | x | Minor: P | <<1, anh | 0 | <<1, subh-anh | | | <<1, anh | | | | |
| 656-2 | Carbonate sediment with volcanic clasts | | | Strong: PA | <<1, anh | 0 | <<1, anh | | | | | | | |
| 657-2 | Carbonate sediment with manganese crust and volcanic clasts | | | Strong: PA | <1, anh | 0,1 | <1, sub-anh, aug, aegirine-aug (anh) | | | x, anh | | | | |
| 657-3 | Amph-bearing basalt or intermediate rock | <80 | x | Minor (P)-none | | | <1, euh/anh, gm | Gm | | <1, sub-euh | | | x minor | Highly vesicular, gradation in vesicle size. Amph is younger than aug |
| 657-4 | Scoriacious alkali basalt | <80 | x | Minor: P | <1, euh-subh, gm | 0 | <10, euh-subh, gm | <10, gm | | | | | | Tachylite |
| 657-6 | Calcarenite with felsic and basaltic volcanic components | | | Strong: PA | <<1, anh | 0 | <1, sub-euh | <1, anh | | <<1, anh | | | | |
| 658-5 | Alkali basalt | <40 | x | Minor: P | <5, euh | 0 | <1, euh-subh | | | | | | x | Tachylite. Glassy rim |
| 658-6 | Alkali basalt | <20 | x | Minor: P, PA. | <5, glcr, euh- anh | 0 | <3, subh. gm: aug | | | | | | x | Tachylite. Spherulitic cpx aggregates and ol in gm |
| 658-7 | Alkali basalt | < 40 | x | Minor: P, PA | <1, euh-subh, glcr | 0 | <1, glcr; gm | | | | | | x | Tachylite. Glassy rim |
| 658-7-II | Alkali basalt | <40 | x | Fresh-minor:P | <5, euh-subh | 0 | <1; glcr | | | | | | x | Tachylite. Glassy rim. Spherulitic cpx aggregates in gm |
| 658-8 | Alkali basalt | <12 | x | Minor-none: P? | <10, subh | 1 | <5, gm: aug | | | | | | x | Tachylite |
| 660-1 | Alkali basalt | <60 | x | Minor: P | <1, euh-subh | 0 | <1, euh-subh, glcr | | | | | | x, minor | Tachylite. Glassy rim (palagonite). Spherulitic cpx aggregates in gm |
| 660-1a | Alkali basalt | <60 | x | Minor(?): P | <8, euh-subh | 0 | <2 glcr | | | | | | x, minor | Tachylite. Vf: partly: zeolites |

| Station no. /rock | Rock type | Vesicles vol | Fresh | Glass alteration | Olivine vol% | Ol alteratio | Cpx vol% | Pl vol% | Alkfsp | Amph vol% | Phl/Bio | Fe-Ti oxides | Mfv: x | Comment |
|---|---|---|---|---|---|---|---|---|---|---|---|---|---|---|
| 660-2 | Alkali basalt | <30 | x | Minor: P, PA | <5, euh-subh, glcr | 0 | 2, euh-subh, glcr | | | | | | x | Spherulitic cpx aggregates in gm. Tachylite. Glassy rim. Vf: partly: zeolites, Fe-hydroxides |
| 662-2 | Felsite | | | Strong: zeolites, sheet silicates | | | | | 5, euh, glcr | <1, subh-anh | 1, bio, euh-subh | <<1 | | Well crystallized trachytic texture. Titanite? Manganese coating |
| 663-3 | Lapillistone with felsic and basaltic clasts | | x | Mafic ash particles: minor? P | <1, subh-anh | 0 | <1 | <<1, anh | <2, subh-anh, gm | <1, subh | <1, phl, euh-anh | <<1, euh | . | Titanite: <<1; cpx: subh aug, Ti-aug, aegirine-aug: subh-anh; aug: gm. Fresh glass basaltic |
| 663-5 | Tuff to fine lapilli-stone with felsic and basaltic clasts | variable | x | Variable. Strong: P,PA, minor: P | <2, anh | 0, 1 | < 2 aug, aegirine-aug; gm | <<1, anh, gm | <1, subh-anh, gm | <1, subh-anh | <1 euh-subh | <1 (tachyl. clasts) | x, minor-none | Hauyne: <<1, subh. Tachylite. Shell debris. Foraminifera |
| 664-2 | Alkali basalt | | x | Minor: P | <1 euh-subh | 0 | 8 | gm | | | | | | Tachylite. Cpx: aug, Ti-aug, euh-subh, glcr; gm: aug, skel |
| 664-3 | Alkali basalt lapillistone with calcareous matrix | Variable: 70-90 | x | Minor: P, PA | <1, euh; glcr | 0 | <8 | | | | | | x, minor | Vf: partly: zeolites, sheet silicates. cpx: aug, Ti-aug, euh-subh, glc, gm. |
| 664-4 | Basaltic lapillistone with calcareous matrix | | x | Variable: Strong : P, minor: P | <5, subh | 0 | <5 | | | | | | | Clast types (a) glassy (b) tachylite. Vf: partly: zeolites, sheet silicates. cpx: aug, Ti-aug, subh, glcr, green-core cpx. gm: aug |
| 664-8 | Alkali basalt | <30 | x | Minor: P, PA | <10, euh-subh | 0 | Ti-aug <1, glcr, gm: aug. | gm | | | | | x, minor-none | Tachylite. Some ol with strong undulose extinction, translation lamellae |
| 665-2 | Alkali basalt with cpx-hornblendite cumulate | <20 | x | Fresh | <1, subh; gm | 0 | < 5, aug, Ti-aug, green-core cpx; gm: aug. | gm | | | | | | Tachylite. Glassy rim. Cumulate: aug, amph, apatite, opaque phase, interstitial glass. Vf: partly: zeolites |
| 666-1 | Carbonate sediment with volcanic clasts | | | Strong: PA | <1, subh-anh | 0 | <1 anh: Aegirine-aug, aug, Ti-aug. | <<1; Lapillus: gm | Lapillus: gm | <1, anh | Lapillus: bio <2 | | | Titanite: <1, anh. Some ol clasts with translation lamellae. Biogenic clasts. Fragments of manganese crusts (?) |
| 666-2 | Felsite | | | Strong. Zeolites, Fe-hydroxides | | | | | <5 euh-subh, gm | <1, subh | 1, bio, euh-subh | <1 | | Titanite: <<1, subh; apatite: <1, euh |
| 666-3 | Alkali basalt | variable 50-30 | x | Minor: P | <3, euh; glcr | 0 | <<1 euh, gm | | | | | | x, minor | Spherulitic aug aggregates in gm. Gradation in vesicle size |

| Station no. /rock | Rock type | Vesicles vol | Fresh | Glass alteration | Olivine vol% | Ol alteratio | Cpx vol% | Pl vol% | Alkfsp | Amph vol% | Phl/Bio | Fe-Ti oxides | Mfv: x | Comment |
|---|---|---|---|---|---|---|---|---|---|---|---|---|---|---|
| 667-1 | Alkali-basaltic lapilli in carbonate matrix | variable 30-50 | x | Variable. Strong PA; Minor P | <1, subh, variable | 0,1 | <1, subh | <5, euh-subh | | | | | x. minor-none | Vf: partly: zeolites |
| 667-2 | Alkali basalt | >20 | x | Minor (?) P, PA | <1, euh-subh | 1 | < 1 | <3, euh-subh, glcr | | | | | x, minor-none | Tachylite. Glassy rim (palagonite). Many vesicles filled with sediment |
| 667-3 | Basalt | >20 | x | Minor-strong (?) P, PA | <1, euh-subh | 1 | | 1, euh-subh, gm | | | | | x, minor-none | |
| ***2. South Hierro ridge*** | | | | | | | | | | | | | | |
| 668-2 | Picritic basalt | <20 | x | Fresh | 10, euh-subh; gm | 0 | >10; gm | gm | | | | <1, skel | x, minor-none | Gradation in vesicle size |
| 668-8 | Basaltic lapillistone | variable 5-20 | x | Minor: P | <1, euh-subh-anh; gm | 0 | <1, euh-subh, glcr, gm | <1, euh-subh, gm | | | | <1 euh-subh | x, minor-none | Spherulitic cpx in gm |
| 668-9 | Basaltic hyaloclastite | variable 30-40 | x | Minor: P, PA | <1, euh-subh | 0 | <1, subh | gm | | | | | x, minor-none | Well sorted. Bubble wall shards |
| 669-2a | Basaltic lapillistone with carbonate matrix | | x(?) | Lapillus: strong (?) P; others: strong PA | <1, subh/anh | 0,1 | <1, subh.gm | | | | | | | Lapillus: Tachylite. Spherulitic cpx aggregates in gm. Vf: partly: zeolites |
| 669-2b | Alkali basaltic lapillistone | <70 | | Strong: P, PA | <1, euh-subh; glcr | 0 | <1: aug, Ti-aug, euh-subh | | | | | | | |
| 669-3 | Alkali basalt | >40 | x | Minor: P | <1, euh-subh, gm | 0 | < 2: aug, Ti-aug, glcr <2; gm: aug | | <<1 auh-anh, xenocr | | | | x | Tachylite. Glassy rim (P). Aug in gm: spherulite-like aggreg. Vf: partly zeolites. Alkfsp xenocr. |
| 670-1 | Alkali basaltic lapillistone with carbonate cemented matrix | variable 30-40 | | Strong: P, PA | <1, euh-subh-anh, glcr | 0 | | <1, euh-subh | | | | <1, subh | x, minor | Vf: partly: zeolites |

| Station no. /rock | Rock type | Vesicles vol | Fresh | Glass alteration | Olivine vol% | Ol alteratio | Cpx vol% | Pl vol% | Alkfsp | Amph vol% | Phl/Bio | Fe-Ti oxides | Mfv: x | Comment |
|---|---|---|---|---|---|---|---|---|---|---|---|---|---|---|
| 671-2 | Alkali basalt | <50 | x | Minor: P | <1, subh-anh, gm | 0 | <1, euh | gm | | | | | x, minor | Tachylite. Glassy rim |
| 672-1 | Alkali basaltic lapillistone with carbonate matrix | <50 | x | Partly: strong P, PA. Clasts with fresh glass. | <1, anh | 0 | <1, sub/anh, glcr, gm | <1, subh | | | | | x, minor | |
| 673-1 | Alkali basalt | <30 | x | Minor: P | <1, euh-subh; glcr; gm | 0 | <1 euh-subh; gm: aug | gm | | | | | x | Tachylite. Glassy rim (P). Alternating layers of filled/ partly filled vesicles. Spherulitic aug-aggregates in gm. Vf: partly: zeolites |
| 673-3 | Hyaloclastite of basaltic to intermediate composition | variable 20-40 | x | Minor: P | <<1, anh | 0 | <<1, anh; gm: aug, Ti-aug | <<1, euh; gm | | | | | | Biogenic clasts |
| 674-1 | Hyaloclastite of basaltic to intermediate composition | | | Strong: P | <<1, anh | 0,1 | ? | <<1, anh; gm | | | | | | Biogenic clasts |
| 674-3 | Basalt-carbonate breccia | Variable 40-70 | | Strong: P,PA | <1, euh-subh | 0 | <1, euh-subh | | | | | | x | Some clasts: tachylite. Vf: partly: sediment, zeolites |
| 675-2 | Alkali basalt | | x | Minor: P | <<1, euh | 0 | <1, gm | <1, gm | | | | <1, subh | x, minor-none | Tachylite. Vf: partly: zeolites |
| 676-2 | Alkali basalt | <40 | | Strong | <3, euh | 2 | <1, euh-subh | gm | | | | | | Vf: completely: carbonate; ol: iddingsite, carbonate |
| 677-1 | Carbonate sediment | | | | | | | | | | | | | No volcaniclastic components |
| 678-2 | Felsic lapillistone with syenite fragments | | | Strong: zeolites, sheet silicates | | | <<1, subh-anh | | <2, euh-subh-anh | <1, subh-anh | <1, bio, anh | <1, anh | | Calcareous matrix. Syenite: alkfsp, bio, cpx, titanite and opaque phases |
| 679-1 | Felsic lapillistone | Variable 20-40 | | Strong:PA | | | | | gm | | | | x | Lapilli: zonation in vesicle size, large vesicles in the interior. Matrix: carbonate, partly open pore space |
| 679-2 | Felsic tuff with intermediate components | Variable 0-5 | | Strong: sheet silicates, zeolites | | | <1, aegirine-aug, aug,anh | | <5, anh | <1, anh | <1, bio, subh | | | Zircon: <<1, subh |
| 682-1 | Lapillistone, hyaloclastite with carbonate cement | | x | Variable: strong/minor: P, PA | <1, euh-subh-anh | 0 | <1, subh-anh | <1, euh-subh | | | | | x | Some clasts: tachylite. Vf: partly: sediment |
| 684-1 | Carbonate sediment with highly altered basaltic ash clasts | Variable 20-40 | | Strong, chlorite/ serpentine | | | | 5 | | | | | | |

| Station no. /rock | Rock type | Vesicles vol | Fresh | Glass alteration | Olivine vol% | Ol alteratio | Cpx vol% | Pl vol% | Alkfsp | Amph vol% | Phl/Bio | Fe-Ti oxides | Mfv: x | Comment |
|---|---|---|---|---|---|---|---|---|---|---|---|---|---|---|
| 684-2 | Intermediate to basaltic rock | <20 | | Strong, layer silicates and secondary carbonates | | | | pl <4, euh-subh and gm | | | | <<1, euh | x, minor | Ab-rich Pl |
| 684-3 | Carbonate sediment with basaltic clasts | <80 | | Strong: P, PA | <1, subh-anh | 0 | <1, subh | | | | | <1, euh-subh | | Vf: partly: sediment, Fe-hydroxides, sheet silicates |
| ***3. Las Hijas Seamounts*** | | | | | | | | | | | | | | |
| 687-2a | Felsite | | | Strong: zeolites, sheet silicates | | | gm: aegirine-aug | | 1-2, euh-subh | | | | | |
| 687-2b | Felsite with inclusion of intermediate composition | | | Strong: zeolites, sheet silicates | | | gm: aegirine-aug | | 1-2, euh-subh | <<1, subh-anh | | | | Inclusion: vesicle volume <20%, cpx, Fsp (pseudomorphs), opaques, apatite |
| 687-3 | Felsite | | | Strong, zeolites | | | <<1, subh | | 1, eu-subh/anh, gm | | | <1, euh | | |
| 687-5 | Intermediate | <20 | x (?) | Minor: P | | | <1, euh-subh, glcrst | <1, euh-subh, gm | | | | <1, euh-subh | x, minor | Vf: partly: sheet silicates |
| 687-7 | Felsite with manganese crust | | | Strong: zeolites, sheet silicates | | | gm | | <1, euh-subh, gm | | | | | |
| 687-8 | Felsite with inclusion of intermediate composition | | x (?) | Felsite: strong. zeolites. Inclusion: minor | | | gm | | 1, eu-/subh, gm | | | <1 anh | | Inclusion: vesicle volume 5-10%, cpx, pl, opaques, fresh (?) glass |
| 689-1 | Felsite | <20 | | Strong, sheet silicates, Fe-hydroxides | | | | | <1, euh, gm | | | | | |
| 689-2 | Amph-bearing felsite with more mafic inclusion | < 5 | | Strong, sheet silicates | | | <1, euh-subh | | < 5, euh | <1, euh-subh | | <5, skel | x | Inclusion: Phenocrysts: pl <3, gm: pl, cpx; , gm: 2 opaque phases |
| 689-3-a | Felsic clast-supported breccia | Variable 0-5 | | Strong: Fe-hydroxides, zeolites, layer silicates | | | | | <1, euh, gm | | | | x | Apatite: <<1, euh, gm: titanite (product of alteration?). Pore space between fragments only partly filled |
| 689-3-b | Felsite | <15 | | Strong: Fe-hydroxides, zeolites, layer silicates | | | | | <1, euh, gm | | | | x, minor | Vf: partly: Sheet silicates, zeolites, Fe-hydroxides |

| Station no. /rock | Rock type | Vesicles vol | Fresh | Glass alteration | Olivine vol% | Ol alteratio | Cpx vol% | Pl vol% | Alkfsp | Amph vol% | Phl/Bio | Fe-Ti oxides | Mfv: x | Comment |
|---|---|---|---|---|---|---|---|---|---|---|---|---|---|---|
| 689-3-C | Felsite breccia with manganese crust | Variable 1-20 | | Strong, zeolites, layer silicates | | | | | <1, euh, gm | | | <<1 | x, minor | Apatite: <<1, euh, gm: titanite (product of alteration?) |
| 689-4 | Felsite | | x(?) | Minor (?): zeolites, layer silicates | | | | | <1, euh-subh, gm | | | <1, euh-subh | | |
| 689-5 | Felsite | | x(?) | Minor (?): zeolites, layer silicates | | | <1, euh-subh | | <1, euh-subh, gm | | | | | |
| 689-6 | Felsite | | | Strong | | | <1, euh-subh | | <1, euh-subh, gm | | | <1 euh-subh | | Glass alteration: zeolites, analcime(?), layer silicates |
| ***4. Tropic Seamount*** | | | | | | | | | | | | | | |
| 692-1 | Amph-bearing alkali basalt/intermediate rock | <1 | x (?) | Minor (?). P | <1; gm | 2 | <3, euh-subh | <1, euh, gm | | <3, euh-subh, glcr | | <1 subh/ anh | x | Titanite: <1, subh, opaque corona. Mafic schlieren (higher contents of Fe-Ti oxides in gm); cpx: aug, green-core cpx, Ti-aug, glcr, gm |
| 692-2 | Felsite | | ? | Minor (?): Fe-hydroxides, analcime (?), zeolites | | | <1 aegirine-aug, euh-subh, gm | | <1, euh-subh, gm | <1, pseudo-morphs | | <1 euh | | Titanite: <1, euh-subh, Amphibole pseudomorphs of opaques + aegirine-aug |
| 692-3 | Amph-bearing alkali basalt/intermediate rock | <1 | x | Minor (?): P | <1, gm; glcr | 2 | <3 euh-subh | <1, euh, gm | | <3, euh-subh, glcr | | <1 subh/ anh | x(?) | Cpx: aug, green-core cpx, Ti-aug, glcr, gm. Same rock as sample 692-1 |
| 693-1 | Alkali basalt tuff | <20 | | Strong: PA | <5, euh-subh | 2 | <2, euh-subh, gm | | | | | <1, euh | x(?) | Vf: partly: zeolites |
| 693-2a | Felsite | | | Strong: zeolites, Fe-hydroxides | | | Aegirine-aegirine aug: gm | | | | | <<1, anh | | Alkfsp: Spherulitic growth in gm |
| 693-2b | Felsic and mafic lapilli in carbonate cement | | | Felsic lapilli: strong: zeolites,PA. Mafic lapilli: strong: PA | | 2 | aug <1 euh-subh, gm: Aegirine-aegirine aug | | <1, euh-subh, gm | <1, euh-subh | | <<1 | | Tachylite clasts |
| 693-3 | Amph-bearing felsite | | | Strong: zeolites, Fe-hydroxides | | | <1, aug, Ti-aug, euh-subh, gm | | <3, euh, gm | <1, euh-subh | | | | Titanite: <1, euh |

| Station no. /rock | Rock type | Vesicles vol | Fresh | Glass alteration | Olivine vol% | Ol alteratio | Cpx vol% | Pl vol% | Alkfsp | Amph vol% | Phl/Bio | Fe-Ti oxides | Mfv: x | Comment |
|---|---|---|---|---|---|---|---|---|---|---|---|---|---|---|
| 694-1 | Alkali basalt. Pillow fragment? | <20 | | Strong, ol: carbonate pseudomorphoses | <1, euh | 2 | <1, euh-subh, glcr, gm | Gm | | | | | x | Moderate quench crystallization. Vf: completely: carbonate. Partly: zeolites |
| 694-2 | Alkali basalt | <30 | | Strong, ol: carbonate pseudomorphoses | <1, euh | 2 | euh-subh, glcr, gm | Gm | | | | <1, subh/anh | x | Moderate quench crystallization. Vf: completely: carbonate |
| 694-3 | Basalt | <25 | | Strong: PA | | | <1, euh-subh, glcr | Gm | | | | <1, euh-subh | | Tachylite |
| 697-2 | Carbonate sediment with highly altered volcanic clast | | | Strong: PA | | | | gm (altered) | | | | | | |
| 699-1a | amph-bearing felsite | <5 | | Strong: zeolites | | | gm | | <1, euh, gm | <<1, euh | | | x | |
| 699-1b | amph-bearing felsite | <5 | | Strong: zeolites | | | gm | | <1, euh, gm | <<1, euh | | | x | Vf: partly: zeolites |
| 703-2 | Basaltic lapillistone, carbonate cemented matrix | <5 | x | Variable: minor-strong, P, PA | <1, euh, | 1; 2 | <2, Ti-aug, aug, gm | | | | | | x(?) | Two major types of clasts (a) glassy (b) tachylite. Vf: completely: carbonate |
| 703-4 | Alkali basaltic lapillistone. Cement: zeolites +carbonate | Variable 0-10 | | Strong: PA | <1, euh | 2 | | | | | | | x, minor | Vf: partly: zeolites, sheet silicates |
| ***5. Paps Seamount*** | | | | | | | | | | | | | | |
| 707-1 | Alkali basalt | <30 | | Strong: PA | <1, euh (?) | 2 | | <1, euh, glcr, gm | | | | | x | Vf: partly: sheet silicates |
| 711-1a,b,c | Coal slag | Vesicles present | | | | | | | | | | | | Mullite, sp, graphite |
| 711-2 | Coal slag | Vesicles present | | | | | | | | | | | | Mullite, graphite |
| ***6. Endeavour Seamount*** | | | | | | | | | | | | | | |
| 715-1a | Basalt | <25 | | Strong: P, PA | <1,euh-subh | 2 | <2, euh, glcr | gm | | <1, euh-subh, glcr | | <1, subh | | Tachylite. Vf: zeolites, carbonate |
| 715-1b | Basalt | <30 | x(?) | Minor(?)-strong: P, PA | <1,euh-subh | 2 | <1, euh | gm | | <1, euh-subh | | <1, subh | | Tachylite. Vf: zeolites, carbonate. Gm: chromite |

| Station no. /rock | Rock type | Vesicles vol | Fresh | Glass alteration | Olivine vol% | Ol alteratio | Cpx vol% | Pl vol% | Alkfsp | Amph vol% | Phl/Bio | Fe-Ti oxides | Mfv: x | Comment |
|---|---|---|---|---|---|---|---|---|---|---|---|---|---|---|
| 716-1b | Basalt | <30 | | Strong: P, PA | <1, euh | 2 | <2, euh-subh, glcr | gm | | | | | x | Tachylite. Vf: nearly completely: carbonate, sheet silicates, minor zeolites |
| 716-2 | Hyaloclastite, large basalt clast | <15 | | Strong: PA | <1, euh-subh | 2 | <1, euh-subh | gm | | | | | x, minor | Tachylite. Vf: partly: carbonates, sheet silicates, zeolites |
| 717-1 | Basalt | <15 | | Strong: PA | <1 | 2 | <1, euh-subh | <1 | | | | <<1 | x | Tachylite. Vf: carbonates |
| ***7. Hierro Seamount*** | | | | | | | | | | | | | | |
| 721-1 | Strongly altered basalt | <8 | | Strong: PA | | | | gm (altered) | | | | | x | Tachylite |
| 721-2 | Strongly altered basalt | <10 | | Strong: PA | | | | gm (altered) | | | | | x | Tachylite |
| 721-3 | Basalt | <25 | | Strong: PA | | | | gm | | | | | x | Tachylite |
| 721-5 | Basalt | <15 | | Strong: PA | | | | | | | | <<1, euh | x | Tachylite |
| ***9. Tenerife, Los Gigantes*** | | | | | | | | | | | | | | |
| 727-1 | Felsite | <5 | | Strong: Sheet silicate | | | | | <10, euh-subh, ± altered | <<1, subh | <1, euh-subh | | x | |
| 727-2 | Carbonate sediment with volcanic clasts | | x(?) | Basaltic clast: minor-strong(?) | <<1, anh | 0; 1 | <<1, anh | <<1, anh | | <<1, anh | | | | Ash-sized tachylitic clast. Biogenic debris |
| 727-3 | Basalt | | x(?) | Minor(?)-strong(?): P | <1, euh-subh; gm | 2 | <10, euh-subh, glcr; gm | <15, euh-subh; gm | | | | <1, euh-subh-anh | | Mafic schlieren (higher contents of Fe-Ti oxides in gm, smaller size of gm crystals) |
| 728-2 | Carbonate sediment with volcanic clasts | | | Strong: PA | | | <<1, anh | <<1, anh | | | | | | Biogenic debris |
| 731-1a | Basalt | | x | None-minor(?) | <3, euh-subh | 0 | <3, euh-subh | gm | | | | | | Mafic schlieren (higher content of Fe-Ti oxides in gm) |
| 731-1b | Basalt | | x | None-minor(?) | <3, euh-subh | 0 | <3, euh-subh | gm | | | | | | Mafic schlieren (higher content of Fe-Ti oxides in gm) |

| Station no. /rock | Rock type | Vesicles vol | Fresh | Glass alteration | Olivine vol% | Ol alteratio | Cpx vol% | Pl vol% | Alkfsp | Amph vol% | Phl/Bio | Fe-Ti oxides | Mfv: x | Comment |
|---|---|---|---|---|---|---|---|---|---|---|---|---|---|---|
| ***10. Tenerife, Punta de la Rasca*** | | | | | | | | | | | | | | |
| 733-1a | Basalt | <10 | x | Minor: P | | | <1, euh-subh | <1, euh-subh glcr | | | | <1, euh | x | Tachylite. Spherulitic growth of cpx in groundmass |
| 733-1d | Basalt | <15 | x | Minor: P | | | <1, euh | <1, euh-subh | | | | | x, minor | Tachylite. Spherulitic growth of cpx in groundmass. Manganese crust |
| 733-2-I | Carbonate sediment with volcanic clasts and altered hyaloclastite | | | Strong: PA | | | <<1, subh | <<1, euh-sub-anh; clast: gm | | <<1, subh | | <1, subh | | Biogenic debris |
| 733-2-II | Carbonate sediment with volcanic clasts and altered hyaloclastite | | | Strong: PA | | | <<1, subh | <<1, euh-subh-anh; clast: gm | | <<1, subh | | <1, subh | | Biogenic debris |
| ***11. Gran Canaria, off Barranco de Veneguera and Barranco de Tasartico*** | | | | | | | | | | | | | | |
| 735 smear slide | Clay sediment with volcanic clasts | | x(?) | Strong(?): P | | | <<1, subh | <<1, subh | | | | | | |
| 736-4 | Rhyolite | | x | None/minor? | | | | | <1 | | | | | Opx: <1, euh; zircon: <1, subh; pl: ab-rich, euh-subh, gm |
| 737-1 | Carbonate sediment with volcanic clasts | | | Strong: PA | | | <<1, subh-anh, aegirine-aug, aug | <<1, anh, gm | gm | | | | | |
| 737-2 | Carbonate sediment with volcanic clasts | | | Mafic clasts: strong, PA; felsic clasts: sheet silicates, zeolites(?) | <<1, anh | 0 | <<1, aug, aegirine-aug, euh-subh/anh | | Gm | | | | | Mafic, tachylitic basalt and felsite |
| 737-3 | Felsite | | x(?) | Minor-strong(?): PA, zeolites, carbonate | | | <1, anh, aegirine-aug; gm: aegirine | | <1, euh-subh | | | <1, sub/anh | | Tachylite. Spherulitic cpx aggregates in gm |
| 739-1 | Intermediate rock | | x | Minor: P, PA | | | <1, euh-subh, glcr | | <2 | | | <<1, subh | | Ab-rich pl, euh-subh, glcr, gm |
| 743-1 | Basalt | <3 | x(?) | Strong? P | <3, euh | 2 | <1, euh-subh, gm | gm | | | | <<1, subh-anh | x, minor | Vf: sheet silicates, zeolites |
| 743-3 | Basaltic lapillistone with carbonate and zeolite matrix | Variable 0-10 | ? | Strong: variable P, PA | | | <<1, euh-subh | | | | | | | Tachylite. Vf: carbonate, zeolites |

| Station no. /rock | Rock type | Vesicles vol | Fresh | Glass alteration | Olivine vol% | Ol alteratio | Cpx vol% | Pl vol% | Alkfsp | Amph vol% | Phl/Bio | Fe-Ti oxides | Mfv: x | Comment |
|---|---|---|---|---|---|---|---|---|---|---|---|---|---|---|
| 744-1a | Basalt | | x | Minor: P, PA | <3, euh-subh; glcr | 1 | <1, euh-subh, glcr; gm | <1, subh, gm | | | | <1, euh-subh | | |
| 744-1b | Picritic basalt | <5 | | Strong: P, PA | <20, euh-subh; glcr | 1 | <5, euh-subh, glcr; gm | Gm | | | | <1, euh-subh | | Tachylite |
| 748-2 | Slag (?) | <20 | x | Minor: P, PA | | | | <20, euh-subh | | | | | x | Tachylite |
| 749-1 | Basalt | <5 | x | Minor(?)-strong: P | <1, euh | 1 | <1, euh-subh; gm | <1, euh-subh, gm | | | | <1, euh-subh | x | Mafic schlieren (higher contents of Fe-Ti oxides in gm). Vf: nearly completely: two zeolite phases |
| 749-2 | Basalt | <3 | | Strong: P, PA | <1, euh-subh | 2 | <1, euh-subh; gm(?) | <1, euh, gm | | | | | x | Vf: completely: zeolites |
| ***12. Gran Canaria, off Barranco de Güigüi Grande and Güigüi Chico*** | | | | | | | | | | | | | | |
| 750-3 | Basalt | | x | Minor: P | <1, euh-subh | 1 | 1, euh-subh, glcr | <20, euh-subh; gm | | | | <1, subh | | Tachylite. More mafic clasts (more Fe-Ti oxides in gm) |
| 750-4 | Basalt | | x | | <<1, subh | 0 | 1, euh-subh, glcr | <15, euh-subh; gm | | | | <1, subh | | |
| 750-6 | Volcaniclastic sediment with felsic and mafic clasts | | x | Variable: minor-strong: Sheet silicates; P, PA | | | <1, subh/anh, aegirine-aug, aug | <<1, anh | | <1, subh/anh | <1, subh/anh | <1, subh | | Felsic glassy and tachylite clasts. Biogenic debris |
| 751-1 | Basalt | | x | Minor: P | | | | <25, euh-subh; gm | | | | <1, euh-subh | | Tachylite |
| ***13. Hijo de Tenerife*** | | | | | | | | | | | | | | |
| 755-1 | Intermediate rock | | x(?) | Sheet silicates | | | Gm (?) | | Gm | | | | | |
| 755-2 | Mafic to intermediate rock | | x | Sheet silicates | <1 | 0 | <1, euh-subh | | <1, euh-subh; gm | <1, euh-subh | <1, euh-subh | | x | Tachylitic domains |
| 755-4 | Felsite to intermediate rock | | x | | | | <1, euh-subh-anh | <1 , euh-subh | <<1, anh | | <1, euh-subh | | x | Tachylitic basalt inclusion: cpx (gm); pl ab-rich |

| Station no. /rock | Rock type | Vesicles vol | Fresh | Glass alteration | Olivine vol% | Ol alteratio | Cpx vol% | Pl vol% | Alkfsp | Amph vol% | Phl/Bio | Fe-Ti oxides | Mfv: x | Comment |
|---|---|---|---|---|---|---|---|---|---|---|---|---|---|---|
| 755-5-I | Mafic to intermediate rock | <15 | x | Minor: P | <1, subh-anh | 0 | <1, euh-subh | <1, euh-subh | | <1, euh-subh | <1, euh-subh | <1, euh-subh | x | Tachylitic domains |
| 755-5-II | Mafic to intermediate rock | <15 | x | Minor: P | | | <1, euh-subh | | | <1, euh-subh | <1, euh-subh | <1, euh-subh | x | Tachylitic domains. Spherulitic cpx aggregates |
| 756-1b | Mafic to intermediate rock | <10 | x | Minor: P | ?<1 subh (inclusion) | 2 | <1, euh-subh | Gm | | <1, euh-subh | <1, euh-subh | | x | |
| 756-3 | Mafic to intermediate lapillistone | Variable: 0-10 | x | Minor: P | <1, subh/anh | 0 | <1, euh-subh | <1, subh-anh | | | <1, euh-subh | | | |
| 756-4 | Mafic to intermediate rock | <20 | x | Minor: P, PA | <1, subh-anh | 0 | <1, euh-subh | <1, euh-subh | | <1, euh-subh | <1, euh-subh | <1, euh-subh | x | Inclusion of calcareous sandstone |
| 756-4b | Mafic to intermediate rock | <25 | x | Minor: P, PA | <1, subh-anh | 0 | <1, euh-subh, gm | <1, euh-subh | | <1, subh | <1, euh-subh; gm | | x | Tachylite |
| 757-2 | Felsite to intermediate rock | <15 | x | Minor: Sheet silicates | | | <1, euh-subh | <1 euh-subh | | | <1, euh-subh | <1, euh-subh | x | Mafic inclusions (higher contents of Fe-Ti oxides in gm) |
| 757-3a | Manganese crust with volcanic clasts | Variable 0-15 | x | Minor: P, PA | <<1, anh | 0 | <1, euh-subh; gm | <<1, subh | | | | | | Tachylitic clasts. Ol grain with strong undulose extinction (translation lamellae) |
| 757-3b | Bbasaltic and intermediate lapillistone; matrix of manganese crust (?) | Variable 0-10 | x | Minor: P, PA | <<1, anh | 0 | <1, euh-subh; gm | <1, euh-subh; gm | | | <1, euh-subh | | | |
| 759-3a | Basaltic lapillistone | Variable: 0-20 | x | Minor: P, PA | <1, subh-anh | 0 | <1, euh-subh | <1, subh/anh | | <1, subh | <1, euh-subh | | x minor | Ol: some grains with strong undulose extinction. Matrix partly filled with manganese crust |
| 759-3b | Basaltic lapillistone | Variable: 0-10 | x | Minor: P, PA | <1, anh | 0 | <1, euh-subh | <1, euh-subh | | <1, euh-subh | <1, euh-subh | | x minor | Matrix partly filled with manganese crust |
| ***14. Submarine flank Gran Canaria, off Agaete*** | | | | | | | | | | | | | | |
| 761-2 | Alkali basalt | <5 | x | Minor: P, PA | <1, euh | 2 | <1, euh; gm | <1, euh-subh; gm | | | | | x | Tachylite. Mafic schlieren (higher content of Fe-Ti oxides in gm). Vf: zeolites |

| Station no. /rock no. | Rock type | Vesicles vol % | Fabric | Glass alteration | Olivine vol% | Ol alteration O (Fresh) | Cpx vol% | Pl vol% | Alkfsp vol% | Amph vol% | Phl/Bio vol% | Fe-Ti oxides | Mfv: x | Comment |
|---|---|---|---|---|---|---|---|---|---|---|---|---|---|---|
| 763-1 | Alkali basalt | <2 | x(?) | Strong: P, PA | <7, euh-subh, glcr; gm | 1 | <5, euh-subh, glcr; gm | Gm | | | | <1, subh | x | Vf: sheet silicates |
| 765-1 | Basalt | <1 | x | Minor: P, PA | <1, euh-subh | 1 | <1, euh-subh | | | | | | x | Tachylitic basalt. Glassy rim (palagonite). Spherulitic cpx aggregates in gm. Vf: partly: zeolites |
| 767-1 | Basalt | | x(?) | Strong (?): P, PA | <10, euh-subh | 1 | <5, euh-subh; gm | Gm | | | | | | Tachylite. Spherulitic cpx aggregates in gm |
| ***15. Submarine flank Tenerife, off Güimar and Anaga*** | | | | | | | | | | | | | | |
| 768-1 | Basalt | <25 | | Strong: P, PA | Gm | 0 | <1, euh-subh; gm | | | | | | x | Vf: zeolites, sediment |
| 768-2 | Basaltic clasts in carbonate sediment | Variable: 5-15 | | Strong: P, PA | <1, subh/anh | 0 | | <1, anh; gm | | | | | | |
| 768-3a-I | Basalt | <20 | x | Minor-strong(?): P, PA | <1, euh-subh | 0 | <1, euh-subh, glcr; gm | <1, euh-subh | | | | <1, euh-subh | x, minor | Strongly tachylitic and less tachylitic domains. Vf: partly zeolites |
| 768-3a-II | Basalt | <20 | x | Minor: P, PA | <1, euh-subh | 0 | <1, euh-subh; gm | <1, euh-subh | | | | <1, euh-subh | x, minor | Strongly tachylitic and less tachylitic domains. Vf: partly zeolites |
| 768-3b-I | Basalt | <20 | x | Minor: P, PA | <1, euh-subh | 0 | <1, euh-subh, glcr; gm | Gm | | | | <1, subh | x | Tachylite. Glassy rim (palagonite). Vf: partly, zeolites |
| 768-3b-II | Basalt | <20 | x | Minor: P, PA | <1, euh-subh | 0 | <1, euh-subh; gm | Gm | | | | <1, subh | x | Tachylite. Glassy rim (palagonite). Vf: partly, zeolites |
| 773-1 | Alkali basalt | <40 | x | Minor: P | | | <1, euh-subh, glcr; gm | | | <1, euh-subh, glcr | | <1, subh-anh | x | Tachylite. Glassy rim |
| 773-4-I | Basaltic lapillistone | Variable 20-50 | x | Minor: P, PA | <<1, subh-anh | 0 | <1, euh-subh; gm | | | <<1 subh | | <1, euh-subh | x | Two major types of clasts (a) glassy (b) tachylite. Spherulitic cpx aggregates in gm |
| 773-4-II | Basaltic lapillistone | Variable 20-50 | x | Minor: P, PA | <<1, subh-anh | 0 | <1, euh-subh; gm | | | | | <1, euh-subh | x | Two major types of clasts (a) glassy (b) tachylite. Spherulitic cpx aggregates in gm |
| 773-5 | Carbonate sediment with volcanic clasts | <20 | x | Variable: Minor-strong: P, PA | <<1, anh | 0 | <<1, subh-euh | <<1, subh | | | | | x | Tachylite clasts |

**Abbreviations**

Textures: anh, euh, subh: anhedral, euhedral, subhedral; glcr: glomerocryst; gm: groundmass; skel: skeletal; vf: vesicle filling; mfv: matrix-filled vesicles.

Minerals: Ab: albite; alkfsp: alkali feldspar; amph: amphibole; aug: augite; bio: biotite; cpx: clinopyroxene; phl: phlogopite; pl: plagioclase.

Glass alteration: strong: > 90 vol%; P: palagonite; PA: altered into sheet silicates/Fe-hydroxides

Olivine alteration: O=Fresh; 1=partly iddingsitic; 2=pseudomorphs. Olivine pseudomorphs consist of sheet silicates, carbonate, Fe-hydroxides.

## 7.2 Leg M43/2

Station List Leg M43/2

| Station | Time UTC | Device | Date | Geographical position Latitude | Longitude | Waterdepth uncorrected (m) | Wire length (m) | Comments |
|---|---|---|---|---|---|---|---|---|
| 1 | 09:27 | CTD 1 | 1.1 | 37° 35,2 N | 010° 38,0 W | 4503m | 800m | |
| | 12:24 | CTD 2 | | 37° 35,5 N | 010° 38,1 W | 4504 | 4000m | |
| 2 | 08:46 | Argos-Drifter 1. | 2.1 | 41° 00,0 N | 009° 24,9 W | 1000m | | |
| | 09:22 | Argos-Drifter 2. | | 40° 59,9 N | 009° 27,8 W | 1210m | | |
| | 09:52 | Argos-Drifter 3. | | 41° 01,8 N | 009° 27,8 W | 1366m | | |
| | 10:29 | Argos-Drifter 4. | | 41° 01,8 N | 009° 25,4 W | 870m | | |
| 3 | 21:03 | CTD 3 | 2.1 | 42° 37,8 N | 010° 03,8 W | 2356m | | break off<br>too heavy sea |
| | 23:09 | ADCP | | 42° 40,0 N | 010° 05,2 W | | | profile start rwK 127° |
| | 23:45 | | | 42° 37,2 N | 009° 59,8 W | | | course change to rwK 090° |
| | 03:02 | | 3.1 | 42° 37,5 N | 009° 30,3 W | | | course change to rwK 180° |
| | 04:32 | | | 42° 27,5 N | 009° 30,0 W | | | course change to rwK 270° |
| | 07:34 | | | 42° 27,5 N | 010° 00,0 W | | | course change to rwK 360° |
| | 08:00 | | | 42° 32,3 N | 010° 00,0 W | | | profile end |
| | 15:32 | ADCP/ | | 42° 38,8 N | 010° 01,9 W | | | profile start rwK 328° |
| | 19:12 | HS / PS | | 43° oo,o N | 010° 20,0 W | | | course change to rwK 090° |
| | 00:06 | | 4.1 | 43° 00,0 N | 009° 37,2 W | | | course change to rwK 180° |
| | 01:53 | | | 42° 52,1 N | 009° 37,0 W | | | course change torwK 160° |
| | 04:46 | | | 42° 37,5 N | 009° 30,0 W | | | profile end |
| 4 | 09:16 | hydro-phon | 4.1 | 42° 38,4 N | 010° 01,7 W | | 2300m | |
| | 09:36 | | | | | | | mooring IM3/2 released |
| | 12:17 | | | 42° 38,4 N | 010° 00,5 W | | | mooring IM3/2 complete on deck |
| 5 | 15:58 | hydro-phone Benthos/ Oceano | | | | 1454m | | mooring IM2/2 released |
| | 15:39 | | | 42° 39,3 N | 009° 42,2 W | | | mooring does not ascend |
| | 18:53 | hydro-phon | | 42° 39,4 N | 009° 41,9 W | 1459m | | mooring still at bottom |
| | 19:00 | | | 42° 39,4 N | 009° 41,9 W | | | break off |
| 5 | 19:00 | ADCP / PS | 4.1 | 42° 39,4 N | 009° 41,9 W | | | profile start rwK 270° |
| | 08:29 | | 5.1 | 42° 44,7 N | 011° 46,4 W | | | profile end |

Abbreviations:

| | |
|---|---|
| BWS: | Bottom water sampler |
| CTD: | Salinity-temperature-water sampling devise with rosette system |
| GKG: | Box corer |
| HS: | Hydrosweep |
| KaL: | Box lead |
| MUC: | Multicorer |
| PS: | Parasound |
| ADCP: | Acoustic Doppler Current Profiler |

Station List Leg M43/2 (continued)

| Station | Time UTC | Device | Date | Geographical position Latitude | Longitude | Waterdepth uncorrected (m) | Wire length (m) | Comments |
|---|---|---|---|---|---|---|---|---|
| 6 | 09:17 | hydro-phon | | 42° 45,0 N | 011° 46,2 W | | | break off of the release of mooring OMEX I |
| | | | | | | | | |
| 7 | 02:56 | CTD 4 | 6.1 | 42° 10,1 N | 009° 18,8 W | 221m | 200m | |
| | 03:14 | | | 42° 10,1 N | 009° 18,8 W | | | |
| | 04:21 | CTD 5 | | 42° 10,2 N | 009° 18,9 W | 222m | 200m | |
| 8 | 07:06 | CTD 6 | | 42° 09,0 N | 009° 27,9 W | 1053m | 1000m | |
| | 08:02 | CTD 7 | | 42° 09,0 N | 009° 27,9 W | 1056m | 300m | |
| | 08:54 | CTD 8 | | 42° 09,0 N | 009° 27,9 W | 1063m | 1000m | |
| 9 | 12:13 | MUC 1 | | 42° 10,0 N | 009° 46,9 W | 2333m | 2343m | failure |
| | 14:15 | GKG 1 | | 42° 08,5 N | 009° 46,6 W | 2323m | 2326m | bottom contact |
| | 16:06 | GKG 2 | | 42° 08,3 N | 009° 46,3 W | 2314m | 2319m | failure |
| | 17:58 | GKG 3 | | 42° 09,6 N | 009° 46,8 W | 2330m | 2339m | failure |
| | 19:48 | BWS | | 42° 09,0 N | 009° 46,9 W | 2334m | 618m | failure |
| 10 | 21:05 | CTD 9 | 6.1 | 42° 09,0 N | 009° 44,4 W | 2265m | 200m | |
| | 21:37 | CTD 10 | | 42° 09,0 N | 009° 44,4 W | 2266m | 150m | |
| | 22:42 | CTD 11 | | 42° 09,0 N | 009° 44,4 W | 2263m | 1700m | |
| | 23:54 | CTD 12 | | 42° 09,0 N | 009° 44,2 W | 2256m | 900m | |
| | 02:12 | CTD 13 | 7.1 | 42° 08,8 N | 009° 43,7 W | 2236m | 2200m | |
| 11 | 04:40 | CTD 14 | | 42° 10,5 N | 009° 35,7 W | 1942m | 1900m | |
| | 05:51 | CTD 15 | | 42° 10,5 N | 009° 35,8 W | 1945m | 200m | |
| | 06:42 | CTD 16 | | 42° 10,5 N | 009° 35,7 W | 1940m | 1400m | |
| | 08:43 | GKG 1 | | 42° 10,5 N | 009° 36,0 W | 1951m | 1951m | bottom contact |
| | 10:06 | GKG 2 | | 42° 10,6 N | 009° 36,0 W | 1949m | 1952m | failure |
| | 11:20 | GKG 3 | | 42° 10,5 N | 009° 36,1 W | 1951m | 1962m | bottom contact |
| | 12:42 | GKG 4 | | 42° 10,5 N | 009° 36,0 W | 1945m | 1954m | bottom contact |
| | 14:27 | MUC 1 | | 42° 10,5 N | 009° 35,9 W | 1952m | 1952m | bottom contact |
| | 16:05 | MUC 2 | | 42° 10,5 N | 009° 35,9 W | 1947m | 1953m | bottom contact |
| | 18:01 | BWS | | 42° 10,5 N | 009° 35,9 W | 1950m | 1973m | bottom contact |
| 12 | 20:05 | CTD 17 | 7.1 | 42° 08,8 N | 009° 31,1 W | 1576m | 1532m | |
| 13 | 22:16 | CTD 18 | 7.1 | 42° 09,0 N | 009° 27,5 W | 968m | 954m | |
| | 23:03 | CTD 19 | | 42° 09,0 N | 009° 27,5 W | 970m | 350m | |
| 14 | 00:14 | CTD 20 | 8.1 | 42° 09,0 N | 009° 26,2 W | 603m | 530m | |
| 15 | 01:33 | CTD 21 | 8.1 | 42° 09,0 N | 009° 23,5 W | 269m | 230m | |
| 16 | 02:23 | CTD 22 | 8.1 | 42° 09,0 N | 009° 20,7 W | 233m | 200m | |
| 17 | 03:09 | CTD 23 | 8.1 | 42° 09,0 N | 009° 18,0 W | 210m | 200m | |
| 18 | 03:53 | CTD 24 | 8.1 | 42° 09,0 N | 009° 15,4 W | 187m | 178m | |
| 19 | 04:37 | CTD 25 | 8.1 | 42° 09,0 N | 009° 13,0 W | 172m | 115m | |
| | 05:00 | CTD 26 | 8.1 | 42° 08,9 N | 009° 13,0 W | 171m | 160m | |
| 20 | 06:26 | GKG 1 | 8.1 | 42° 09,0 N | 009° 18,7 W | 216m | 214m | bottom contact |
| | 06:59 | GKG 2 | | 42° 09,0 N | 009° 18,7 W | 216m | 218m | bottom contact |
| | 07:33 | GKG 3 | | 42° 09,0 N | 009° 18,7 W | 217m | 219m | bottom contact |
| | 08:10 | GKG 4 | | 42° 09,0 N | 009° 18,8 W | 217m | 217m | bottom contact |
| | 08:39 | GKG 5 | | 42° 09,0 N | 009° 18,7 W | 217m | 219m | bottom contact |
| | 09:15 | MUC 1 | | 42° 09,0 N | 009° 18,7 W | 217m | 222m | bottom contact |
| | 09:55 | MUC 2 | | 42° 09,0 N | 009° 18,7 W | 216m | 221m | bottom contact |
| | 10:46 | MUC 3 | | 42° 09,0 N | 009° 18,7 W | 216m | 220m | bottom contact |
| 21 | 11:49 | CTD 27 | 8.1 | 42° 07,0 N | 009° 18,8 W | 207m | 180m | |
| | 12:22 | MUC 1 | | 42° 07,0 N | 009° 18,8 W | 206m | 214m | bottom contact |
| 22 | 13:19 | MUC 1 | | 42° 11,0 N | 009° 18,8 W | 222m | 233m | bottom contact |
| 23 | 14:52 | BWS | | 42° 09,0 N | 009° 18,8 W | 216m | 226m | bottom contact |

Station List Leg M43/2 (continued)

| Station | Time UTC | Device | Date | Geographical position Latitude | Longitude | Waterdepth uncorrected (m) | Wire length (m) | Comments |
|---|---|---|---|---|---|---|---|---|
| 24 | 20:20 | CTD 28 | 8.1 | 42° 09,1 N | 010° 30,0 W | 2762m | 300m | |
| | 20:52 | CTD 29 | | 42° 09,1 N | 010° 29,8 W | 2763m | 30m | |
| | 21:15 | CTD 30 | | 42° 09,0 N | 010° 29,8 W | 2761m | 10m | |
| | 21:51 | CTD 31 | | 42° 09,1 N | 010° 29,9 W | 2762m | 1000m | |
| | 22:22 | CTD 32 | | 42° 09,0 N | 010° 29,9 W | 2768m | 50m | |
| | 23:18 | CTD 33 | | 42° 09,0 N | 010° 29,9 W | 2763m | 2700m | |
| | 01:09 | CTD 34 | 9.1 | 42° 09,0 N | 010° 30,0 W | 2763m | 2700m | |
| | 02:40 | CTD 35 | | 42° 09,0 N | 010° 30,0 W | 2761m | 1000m | |
| | 03:33 | CTD 36 | | 42° 09,0 N | 010° 30,0 W | 2766m | 1000m | |
| | 04:25 | CTD 37 | | 42° 09,0 N | 010° 30,0 W | 2764m | 1000m | |
| | 05:19 | CTD 38 | | 42° 09,0 N | 010° 30,0 W | 2765m | 700m | |
| | 07:23 | CTD 39 | | 42° 09,0 N | 010° 30,0 W | 2766m | 2700m | |
| | 09:21 | GKG 1 | | 42° 09,0 N | 010° 30,0 W | 2764m | 2768m | bottom contact |
| | 11:01 | GKG 2 | | 42° 09,0 N | 010° 29,9 W | 2763m | 2765m | bottom contact |
| | 12:59 | MUC 1 | | 42° 09,1 N | 010° 30,0 W | 2765m | 2776m | bottom contact |
| | 13:56 | CTD 40 | | 42° 09,0 N | 010° 29,9 W | 2762m | 200m | |
| | 14:55 | MUC 2 | | 42° 09,0 N | 010° 29,9 W | 2762m | 2774m | bottom contact |
| | 16:00 | CTD 41 | | 42° 09,0 N | 010° 30,0 W | 2763m | 200m | |
| | 16:11 | MUC 3 | | 42° 08,9 N | 010° 29,9 W | 2762m | 2780m | bottom contact |
| | 19:04 | KaL | | 42° 09,0 N | 010° 30,0 W | 2761m | 2783m | bottom contact |
| | 21:35 | BWS | | 42° 09,0 N | 010° 30,1 W | 2766m | 2783m | bottom contact |
| 25 | 13:52 | GKG 1 | | 39° 29,8 N | 009° 55,3 W | 3469m | 3505m | failure |
| | 15:53 | GKG 2 | | 39° 29,8 N | 009° 55,4 W | 3612m | 3601m | failure |
| | 17:51 | GKG 3 | | 39° 29,7 N | 009° 55,4 W | 3514m | 3510m | bottom contact |
| | 20:12 | MUC 1 | | 39° 29,7 N | 009° 55,5 W | 3526m | 3549m | bottom contact |
| | 22:37 | MUC 2 | | 39° 29,7 N | 009° 55,5 W | 3554m | 3554m | bottom contact |
| | 00:56 | MUC 3 | 11.1 | 39° 29,7 N | 009° 55,5 W | 3509m | 3562m | bottom contact |
| | 02:28 | CTD 42 | | 39° 29,8 N | 009° 55,5 W | 3456m | 900m | |
| | 04:56 | CTD 43 | | 39° 29,8 N | 009° 55,4 W | 3602m | 3500m | |
| | 06:14 | HS / PS | | 39° 29,8 N | 009° 55,5 W | | | profile start various courses in the Nazare Canoyn |
| | 08:00 | | | 39° 31,8 N | 009° 48,5 W | | | various courses |
| | 08:21 | | | 39° 31,7 N | 009° 46,1 W | | | course change to rwK151° |
| | 09:10 | | | 39° 29,0 N | 009° 45,1 W | | | profile end |
| 26 | 09:20 | GKG 1 | 12.1 | 39° 29,0 N | 009° 45,1 W | 2816m | 2859m | bottom contact |
| | 12:05 | GKG 2 | | 39° 29,0 N | 009° 45,1 W | 2894m | 2883m | bottom contact |
| | 14:13 | MUC 1 | | 39° 29,0 N | 009° 45,1 W | 2878m | 2890m | bottom contact |
| | 16:14 | MUC 2 | | 39° 29,1 N | 009° 45,0 W | 2898m | 2916m | bottom contact |
| | 18:03 | MUC 3 | | 39° 29,0 N | 009° 45,0 W | 2893m | 2890m | bottom contact |
| 27 | 12:57 | GKG 1 | 12.1 | 39° 34,0 N | 010° 10,3 W | 4141m | 4183m | bottom contact |
| | 16:08 | MUC 1 | | 39° 33,9 N | 010° 10,0 W | 4121m | 4176m | bottom contact |
| | 18:54 | KaL | | 39° 33,9 N | 010° 09,9 W | 4121m | 4194m | failure KaL got bent |
| | 21:21 | CTD 44 | | 39° 34,0 N | 010° 09,9 W | 4120m | 4000m | |
| 28 | 17:23 | CTD 45 | 13.1 | 36° 33,1 N | 008° 30,0 W | 2260m | 300m | |
| | 19:03 | CTD 46 | | 36° 33,1 N | 008° 30,2 W | 2172 | 2000m | |
| | 00:02 | HS / PS | 14.1 | 37° 00,0 N | 008° 10,0 W | | | profile start (Faro) rwK 104° |
| | 01:08 | | | 36° 58,0 N | 008° 00,0 W | | | course change to rwK122° |
| | 01:48 | | | 36° 55,5 N | 007° 55,0 W | | | course change to rwK058° |
| | 02:17 | | | 36° 58,0 N | 007° 50,0 W | | | course change to rwK076° |
| | 03:44 | | | 37° 00,0 N | 007° 40,0 W | | | profile end |

End of station work, departure to cardiz

## 8 Concluding Remarks

METEOR Cruise M 43 was very international, with participants from 11 countries and 21 institutions.

The quantity and quality of the rocks dredged during the METEOR cruise M 43/1 exceeded our expectations. Using the HYDROSWEEP and HYDROMAP facilities of FS METEOR in addition to previously collected data, bathymetric maps were produced on board of the entire, or at least larger parts, of the survey area. Such maps are an important tool for selecting sampling sites or areas for more detailed data collection. Our understanding of the structure and evolution of oceanic intra-plate volcanic systems and their peripheral sedimentary basins will be greatly advanced.

METEOR cruise M 43/2 was a successful winter cruise providing very important samples for the OMEX project. The results will significantly contribute to construct seasonal budgets for the upwelling area off Portugal and will help to validate physical models of the area.

Our thanks go to all funding institutions, especially BMBF, DFG and the EU who provided the bulk of the cruise and ship support as well as the associated research. Support for some members of the scientific crew came from institutions in Portugal, Ireland, Switzerland, Netherlands, Belgium, France, and Great Britain. We also like to address our thanks to the Leitstelle METEOR in Hamburg for their help in the planning and realisation of the cruise.

The success of our work very much depended on the close co-operation with Captain Kull and his crew especially in view of our frequent change in the program demanding a high degree of flexibility. Working under such professional conditions was a very good experience indeed.

## 9 References


BEHR, H. D. (1990): Radiation Balance at the Sea Surface in the Atlantic Ocean Region between 40° S and 40° N. J. Geophys. Res., D95, 20633-20640.

BEHR, H. D. (1992): Net total and UV-B Radiation at the Sea Surface, J. Atmospher. Chem., 15, 299-314.

BLUM, N., P. HALBACH, U. MÜNCH AND M. VAN GERVEN (1996): Pb-Sr-Nd isotopic data of Mesozoic ocean island basalts from the eastern Atlantic ocean continental margin. Chem. Erde, 56, 193-205.

HALBACH, P. (1993): Technical cruise report, RV SONNE Cruise 83 - MARFLUX 4, 26.11. - 31.12.1992, Bremerhaven - Las Palmas de Gran Canaria, The Free University of Berlin.

IQBAL, M. (1983): An Introduction to Solar Radiation, Academic Press Toronto, New York, London, 390 pages.

KASTEN, F. (1996): The Linke Turbidity Factor Based on Improved Values of the Integral Rayleigh-optical Thickness, Solar Energy, 56, 239-244.

KASTEN, F. AND YOUNG, A. T. (1989): Revised Optical Air Mass Tables and Approximation Formula, Applied Optics, 28, 4735-4738.

MASSON, D.G., R.B. KIDD, J.V. GARDNER, Q.J. HUGGETT AND P.P.E. WEAVER (1992): Saharan continental rise: facies distribution and sediment slides. In: Poag, C. W. and P. C. de Graciansky (eds.): Geologic evolution of Atlantic continental rises. 327-343.

MOORE, J.G., D.A. CLAGUE, R.T. HOLCOMB, P.W. LIPMAN, W.R. NORMARK AND M.E. TORRESAN (1989): Prodigious submarine landslides on the Hawaiian Ridge. J. Geophys. Res., 94, 17465-17484.

MOORE, J.G., W.R. NORMARK AND R.T. HOLCOMB (1994): Giant Hawaiian landslides. Annu. Rev. Earth Planet. Sci., 22, 119-144.

RIHM, R., C.L. JACOBS, S. KRASTEL, H.-U. SCHMINCKE AND B. ALIBES (1998): Las Hijas Seamounts - the next Canary Island? Terra Nova, 10, 121-125.

SCHMINCKE, H.-U. (1982): Volcanic and chemical evolution of the Canary Islands. In: von Rad, U., K. Hinz, M. Sarnthein and E. Seibold (eds.): Geology of the Northwest African continental margin. 273-306.

SCHMINCKE, H.-U. AND R. RIHM (1994). Ozeanvulkan 1993, Cruise No. 24, 15 April - 9 May 1993. METEOR-Berichte, 94-2. Univ. Hamburg: 1-88.

SCHMINCKE, H.-U. AND B. SEGSCHNEIDER (1998): Shallow submarine to emergent basaltic shield volcanism of Gran Canaria: Evidence from drilling into the volcanic apron. In: Weaver, P. P. E., H.-U. Schmincke, J. V. Firth and W. Duffield (eds.): Proc. ODP. Sci. Results, 157. 141-181.

SCHMINCKE, H.-U. AND M. SUMITA (1998): Volcanic evolution of Gran Canaria reconstructed from apron sediments: Synthesis of VICAP project drilling. In: Weaver, P. P. E., H.-U. Schmincke, J. V. Firth and W. Duffield (eds.): Proc. ODP. Sci. Results, 157. 443-469.

SMITH, W.H.F. AND D.T. SANDWELL (1997): Global seafloor topography from satelite altimetry and ship depth soundings. Science, 277, 1956-1962.

SPIEß , V. (1992): Paradigma. Handbuch zur Digitalisierung von Parasound-Seismogrammen, Universität Bremen, 1-39.

STAUDIGEL, H. AND H.-U. SCHMINCKE (1984): The Pliocene seamount series of La Palma/Canary Islands. J. Geophys. Res., 89, 11195-11215.

WATTS, A.B. AND D.G. MASSON (1995): A giant landslide on the north flank of Tenerife, Canary Islands. J. Geophys. Res., 100, 24487-24498.

**Publications from METEOR expeditions**
**in other reports**

---


GERLACH, S.A., J. THIEDE, G. GRAF UND F. WERNER (1986): Forschungsschiff Meteor, Reise 2 vom 19. Juni bis 16. Juli 1986. Forschungsschiff Poseidon, Reise 128 vom 7. Mai bis 8. Juni 1986. Ber. Sonderforschungsbereich 313, Univ. Kiel, 4, 140 S.

SIEDLER, G., H. SCHMICKLER, T.J. MÜLLER, H.-W. SCHENKE UND W. ZENK (1987): Forschungsschiff Meteor, Reise Nr. 4, Kapverden - Expedition, Oktober - Dezember 1986. Ber. Inst. f. Meeresk., 173, Kiel, 123 S.

WEFER, G., G.F. LUTZE, T.J. MÜLLER, O. PFANNKUCHE, W. SCHENKE, G. SIEDLER UND W. ZENK (1988): Kurzbericht über die Meteor - Expedition Nr. 6, Hamburg - Hamburg, 28. Oktober 1987 - 19. Mai 1988. Berichte, Fachbereich Geowissenschaften, Universität Bremen, 4, 29 S.

MÜLLER T.J., G. SIEDLER UND W. ZENK (1988): Forschungsschiff Meteor, Reise Nr. 6, Atlantik 87/88, Fahrtabschnitte Nr. 1 - 3, Oktober - Dezember 1987. Ber. Inst. f. Meeresk., 184, Kiel, 77 S.

LUTZE, G.F., C.O.C. AGWU, A. ALTENBACH, U. HENKEN-MELLIES, C. KOTHE, N. MÜHLHAN, U. PFLAUMANN, C. SAMTLEBEN, M. SARNTHEIN, M. SEGL, TH. SOLTWEDEL, U. STUTE, R. TIEDEMANN UND P. WEINHOLZ (1988): Bericht über die "Meteor" -Fahrt 6-5, Dakar - Libreville, 15.1.- 16.2.1988.Berichte - Reports, Geol. Paläont. Inst., Univ. Kiel, 22, 60 S.

WEFER, G., U. BLEIL, P.J. MÜLLER, H.D. SCHULZ, W.H.BERGER, U. BRATHAUER, L. BRÜCK, A. DAHMKE, K. DEHNING, M.L. DURATE-MORAIS, F. FÜRSICH, S. HINRICHS, K. KLOCKGETER, A. KÖLLING, C. KOTHE, J.F. MAKAYA, H. OBERHÄNSLI, W. OSCHMANN, J. POSNY, F. ROSTEK, H. SCHMIDT, R. SCHNEIDER, M. SEGL, M. SOBIESIAK, T. SOLTWEDEL UND V. SPIEß (1988): Bericht über die Meteor - Fahrt M 6-6, Libreville - Las Palmas, 18.2.1988 - 23.2.1988. Berichte, Fachbereich Geowissenschaften, Universität Bremen, 3, 97 S.

HIRSCHLEBER, H., F. THEILEN, W. BALZER, B. V. BODUNGEN UND J. THIEDE (1988): Forschungsschiff Meteor, Reise 7, vom 1. Juni bis 28. September 1988, Ber. Sonderforschungsbereich 313, Univ. Kiel, 10, 358 S.

**METEOR-Berichte**
List of publications

| | | |
|---|---|---|
| 89-1 | (1989) MEINCKE, J., QUADFASEL, D. | GRÖNLANDSEE 1988-Expedition, Reise Nr. 8, 27. Oktober 1988 - 18. Dezember 1988. Universität Hamburg, 40 S. |
| 89-2 | (1989) ZENK, W., MÜLLER, T.J., WEFER, G. | BARLAVENTO-Expedition, Reise Nr. 9, 29. Dezember 1988 - 17. März 1989. Universität Hamburg, 238 S. |
| 90-1 | (1990) ZEITSCHEL, B., LENZ, J., THIEL, H., BOJE, R., STUHR, A., PASSOW, U. | PLANKTON'89 - BENTHOS'89, Reise Nr. 10, 19. März - 31. August 1989. Universität Hamburg, 216 S. |
| 90-2 | (1990) ROETHER, W., SARNTHEIN, M., MÜLLER, T.J., NELLEN, W., SAHRHAGE, D. | SÜDATLANTIK-ZIRKUMPOLARSTROM, Reise Nr. 11, 3. Oktober 1989 - 11. März 1990. Universität Hamburg, 169 S. |
| 91-1 | (1991) WEFER, G., WEIGEL, W., PFANNKUCHE, O. | OSTATLANTIK 90 - EXPEDITION, Reise Nr. 12, 13. März - 30. Juni 1990. Universität Hamburg, 166 S. |
| 91-2 | (1991) GERLACH, S.A., GRAF, G. | EUROPÄISCHES NORDMEER, Reise Nr. 13, 6. Juli - 24. August 1990. Universität Hamburg, 217 S. |
| 91-3 | (1991) HINZ, K., HASSE, L., SCHOTT, F. | SUBTROPISCHER & TROPISCHER ATLANTIK, Reise Nr. 14/1-3, Maritime Meteorologie und Physikalische Ozeanographie, 17. September - 30. Dezember 1990. Universität Hamburg, 58 S. |
| 91-4 | (1991) HINZ, K. | SUBTROPISCHER & TROPISCHER ATLANTIK, Reise Nr. 14/3, Geophysik, 31. Oktober - 30. Dezember 1990. Universität Hamburg, 94 S. |
| 92-1 | (1992) SIEDLER, G., ZENK, W. | WOCE Südatlantik 1991, Reise Nr. 15, 30. Dezember 1990 - 23. März 1991. Universität Hamburg, 126 S. |
| 92-2 | (1992) WEFER, G., SCHULZ, H.D., SCHOTT, F., HIRSCHLEBER, H. B. | ATLANTIK 91 - EXPEDITION, Reise Nr. 16, 27. März - 8. Juli 1991. Universität Hamburg, 288 S. |

| | | |
|---|---|---|
| 92-3 | (1992) SUESS, E., ALTENBACH, A.V. | EUROPÄISCHES NORDMEER, Reise Nr. 17, 15. Juli - 29. August 1991. Universität Hamburg, 164 S. |
| 93-1 | (1993) MEINCKE, J., BECKER, G. | WOCE-NORD, Cruise No. 18, 2. September - 26. September 1991. NORDSEE, Cruise No. 19, 30 September - 12 October 1991. Universität Hamburg, 105 pp. |
| 93-2 | (1993) WEFER, G., SCHULZ, H.D. | OSTATLANTIK 91/92 - EXPEDITION, Reise Nr. 20, M 20/1 und M 20/2, 18. November 1991 - 3. Februar 1992. Universität Hamburg, 248 S. |
| 93-3 | (1993) WEFER, G., HINZ, K., ROESER, H.A. | OSTATLANTIK 91/92 - EXPEDITION, Reise Nr. 20, M 20/3, 4. Februar - 13. März 1992. Universität Hamburg, 145 S. |
| 93-4 | (1993) PFANNKUCHE, O., DUINKER, J.C., GRAF, G., HENRICH, R., THIEL, H., ZEITSCHEL, B. | NORDATLANTIK 92, Reise Nr. 21, 16. März - 31. August 1992. Universität Hamburg, 281 S. |
| 93-5 | (1993) SIEDLER, G., BALZER, W., MÜLLER, T.J., RHEIN, M., ONKEN, R., ZENK, W. | WOCE South Atlantic 1992, Cruise No. 22, 22 September 1992 - 31 January 1993. Universität Hamburg, 131 pp. |
| 94-1 | (1994) BLEIL, U., SPIEß , V., WEFER, G. | Geo Bremen SOUTH ATLANTIC 1993, Cruise No. 23, 4 February - 12 April 1993. Universität Hamburg, 261 pp. |
| 94-2 | (1994) SCHMINCKE, H.-U., RIHM, O. | OZEANVULKAN 1993, Cruise No. 24, 15 April - 9 May 1993. Universität Hamburg, 88 pp. |
| 94-3 | (1994) HIEKE, W., HALBACH, P., TÜRKAY, M., WEIKERT, H. | MITTELMEER 1993, Cruise No. 25, 12 May - 20 August 1993. Universität Hamburg, 243 pp. |
| 94-4 | (1994) SUESS, E., KREMLING, K., MIENERT, J. | NORDATLANTIK 1993, Cruise No. 26, 24 August - 26 November 1993. Universität Hamburg, 256 pp. |

| | | |
|---|---|---|
| 94-5 | (1994) Bröckel, K. von, Thiel, H., Krause, G. | ÜBERFÜHRUNGSFAHRT, Reise Nr. 0, 15. März - 15. Mai 1986. ERPROBUNGSFAHRT, Reise Nr. 1, 16. Mai - 14. Juni 1986. BIOTRANS IV, Skagerrak 86, Reise Nr. 3, 21. Juli - 28. August 1986. Universität Hamburg, 126 S. |
| 94-6 | (1994) Pfannkuche, O., Balzer, W., Schott, F. | CARBON CYCLE AND TRANSPORT OF WATER MASSES IN THE NORTH ATLANTIC - THE WINTER SITUATION, Cruise No. 27, 29 December - 26 March 1994. Universität Hamburg, 134 pp. |
| 95-1 | (1995) Zenk, W., Müller, T.J. | WOCE Studies in the South Atlantic, Cruise No. 28, 29 March - 14 June 1994. Universität Hamburg, 193 pp. |
| 95-2 | (1995) Schulz, H., Bleil, U., Henrich, R., Segl, M. | Geo Bremen SOUTH ATLANTIC 1994, Cruise No. 29, 17 June - 5 September 1994. Universität Hamburg, 323 pp. |
| 96-1 | (1996) Nellen, W., Bettac, W., Roether, W., Schnack, D., Thiel, H., Weikert, H., Zeitschel, B. | MINDIK (Band I), Reise Nr. 5, 2. Januar - 24. September 1987. Universität Hamburg, 275 S. |
| 96-2 | (1996) Nellen, W., Bettac, W., Roether, W., Schnack, D., Thiel, H., Weikert, H., Zeitschel, B. | MINDIK (Band II), Reise Nr. 5, 2. Januar - 24. September 1987. Universität Hamburg, 179 S. |
| 96-3 | (1996) Koltermann, K.P., Pfannkuche, O., Meincke, J. | JGOFS, OMEX and WOCE in the North Atlantic 1994, Cruise No. 30, 7 September - 22 December 1994. Universität Hamburg, 148 pp. |
| 96-4 | (1996) Hemleben, Ch., Roether, W., Stoffers, P. | Östliches Mittelmeer, Rotes Meer, Arabisches Meer, Cruise No. 31, 30 December 1994 - 22 March 1995. Universität Hamburg, 282 pp. |
| 96-5 | (1996) Lochte, K., Halbach, P., Flemming, B.W. | Biogeochemical Fluxes in the Deep-Sea and Investigations of Geological Structures in the Indian Ocean, Cruise No. 33, 22 September - 30 December 1995. Universität Hamburg, 160 pp. |

| | | |
|---|---|---|
| 96-6 | (1996) SCHOTT, F., POLLEHNE, F., QUADFASEL, D., STRAMMA, L., WIESNER, M., ZEITZSCHEL, B. | ARABIAN SEA 1995, Cruise No. 32, 23 March - 19 September 1995. Universität Hamburg, 163 pp |
| 97-1 | (1997) WEFER, G. BLEIL, U. SCHULZ, H. FISCHER, G. | Geo Bremen SOUTH ATLANTIC 1996 (Volume I), Cruise No. 34, 3 January - 18 February 1996. Universität Hamburg, 254 pp. |
| 97-2 | (1997) WEFER, G. BLEIL, U. SCHULZ, H. FISCHER, G. | Geo Bremen SOUTH ATLANTIC 1996 (Volume II), Cruise No. 34, 21 February - 15 April 1996. Universität Hamburg, 268 pp. |
| 97-3 | (1997) WEFER, G. | 10 Jahre Forschungsschiff METEOR (1986 - 1996) - Dokumentation der Fahrten M0 - M34 (Volume I), Cruise No. 0-17. Universität Hamburg, 269 pp. |
| 97-4 | (1997) WEFER, G. | 10 Jahre Forschungsschiff METEOR (1986 - 1996) - Dokumentation der Fahrten M0 - M34 (Volume II), Cruise No. 18-34. Universität Hamburg, 236 pp. |
| 98-1 | (1998) WEFER, G. MÜLLER, T.J. | Canary Islands 1996/97, Cruise No. 37, 4 December 1996 - 22 January 1997. Universität Hamburg, 134 pp. |
| 98-2 | (1998) MIENERT, J. GRAF, G. HEMLEBEN, C. KREMLING, K. PFANNKUCHE, O. SCHULZ-BULL, D. | Nordatlantik 1996, Cruise No. 36, 6 June 1996 - 4 November 1996. Universität Hamburg, 302 pp. |
| 98-3 | (1998) HEMLEBEN, Ch. ZAHN, R. MEISCHNER, D. | Karibik 1996, Cruise No. 35, 18 April - 3 June 1996. Universität Hamburg, 208 pp. |
| 98-4 | (1998) BLEIL, U. FISCHER, G. | Geo Bremen South Atlantic 1997, Cruise No. 38, 25 January - 14 April 1997. Universität Hamburg, 244 pp. |
| 99-1 | (1999) SCHOTT, F. KOLTERMANN, K.-P. STRAMMA, L. SY, A. ZAHN, R. ZENK, W. | North Atlantic 1997, Cruise No. 39, 18 April - 14 September 1997. Universität Hamburg, 197 pp. |

| | | | |
|---|---|---|---|
| 99-2 | (1999) | HIEKE,W.<br>HEMLEBEN, Ch.<br>LINKE, P.<br>TÜRKAY, M.<br>WEIKERT, H. | Mittelmeer 1997/98, Cruise No. 40, 28 October 1997-10 February 1998. Universität Hamburg, 286 pp. |
| 99-3 | (1999) | SCHULZ, H.D.<br>DEVEY, C.W.<br>PÄTZOLD, J.<br>FISCHER, G. | Geo Bremen / GPI Kiel South Atlantic 1998, Cruise No. 41, 13 February - 13 June 1998. Universität Hamburg, 341 pp. |
| 00-1 | (2000) | PFANNKUCHE, O.<br>MÜLLER, T.J.<br>NELLEN, W.<br>WEFER, G. | Ostatlantik 1998, Cruise No. 42, 16 June - 26 October 1998. Universität Hamburg, 259 pp. |
| 00-2 | (2000) | SCHMINCKE, H.-U.<br>GRAF, G. | DECOS / OMEX II, Cruise No. 43, 25 November 1998-14 January 1999, Universität Hamburg, 99 pp. |